UNIVERSITY OF ZULULAND

A STUDY OF THE PROTECTIVE EFFECTS OF AN ASPALATHIN ENRICHED GREEN ROOIBOS EXTRACT ON EXPERIMENTALLY INDUCED HEPATIC STEATOSIS

BY

NOXOLO THOBILE KHUBONI

201237092

A dissertation submitted to fulfill the requirements of a

MASTER OF SCIENCE

In the study field of

Biochemistry

Department of Biochemistry and Microbiology, Faculty of Science and Agriculture,

University of Zululand, KwaDlangezwa, KwaZulu Natal

SUPERVISOR: DR. K.B. GABUZA AND PROF. A.P. KAPPO

CO-SUPERVISOR: PROF. C.J.F. MULLER

Date of submission:

March 2019

ABSTRACT

Background: Non-alcoholic fatty liver disease (NAFLD) is a hepatic manifestation of the metabolic syndrome, and is strongly associated with insulin resistance, obesity and type 2 diabetes (T2D). Growing evidence shows NAFLD as a multi-system disease, affecting several extra hepatic organs and regulatory pathways (Byrne et al., 2015). The prevalence of NAFLD is expected to escalate dramatically with the upsurge in metabolic diseases, particularly obesity and type 2 diabetes. However, an optimal treatment regime to cure NAFLD has not been established. Rooibos is gaining increasing recognition for its ability to improve health and has demonstrated hepatoprotective effects against carbon tetrachloride (CCl_4) and tert-butyl hydroperoxide induced hepatotoxicity in rodents. This study will establish if an aspalathin rich green rooibos extract (Afriplex GRT™) is able to modulate or prevent the excessive fat accumulation in experimental models of NAFLD.

Aim: The aim of the study was to assess the modulatory effect of GRT extract in *in vitro* and *in vivo* models of experimentally induced NAFLD.

Methods: The study used immortalized C3A liver cells and oleic acid to induce steatosis. Assessment of the effect of GRT on oleic acid induced steatosis was determined using different concentrations of aspalathin-enriched rooibos (GRT) extract. Cells not exposed to oleic acid were included as controls. Pioglitazone was used as a positive control. Steatosis of C3A cells was induced using 1 mM oleic acid for 24 hours. Treatment with GRT and pioglitazone for 24 hours, either commenced in the presence of oleic acid (simultaneous treated group) or 24 hours after oleic acid induced steatosis (post-treated group). MTT assay was performed to determine cell viability, while lipid content was measured using oil red O staining normalized for cell number by crystal violet staining. The effect of GRT extract on mRNA relevant to lipogenic genes (PPAR-α, SREBP, FASN and CPT1), inflammation (TNF-α) and glucose metabolism (GCK and ChREBP) were assessed.

Further investigation was done using leptin-receptor deficient C57BL6/J *db/db* mice (n=8/group) and their lean littermates (*db*/+) (n=8/group). The mice received standard

rodent chow *ad libitum*. Treatments were given daily with powdered chow containing a calculated dose equal to 74 mg/kg BW and 740 mg/kg BW GRT or 10 mg/kg BW pioglitazone. Food intake, water intake, body weight and fasting glucose was monitored weekly for the duration of the study. A week prior to termination of the study, oral glucose tolerance tests were performed. At termination the livers were collected and either fixed in formalin or snap frozen for storage at -80^{o}C. Gene and protein expression were performed using qPCR and Western blot, respectively, for the genes and proteins related to the development of NAFLD. The effect of GRT extract on the liver was confirmed by histology. The data was analysed using one-way analysis of variance (ANOVA) followed by Dunnet multiple comparison *post hoc* test. Statistical significance was set at $p < 0.05$.

Results: This study showed that 1 mM oleic acid for 24 hrs induced lipid accumulation in C3A cells and produced a good *in vitro* model for studying NAFLD. GRT extract displayed protective effects against NAFLD in oleic acid induce steatosis and decreased lipid content by < 80% in steatotic C3A cells. The reduction was comparable to pioglitazone (control drug). mRNA analysis revealed that GRT extract regulated fatty acid synthesis by downregulating genes involved in lipogenesis (SREBP 1c and FASN) and glucose metabolism (GCK and ChREBP) as well as inflammation (TNF-α).

In *db/db* mice, GRT improved glucose tolerance and reduced the liver weight to body weight ratio. In terms of genes and proteins that are involved in NAFLD, GRT increased key lipolytic genes PPAR-α and CPT 1 involved in the regulation of beta-oxidation of lipids and reduced HMG-CoA synthase 1 (HMGCS1), the gene regulating cholesterol synthesis. Histology confirmed increased steatosis limited to zone 3 of the liver acinus synonymous with NAFLD. Treatment with GRT did not significantly affect the steatotic severity score of the *db/db* mice.

Conclusion: GRT was effective at reducing oleic acid induced steatosis in C3A cells by regulating key genes involved in fatty acid and cholesterol synthesis, and inflammation. In *db/db* mice GRT extract modulated glucose tolerance and increased the expression of effector proteins involved with beta-oxidation in the liver but was not effective at reducing NAFLD.

Key Words: Non-alcoholic fatty liver disease, aspalathin rich unfermented rooibos extract.

DECLARATION

I, **Noxolo Thobile Khuboni** (Student Number: **201237092**), declare that this thesis is my own work. It is being submitted for the Master of Science in the study field of Biochemistry in Department of Biochemistry and Microbiology, University of Zululand, Empangeni. It has not been submitted before for any degree or examination at this or any other university.

Signature (Candidate): …….

Date: .....

ACKNOWLEDGEMENTS

"I will give thanks to you, LORD, with all my heart; I will tell of all your wonderful deeds." Ps. 9:1

I am grateful to my supervisor, Dr. K. B. Gabuza, whose expertise, understanding, generous guidance and support made it possible for me to work on a topic that was of great interest to me. It was a pleasure working with him.

I would like to extend my gratitude to my co-supervisors Prof. C.J.F. Muller for your assistance and guidance, for finding time to reply to my emails, for being ever so kind to show interest in my research. I would also like to thank my academic father Prof. A.P. Kappo for granting me this opportunity.

To my colleagues from BRIP. Ms. Amsha Viraragavan (tissue culture training), Dr. Carmen Pheiffer (PCR analysis) and Ms. Asive Myataza for giving your precious time when I needed assistance and kind advice regarding my research. Desmond Linden Thank you.

This journey would not have been possible without the support and love of my family. Thank you for supporting me in every way possible.

Mukelwe Sibisi, you have made me stronger, better and more fulfilled than I could have ever imagined. Thank you.

To Smangaliso Dlamini, Hlulukwenza Ngubane, Retsetse Ramtholo and Khanyisani Ziqubu thank you for the support you gave me, for the right advice at the right time and for being a source of motivation throughout this study.

Prof. Johan Louw, for the opportunity to conduct my M.Sc. research at the Biomedical Research and Innovation Platform (BRIP), South African Medical Research Council (SAMRC). Thank you.

Thanks to University of Zululand, Department of Biochemistry and Microbiology, and my gratitude to the SAMRC Research Internship Scholarship Programme (Masters and Ph.D. Scholarships). National Research Foundation and thank you for your sponsorship.

DEDICATION

This work is dedicated to my beloved parents

Dedicated to the memory of my late father **Mr. M.P. Khuboni** who always believed in my ability to be successful in the academic arena. You are gone but your belief in me has made this journey possible.

My mother **A.N. Khuboni** a strong and gentle soul who always picked me up on time and encourage me to go on every adventure especially this one. Thank you for supporting me in every way possible "***Ngiyabonga Ndlovukazi!".***

OUTPUTS FROM THE PRESENT STUDY

Symposia, conference proceedings, workshop(s) and publications

Symposia

N.T. Khuboni, A.P. Kappo, C.J.F Muller and K.B. Gabuza. The hepatoprotective effects of an aspalathin enriched green rooibos extract on experimentally induced hepatic steatosis. Stellenbosch, Cape Town, Joint SAMRC, University of Limpopo and University of Zululand research meeting, 25-27 July 2018

N.T. Khuboni, A.P. Kappo, C.J.F. Muller and K.B. Gabuza. The effects of an aspalathin enriched green rooibos extract on experimentally induced hepatic steatosis. SAMRC Conference Centre. Biomedical Research and Innovation Platform Symposium. 16 October 2018.

Conferences

N.T. Khuboni, A.P. Kappo, C.J.F. Muller and K.B. Gabuza. An anti-steatotic effect of aspalathin-enriched green rooibos extract on oleic acid induced steatosis in C3A liver cells. Spier Estate, Stellenbosch. 1st Conference of Biomedical and Natural Sciences and Therapeutics (CoBNest), 7-10 October 2018.

N.T. Khuboni, A. P. Kappo, C.J.F. Muller and K.B. Gabuza. The effects of an aspalathin enriched green rooibos extract on experimentally induced hepatic steatosis. ICCT, Cape Town.18th International Congress of Endocrinology, 53rd SEMDSA Congress. 1-4 December 2018.

Workshop

N.T. Khuboni. SAMRC Conference Centre, 12th Annual Early Career Scientist Convention: Western Cape, South Africa, 17-19 October 2018

Publications

To be submitted research papers

N.T. Khuboni, A.P. Kappo, C.J.F. Muller and K.B. Gabuza. **Experimental paper titled:** An anti-steatotic effect of aspalathin-enriched green rooibos extract on oleic acid induced steatosis in C3A liver cells.

N.T. Khuboni, A.P. Kappo, C.J.F. Muller and K.B. Gabuza. **Experimental paper titled:** Hepatoprotective effects of aspalathin-enriched green rooibos extract in leptin resistance male C57BL6/J (*db/db*) mice.

To be submitted review paper

N.T. Khuboni, A.P. Kappo, C.J.F. Muller and K.B. Gabuza **Review article titled:** Therapeutic potentials of medicinal plants in experimentally induced hepatic steatosis.

LIST OF ABBREVIATIONS

ALT	Alanine aminotransferase
ANOVA	Analysis of variance
AST	Aspartate aminotransferase
ATP	Adenosine triphosphate
BSA	Bovine serum albumin
DNL	*De novo* lipogenesis
BMI	Body mass index
BW	Body weight
ACC	Acetyl-CoA carboxylase
CVD	Cardiovascular disease
CBH	Carbohydrates
DMSO	Dimethyl sulfoxide
EMEM	Eagle's minimal essential medium
I-kB	Inhibition of NF-kB
IR	Insulin resistance
MTT	2-(4,5-dimethylthiazol-2-yl)-2,5-diphenyltetrazolium bromide
NaOH	Sodium hydroxide
PBS	Phosphate buffered saline
ROS	Reactive oxygen species
Rpm	Revolutions per minute
STZ	Streptozotocin
T2DM	Type 2 Diabetes Mellitus
WHO	World Health Organization
APS	Ammonium persulfate
CYP_{450}	Cytochrome P_{450} enzymes
SREBP	Sterol regulatory element-binding protein
NAFLD	Non-alcoholic fatty liver disease
NF-kB	Nuclear factor-kappa B
NASH	Non-alcoholic steatohepatitis

PVDF	Polyvinylidene difluoride
TEMED	Tetramethylethylenediamine tetraacetic acid
RNS	Reactive nitrogen species
RT	Room temperature
TNF	Tumor necrosis factor
SEM	Standard error of the mean
GRT	Green Rooibos extract
GLUT 4	Glucose transporter type 4
AMPK	Adenosine monophosphate-activated protein kinase
CO_2	Carbon dioxide
GSH	Glutathione
CCl_4	Carbon tetrachloride
MW	Molecular weight
NADPH	Nicotinamide adenine dinucleotide phosphate
PEP	phosphoenolpyruvate
GBD	Global burden of disease
FFA	Free fatty acid
HCC	Hepatocellular carcinoma
LPS	Lipopolysaccharide
TZDs	Thiazolidinediones
Act β	Beta actin
Pen/ strep	Penicillin- streptomycin
PUDAC	Primate unit and delft animal centre
qRT-PCR	Quantitative reverse transcription polymerase chain reaction

UNITS OF MEASUREMENTS

µl	Microliter
ml	Milliliter
l	Liter
ng	Nanogram
µg	Microgram
mg	Milligram
g	Gram
kg	Kilogram
kDa	Kilo Dalton
µM	Micromolar
mM	Millimolar
M	Molar
mm	Millimeters
µm	Micrometer
min	Minute
sec	Second
Hrs	Hours
°C	Degree Celsius
× g	Centrifugal gravity
%	Percentage

SYMBOLS

α	Alpha
β	Beta
γ	Gamma

LIST OF TABLES

LIST OF FIGURES

TABLE OF CONTENTS

CHAPTER ONE

INTRODUCTION TO THE PRESENT STUDY

1. INTRODUCTION

Obesity, insulin resistance, and type 2 diabetes (T2D) are associated with a concurrent increase in non-alcoholic fatty liver disease (NAFLD). Fatty liver affects between 70% and 90% of people with obesity and T2D (Downman *et al*., 2011; Fabbrini, Sullivan, and Klein, 2010; Souza *et al*., 2012). Non-alcoholic fatty liver disease is defined by the presence of excessive amounts of fat in the liver, exceeding 5% of the liver mass (Chalasani *et al*., 2017). The diagnosis of NAFLD is based either on sonar imaging or on liver histology without secondary causes such as significant alcohol consumption and certain medications (Puri *et al*., 2012).

NAFLD is the commonest liver disorder in Western countries (Bellentani *et al*., 2010). Fatty liver disease was initially linked to chronic alcoholism (Lieber *et al*., 1965). However, Judwing in 1981 discovered that similar fat accumulation occurs in absence of excessive alcohol consumption, and this was classified as NAFLD. It embraces a disease spectrum, ranging from simple steatosis (fatty liver) to non-alcoholic steatohepatitis (NASH) and cirrhosis (Benedict and Zhang, 2017). Simple steatosis is benign, whereas steatohepatitis (NASH) is characterized by hepatocyte injury, inflammation and fibrosis, which can lead to cirrhosis, liver failure and hepatocellular carcinoma (HCC) (Abd El-Kader and El-Den Ashmawy, 2015).

The liver performs an essential role in lipid metabolism, importing free fatty acids (FFAs) and manufacturing, storing and exporting lipids. Fat accumulation in the liver occurs as a result of metabolic dysfunction that may have long term consequences (Musso, Gambino and Cassader, 2009). A strong relationship exists between insulin resistance and NAFLD (Dowman, Tomlinson, and Newsome, 2009; Takahashi *et al*., 2010 Kristina, Utzschneider and Steven, 2006). When people are insulin resistant, their muscle, fat and liver cells don’t respond normally to insulin, with a resultant increase in blood glucose and the amount of free fatty acids circulating in the blood (Petta, Muratore, and Craxì, 2009). Hyperinsulinaemia, a feature of insulin resistance, reduces mitochondrial fatty acid beta-oxidation, and augments endogenous fatty acid synthesis in the liver (Anstee *et al*., 2006).

Clinically, pharmacological agents used to treat other metabolic diseases, such as insulin sensitizers, antioxidants, lipid-lowering drugs, pentoxifylline and medicinal herb/natural products, are prescribed for NAFLD with limited success.

Aspalathus linearis, popularly known as Rooibos, is a South African indigenous plant that has gained attention for its health promoting benefits. Rooibos is unique because it contains aspalathin to which many of its bioactivity has been attributed including its anti-oxidant, glucose and cholesterol lowering activity. Afriplex GRT^{TM} is an aspalathin rich unfermented rooibos extract containing 12.8% aspalathin. The extract was developed by Afriplex in partnership with the Biomedical Research and Innovation Platform at the South African Medical Research Council.

The therapeutic probability that rooibos can modulate or prevent NAFLD is based on previous studies confirming the hypoglycaemic activity of an aspalathin-enriched green rooibos extract *in vitro* and *in vivo* (Muller *et al*., 2012). In addition, Beltrán-Debón et al*.* (2011) demonstrated hypolipidaemic effects of rooibos in *LDLr-/-* mice fed a high fat diet, but this effect was stringently dependent on diet type. Mazibuko et al. (2013) demonstrated that rooibos reduced insulin resistance in insulin resistant muscle cells by activating the AKT and the AMPK pathways, and increasing glucose uptake via GLUT 4.

This finding was confirmed by Son et al. (2013) who reported that aspalathin isolated from rooibos increased glucose uptake in L6 myotubes by increasing AMPK phosphorylation and GLUT 4 translocation to the membrane. Further, in the *ob/ob* mouse model, aspalathin reduced fasting blood glucose levels, increased adiponectin levels and reduced hypertriglyceridaemia and serum thiobarbituric acid reactive substance (TBARS) levels, a marker of ROS. In addition, enzymes related to gluconeogenesis, glycogenolysis and lipogenesis were reduced by aspalathin, while the mRNA expression of glycogen synthase was increased in the liver of these obese IR mice (Son *et al.,* 2013). Rooibos also demonstrated a protective role in carbon tetrachloride (CCl_4) and tert-butyl

hydroperoxide induced hepatotoxicity in Wistar rats by reducing conjugated dienes (CD) and malondialdehyde (MDA) levels in the liver and reduced serum level of ALT, AST, and LDH.

1.1 STUDY OUTLINE

1.2 Aim

The primary aim of the study is to assess the modulatory or protective potential of an aspalathin rich green rooibos extract (Afriplex GRT) against experimentally induced NAFLD and then to establish the mechanisms whereby GRT protects the liver against NAFLD.

1.3 Objectives

Cell based models

- Examine the effects of oleic acid and inflammation on lipid metabolism and accumulation at a functional level including gene and protein expression in C3A liver cells.
- Examine the effects of GRT as treatment and/or preventative measure on the NAFLD lipid accumulation.

In-vivo work

- Assess the hepato-protective effects of an aspalathin-enriched rooibos extract on NAFLD in diet induced NAFLD C57BL6/J mice.

1.4 Intended contribution to the body of knowledge

This study will be crucial in understanding the effects of GRT extract on lipid accumulation in the liver leading to steatosis. Pioglitazone, a known insulin sensitizer was used as a reference treatment, as one of the contributors to NAFLD is insulin resistance. The protective effect of GRT against NAFLD is currently not known and thus this study will contribute new knowledge regarding the potential therapeutic effect of GRT.

1.5 This dissertation will be divided into 8 chapters:

1. Introduction
2. Literature review
3. Materials and methodology
4. Results
5. Discussion
6. Conclusion and limitations
7. References
8. Appendix

CHAPTER TWO

LITERATURE REVIEW

2.0 LITERATURE REVIEW

2.1 Non-Alcoholic Fatty Liver Disease (NAFLD)

Non-alcoholic fatty liver disease is one of the most prevalent liver diseases in the world (Mavrogiannaki and Migdalis, 2013). It is defined as a hepatic indicator of metabolic syndrome that also encompasses abdominal obesity (Milić, Lulić, and Štimac, 2014). About 20-30% of NAFLD patients develop non-alcoholic steatohepatitis (NASH) which further advances to more significant liver injury such as fibrosis, cirrhosis and for some people, hepatic carcinoma which leads to increased liver-related mortality (Petta, Muratore, and Craxì, 2009). The strong link between obesity and NAFLD arises from statistics which show that 80% of patients with NAFLD are obese (Kohli *et al.*, 2010; Sartorio *et al.*, 2007). Studies conducted by Hruby and Hu, (2015) show that obesity affects 1 in 3 worldwide and, subsequently, NAFLD has become the leading chronic form of liver disorder with a frequency comparable to obesity (Mirza, 2011).

2.2 Obesity

Obesity results from a disproportion between food consumption and energy outflow, resulting in increased accumulation of adipose tissue mass. Adipose tissue is comprised of adipocytes, connective tissue matrix, nerve tissue, blood vessels and immune cells functioning as a unit (Kershaw and Flier, 2004). However excess energy, stored as accumulated lipid in adipocytes, increases the adiposity and can result in obesity (Dyson, Anstee and Mcpherson, 2014; Kershaw and Flier, 2004). In addition, adipose tissue functions as an endocrine organ that produces adipokines, cytokines and hormones essential for maintaining metabolic homeostasis (Jung and Choi, 2014).

Obesity is a chronic disease, defined as a state of excess adipose mass (Caballero, 2007), clinically characterized by a body mass index (BMI) greater than or equal to thirty kg/m^2, (Rouabhia, Milic, and Abenavoli, 2014). In developed countries, obesity is more common in men while in developing countries women are more susceptible (Pinto *et al.*, 2018). A study conducted by Chalasani *et al*. (2018) shows a linear relationship between obesity and metabolic disorders, including liver-related disease (Figure 2.1). They further

showed that obesity is one of the major risk factors for metabolic disease (Chalasani *et al*., 2018).

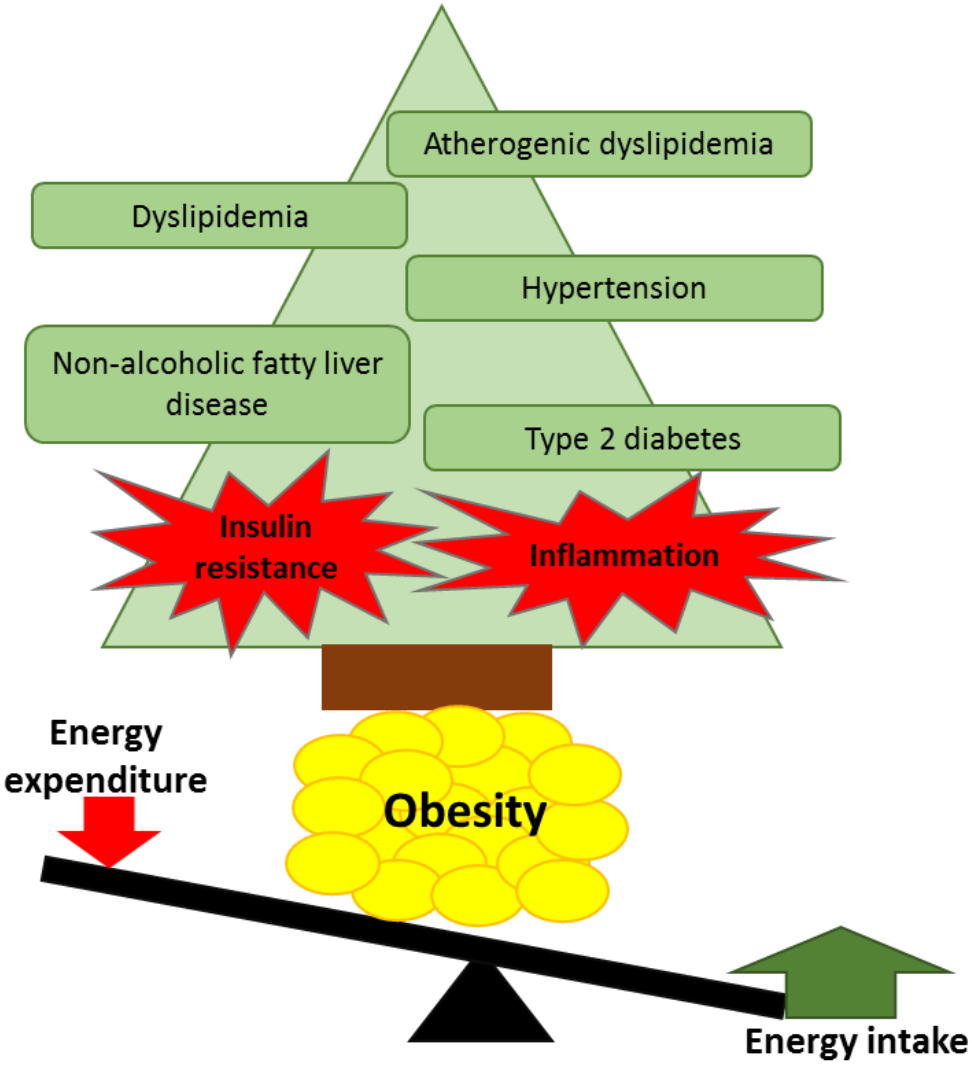

Figure 2.1 Representation of obesity as the main causative factor for metabolic syndrome. Illustration adapted from Jung and Choi., (2014). Obesity defined as an imbalance between energy intake and expenditure, underlies several other comorbidities fueled by insulin resistance and inflammation.

2.3 Obesity prevalence

Obesity is an epidemic which is increasing exponentially all over the world and presents a growing global public health disaster (Masuoka and Chalasani, 2013). According to the global burden of disease (GBD) 2016 obesity collaborators, there were more than 107.7 million obese children and 603.7 million obese adults in 2015, worldwide. Such statistics highlight obesity as a major public health concern, both in developed and developing countries. However, the prevalence of obesity is climbing more in developing countries (Serván, 2013). According to the World Health Organization (2018), the rapid increase of obesity has shown to have tripled since 1975.

2.3.1 Metabolic alterations and diseases related to obesity

Metabolic syndrome is a collection of metabolic malfunctions and contributes to the development of serious metabolic diseases such as cardiovascular disease and type 2 diabetes (T2D) (McCracken, Monaghan, and Sreenivasan, 2018). The metabolic syndrome is commonly characterized by increased visceral adiposity, compromised glucose tolerance, enhanced triglyceride levels, reduced levels of high-density lipoproteins and hypertension, causing an amplified rate of inflammation and increasing the risk of developing cardiovascular disease (Serván, 2013; Carr, Friedman and Jaffe, 2007). A study by Han and Boyko (2018) confirmed that strong links exist between obesity and T2D patients.

Hypertension is also associated with the worldwide obesity epidemic (Lu *et al*., 2013). Hall et al., (2010) showed that obesity contributes up to 75% to the development of hypertension. In patients with obesity, vascular impairment, systemic insulin resistance and the dysfunction of the sympathetic nervous system contribute to hypertension (Hall *et al*., 2010). Insulin resistance and hyperinsulinaemia, which result from obesity, independently activate the renal sympathetic nervous system. This causes the constriction of blood vessels and increases blood pressure (Kotsis *et al*., 2010). Obesity is one of the major risk factors for metabolic syndrome as shown in (Figure 2.2) below.

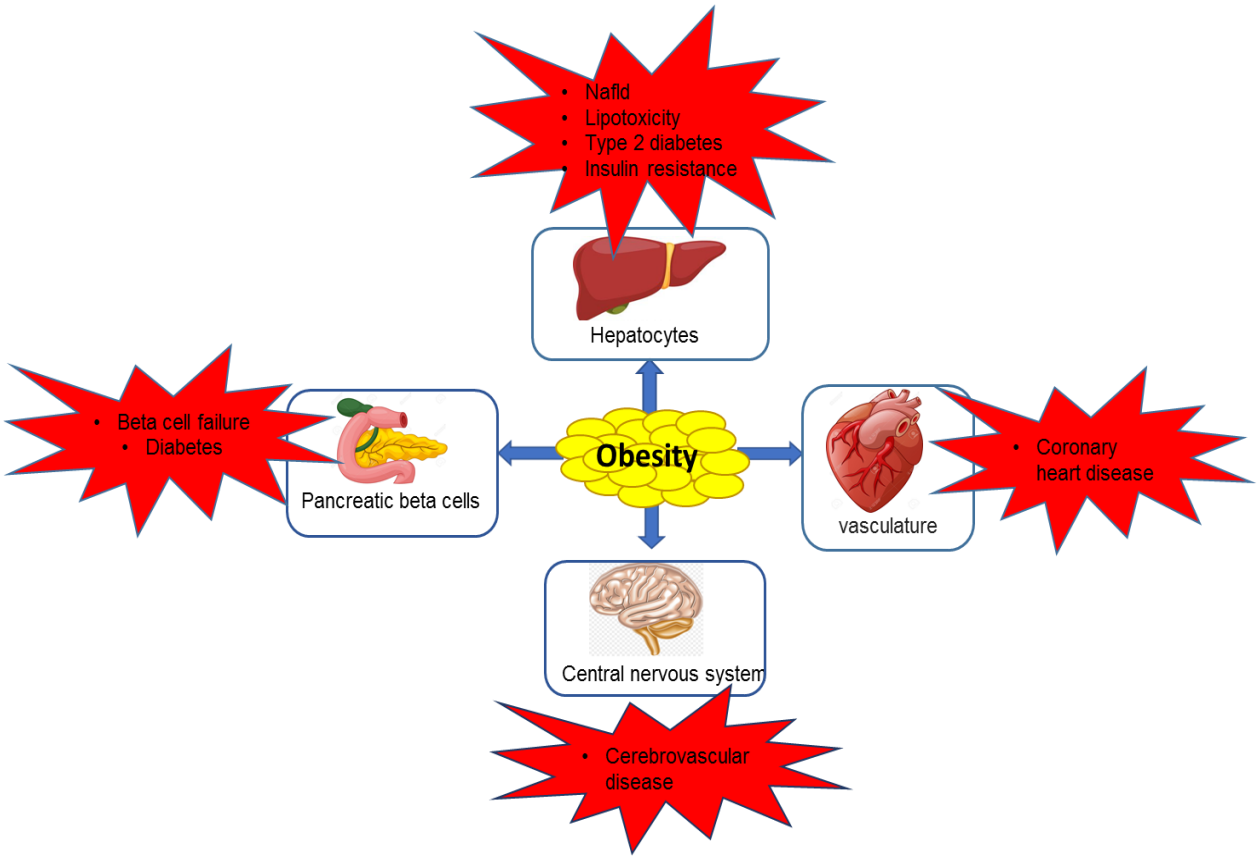

Figure 2.2 Illustration showing obesity as a major consequence of metabolic disorders.
Almost all organ systems are adversely affected by obesity as shown in the diagram.

2.3.1.1 Insulin resistance, type 2 diabetes and non-alcoholic fatty liver disease

In the presence of increased blood glucose, beta cells of the pancreas secrete insulin (a small protein composed of two amino acid chains interconnected by disulphide bridges) which is then released into the bloodstream and usually promotes glucose uptake into cells (Linardi, 2018). Obesity contributes to metabolic complications such as inflammation and insulin resistance. Insulin resistance (IR) can be defined as a condition where insulin responsive cells fail to respond efficiently to insulin resulting in glucose intolerance and increased post prandial blood glucose levels (Boden and Shulman, 2002). This condition normally precedes the onset of T2D (Nadulska, Szwajgier, and Opielak, 2017).

Type 2 diabetes is a disease that is characterized by hyperglycaemia and insulin resistance (Serván, 2013). Increased circulation of free fatty acids is another of the major consequences of T2D, which, further impairs insulin resistance and causes lipotoxicity (Oh *et al*., 2018). This usually triggers overproduction of proinflammatory cytokines and a comparative reduction of anti-inflammatory factors such as the adipokine adiponectin (Oh *et al*., 2018). This metabolic dysfunction causes intracellular fat to build up in the liver, a condition called non-alcoholic fatty liver disease (NAFLD).

2.4 Anatomy and physiology of the liver

The liver is the organ responsible for regulating metabolism and maintaining homeostasis (Limdi and Hyde, 2003). It is a multi-purpose organ that fulfills numerous physiological requirements such as gluconeogenesis, fat metabolism, protein metabolism and detoxification (Pauli *et al.*, 2012). The liver is composed of several cell types adapted to perform different specific functions. However, the principal cell type found in the hepatic parenchyma are hepatocytes which facilitate most of the vital biochemical reactions necessary for normal functioning (Lee *et al*., 2018). Hepatocytes account for 70-85% of the total cell population and 80% of the volume of the organ (Zhou, Xu and Gao, 2015). Better knowledge and understanding of the anatomy and segmental nature of the liver is essential in the management of patients with a liver-related disease such as NAFLD, as the liver plays a key role in metabolism to maintain the normal functioning of most physiological processes.

2.4.1 Gross anatomy of the liver

The liver weighs about 1.44–1.66 kg in humans and extends from the right hypochondrium and epigastrium to the left hypochondrium (Parkash and Patel, 2015). The liver is divided into two lobes and eight segments. It is partially separated into two major lobes; the right lobe, which is the largest lobe and occupies the right hypochondrium, and the left lobe which lies in the epigastric and left hypochondriac

regions. They are divided into anterior and posterior sections by the falciform ligament (Abdel-Misih and Bloomston, 2010).

2.4.2 Microscopic anatomy of the liver

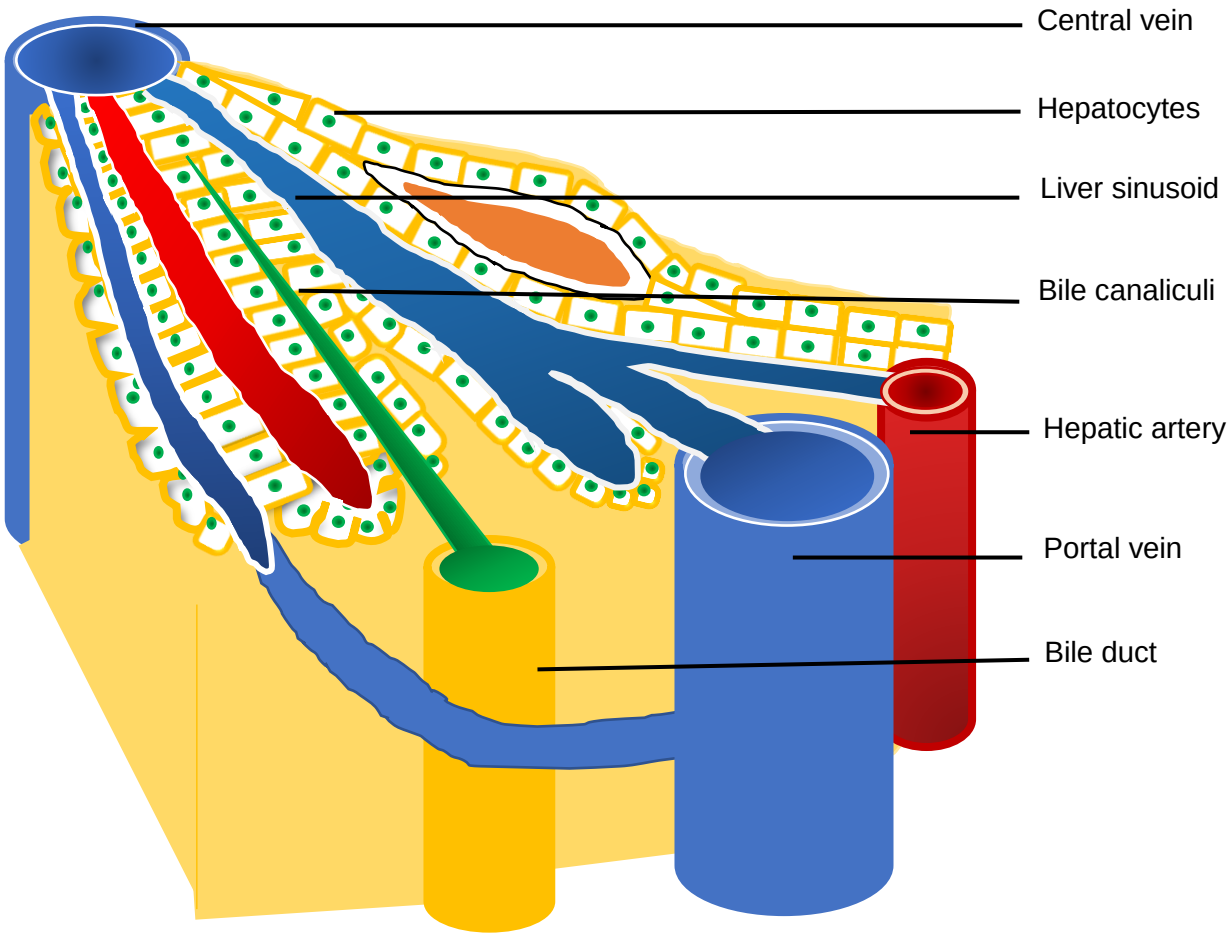

Figure 2.3 Microscopic anatomy of the liver (hepatic lobule).
The hepatic lobule is the classical functional unit in which the liver is divided. This represented the flow of blood from the portal area, comprising of the portal vein, hepatic artery and the bile duct. The blood from the hepatic artery and portal vein percolate through the liver sinusoids. The hepatocytes metabolize and detoxify nutrients and other substances from the blood. Bile secreted by the hepatocytes flows back towards the bile duct for excretion.

Hepatocytes are dynamic cells containing abundant mitochondria. They diverge from the central vein towards the periphery of the lobule (Majno *et al*., 2014). The spaces found in

between hepatocytes are called sinusoids, which are lined by fenestrated endothelium, separated from the hepatocytes by the extracellular space of Disse (Ober and Lemaigre, 2018). The main function of sinusoids is to drain blood from the portal triad into the central vein. From the central vein, the blood collects in the hepatic vein and then travel to the heart.

The portal triad consists of the hepatic vein, portal vein and bile duct (Krishna, 2013). The hepatic artery delivers oxygenated blood to the hepatocytes while the portal vein carries deoxygenated blood and nutrients from the gastrointestinal tract to the liver. The arterial and portal blood initially percolate through the hepatic sinusoids prior to draining into the systemic circulation (Abdel-Misih and Bloomston, 2010).

2.5 Metabolic functions of the liver:

As mentioned earlier, the liver plays a central role in maintaining metabolic homeostasis. This entails various processes that regulate the nutritional needs of the body during times of fast and stores energy postprandially. The liver also protects the body from potentially toxic substances (Pauli *et al.*, 2012).

2.5.1 Glucose production

As the brain and erythrocytes need a constant supply of glucose (Han *et al*., 2016), producing and maintaining blood glucose levels during periods of fast is a primary function of the liver. During the fasting state, the liver degrades its glycogen stores in a process called glycogenolysis. Glycogen degradation is under the hormonal control of glucagon and epinephrine. Glucagon is secreted by the pancreas in response to the low levels of glucose in the bloodstream. Glucagon binds to glucagon receptors on the surface of the liver cells, causing the release of cyclic AMP which activates the glycogen degradation (Zhang *et al*., 2018; Kolnes *et al*., 2015).

The degradation process is coupled by an enzymatic reaction i.e. glycogen phosphorylase catalyzes the breakdown of glycogen to yield glucose 1 phosphate, which is then converted to glucose by glucose 6 phosphatase. The glucose that is released can be transported from the liver to the blood stream as shown in Figure 2.4. The second hormone is epinephrine, which is released into the blood stream, and binds both alpha and beta receptors on the outer surface of the liver cells. In response, the alpha receptor causes an increase in calcium ion concentration and the beta receptors increase cyclic AMP (Kolnes *et al*., 2015). The second messenger stimulates glycogen degradation and helps to export the glucose into blood stream (Han *et al*., 2016).

During glycogenolysis, glycogen phosphorylase breaks down the alpha 1,4 glycosidic bond in glycogen, while the debranching enzyme amylo-α-1,6 glucosidase, breaks the branching alpha 1,6 glycogen bond to release a single glucose molecule. However, as the supply of glucose from glycogen stores is limited, during prolonged fasting glucose is produced by gluconeogenesis (Puigserver *et al*., 2003; Hatting *et al*., 2017).

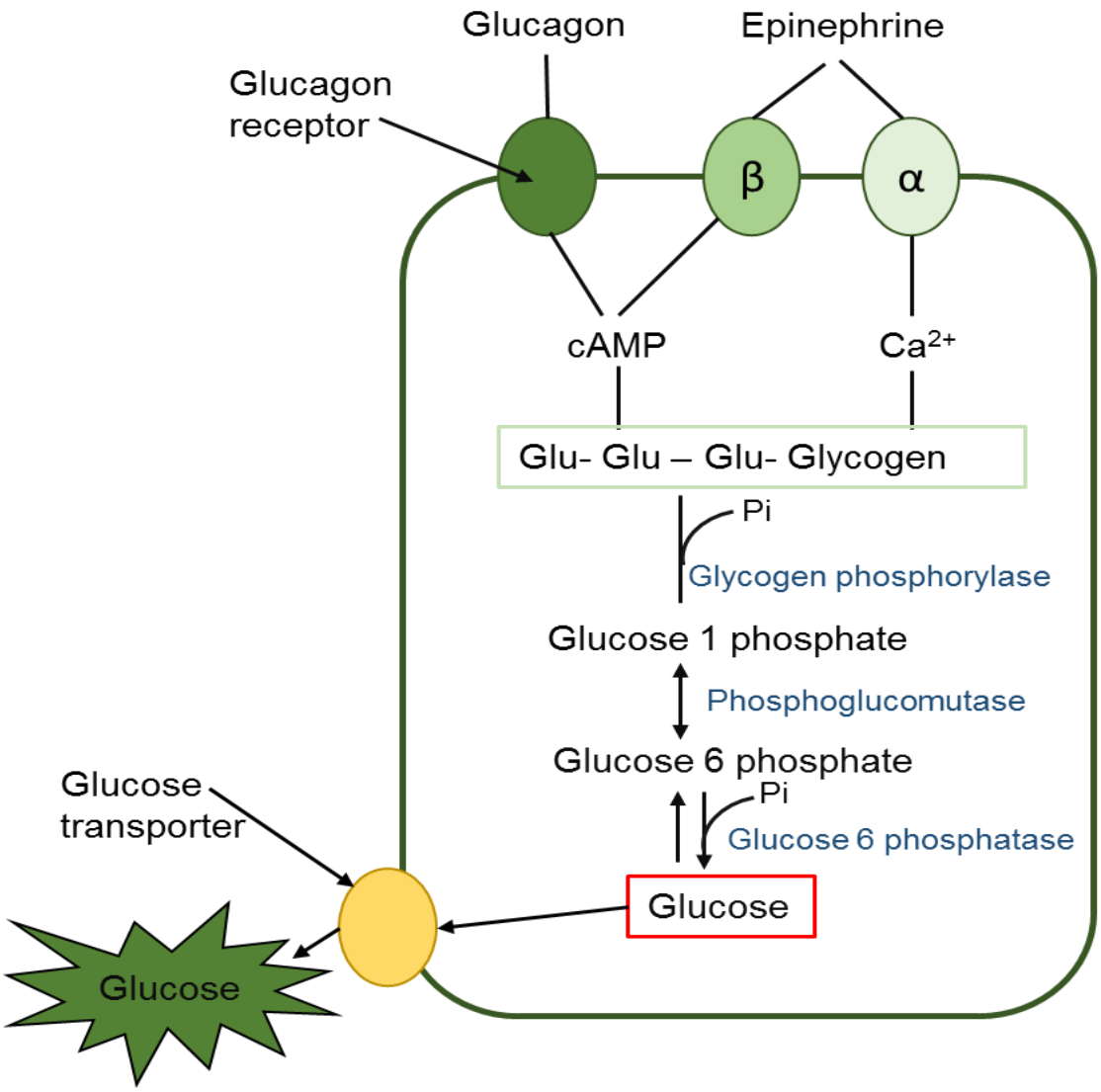

Figure 2.4 Hormonal and enzymatic control of glycogen degradation.
Glucagon and epinephrine hormones control the degradation of glycogen by activating cyclic AMP and calcium ions, degradation of glycogen also requires enzymatic reactions to occur facilitated by glycogen phosphorylase, phosphoglucomutase and glucose 6 phosphatase.

Gluconeogenesis is an anabolic process that generates glucose from non-carbohydrate sources such as amino acids and lactate glycerol under prolonged fasting (Han *et al.*, 2016; Kaleta *et al.*, 2011). Gluconeogenesis primarily occurs in the liver and secondarily in the kidneys (Hatting *et al*., 2017). Gluconeogenesis is a process by which pyruvate is converted into glucose, a sole energy source for brain and red blood cells. The first step of glucose production involves the conversion of pyruvate into oxaloacetate via pyruvate carboxylase which occurs in the mitochondria, while the following conversion occurs in

the cytosol (Wu *et al*., 2016). Pyruvate carboxylase consists of four identical subunits that each consists of a domain that is covalently attached to a biotin prosthetic group. This biotin-binding domain is used to bind the carbon dioxide molecule to the active site of the enzyme. It also consists of a domain that binds ATP needed to activate the carbon dioxide (Han *et al*., 2016).

Carbon dioxide exists as bicarbonate ions in the cytoplasm. In the first process (carboxylation), ATP is used to activate the carbon dioxide by forming carboxyphosphate. The phosphorylated carbon dioxide then attaches to the biotin of the enzyme and forms the carboxybiotin enzyme intermediate. The bond holding the carbon dioxide and biotin enzyme is quite unstable. In the final step, the carboxylated biotin-binding domain rotates into the active site containing the pyruvate substrate, forming oxaloacetate (Wu *et al.*, 2016; Hatting *et al.*, 2017).

The conversion of pyruvate into oxaloacetate by pyruvate carboxylase occurs in the mitochondria. Before step two of gluconeogenesis can occur, oxaloacetate is converted to malate and transported across the mitochondrial membrane into the cytoplasm. In the cytoplasm, phosphoenolpyruvate carboxykinase converts oxaloacetate into phosphoenolpyruvate (PEP). This highly endergonic decarboxylation step is coupled to the highly exergonic decarboxylation. The goal of these steps is to bypass the last irreversible steps of glycolysis as this is a highly exogenic process (Han *et al*., 2016; Hatting *et al.*, 2017).

2.5.2 Fat Metabolism

The liver plays a crucial role in fat synthesis and metabolism as illustrated in the lipid pathway shown in Figure 2.5**,** including fatty acid catabolism, fatty acid synthesis, ketogenesis (synthesis of ketone bodies), cholesterol synthesis and lastly synthesis of other lipids (Lavoie and Gauthier, 2006). All these pathways converge at acetyl-CoA. Triacylglycerol contains fatty acids attached to a glycerol backbone. Fatty acids are then

broken down into two and three carbon intermediates that feed into several lipid pathways.

Post-prandially triacylglycerol, derived from fats in food, undergoes lipolysis in a series of processes to produce fatty acids and glycerol (Rui, 2014). During this process fatty acids are esterified to triacylglycerol. In contrast, during starvation fatty acids undergo beta-oxidation in the liver cell mitochondria producing acetyl CoA (Nguyen *et al*., 2008). The liver also provides energy through oxidation of fatty acids from proteins and carbohydrates, resulting in a formation of acetyl CoA.

Acetyl CoA produced from the above mentioned pathways undergoes different processes according to the need of the body, which is integrated into the citric acid cycle and oxidized to produce energy (Nguyen *et al*., 2008). It also synthesizes cholesterol, phospholipids and lipoproteins (Tall, 2008). Lastly, acetyl CoA is used to produce ketone bodies through ketogenesis which acts as fuel for muscle and adipose tissue when blood glucose levels decrease (Puchalska and Crawford, 2017). However, in excess glucose levels, acetyl CoA is converted to fatty acids in a process called lipogenesis (fatty acid synthesis) and is stored primarily in the adipose tissue, but also in the liver and muscle (Ipsen *et al.*, 2018).

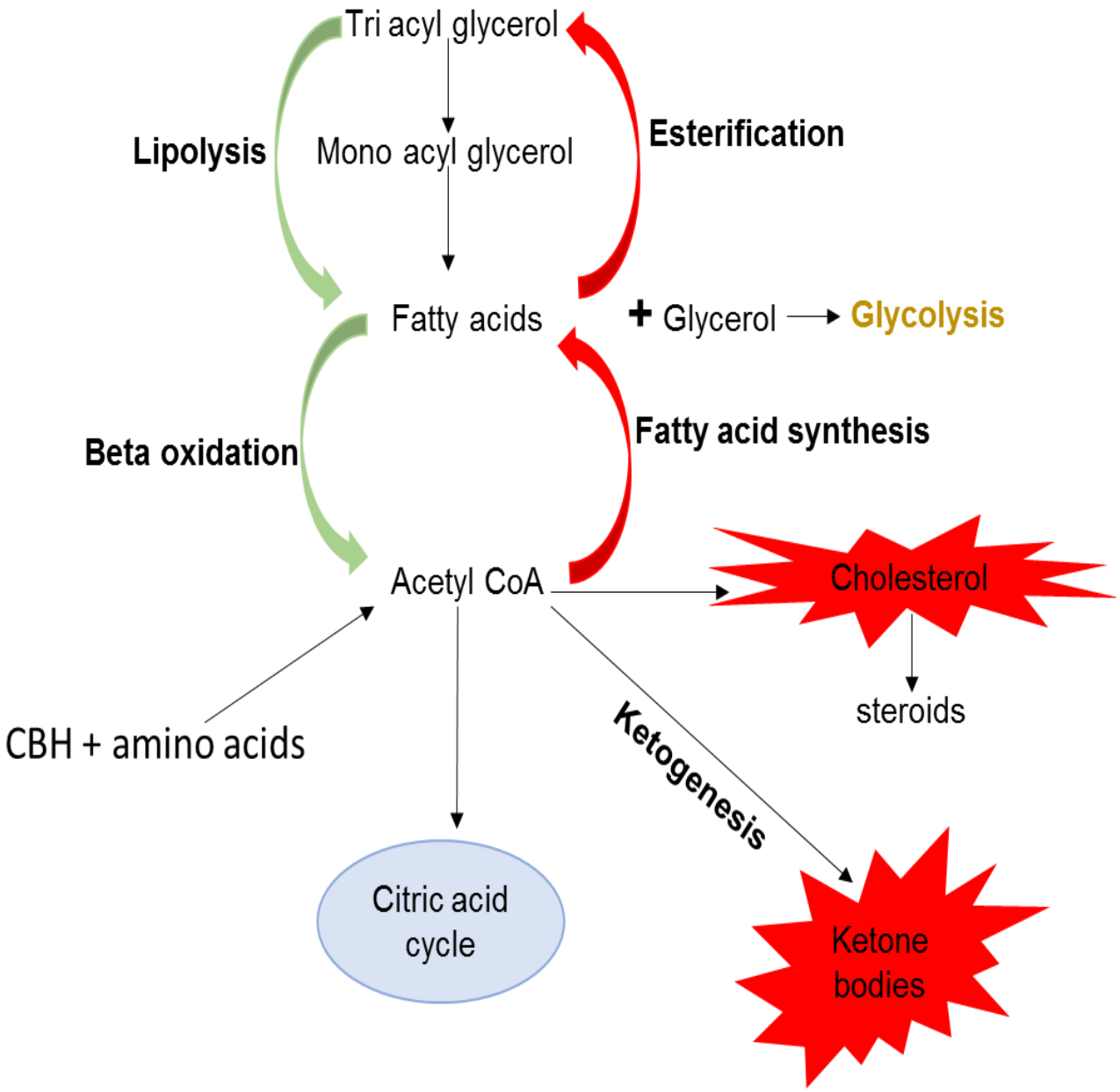

Figure 2.5 Illustration showing role of liver in fat metabolism.

Illustration adapted from (Ipsen *et al.,* 2018). After a fat containing meal, fatty acids and glycerol are produced via lipolysis, glycerol goes to glycolysis and the fatty acids undergo beta oxidation to yield acetyl CoA, which then can undergo several processes depending on the requirement of the body at that moment.

2.5.3 Protein Metabolism

Liver cells are responsible for the synthesis of most plasma proteins as well as non-essential amino acids (Zhou, Xu and Gao, 2015). The liver also plays a pivotal role in deamination of amino acids before conversion into carbohydrates or fats. The deamination process results in the formation of large quantities of ammonia which is removed by the liver through the formation of urea (Kraft *et al.*, 2017).

2.5.4 Other Metabolic Functions of the Liver

In addition to the above-listed functions, the liver participates in detoxification by clearing the blood of drugs and other poisonous substances. Drug metabolism primarily takes place in the liver and secondarily, in the lungs or the gut. The fact that most drugs get metabolized in the liver makes the liver a vital organ. The drug-metabolizing enzymes cytochrome (CYP) P450 are abundant in the liver because of its location between the gastrointestinal tract and the systemic circulation. Additionally, different enzymes metabolize different drugs (Singh, Sharma, and Alam, 2018).

Orally administered drugs get metabolized in the liver before they reach the systemic circulation, reacting with cytochrome P450 (heme-containing) enzymes. This phenomenon is known as first pass metabolism, characterized by oxidation (drug becomes electrophilic), reduction (drug becomes nucleophilic through reductase enzymes including aldo-keto reductases) and hydrolysis (the addition of water across a bond resulting in a more water-soluble metabolite) (Schonborn, 2010). The drug metabolism begins with a hydrophobic drug so the main aim of first pass or phase one metabolism is to produce a more hydrophilic molecule to be easily removed from the body. (Arshad, Butt, and Ijaz, 2018).

The drug then undergoes the phase II reaction called conjugation, by the addition of small polar molecules to the drug, to increase polarity. The conjugation reaction uses an enzyme, transferase, to transfer the large polar molecule called a co-factor to the drug,

while glucuronic acid adds a significant amount of hydrophilicity to the molecule facilitating its excretion process (Schonborn, 2010). Another popular reaction is glutathione conjugation which results from the addition of a glutathione molecule to an electrophilic substrate. Being a nucleophile, glutathione generally acts to detoxify electrophiles. Glutathione-s-transferase is the enzyme responsible for the reaction of glutathione with electrophiles like epoxides and halides. After conjugation, the product is excreted as mercapturic acid in the urine.

2.6 Definition of Non-Alcoholic Fatty Liver Disease

Non-alcoholic fatty liver disease (NAFLD) is the cluster of conditions that occur as a consequence of excess deposition or accumulation of hepatic fat greater than 5% of liver weight and is unrelated to alcohol consumption or viruses (Antonucci *et al*., 2017; Yoneda *et al.*, 2008). People suffering from metabolic dysfunctions are more susceptible to develop NAFLD (Genel *et al*., 2015).

2.6.1 Non-Alcoholic fatty liver disease background

Non-alcoholic fatty liver disease mutually affects a large proportion of people with obesity and/or diabetes (Kim *et al.*, 2012; Boursier *et al.*, 2016) and includes a spectrum of diseases which was initially dominant in the prosperous industrialized Western countries (Albhaisi and Sanyal, 2018). In simple terms, due to overnutrition, triglycerides are stored and build up in the liver. Non-alcoholic fatty liver disease is a reversible condition that can progress to dangerous irreversible stages, such as liver dysfunction and scarring. Although generally regarded as a benign condition, NAFLD sometimes progresses to hepatic carcinoma (Trauner, Arrese, and Wagner, 2009).

Obesity and type 2 diabetes have been well-known as mutual risk factors for NAFLD and cardiovascular disease. The elevated levels of inflammatory cytokines and circulating free fatty acids in obese individuals account for most of the liver lipids in NAFLD (Berlanga *et al*., 2014). NAFLD can be considered as the hepatic manifestation of the metabolic

syndrome and is particularly associated with insulin resistance, obesity and irregularities of glucose and lipid metabolism (Byrne and Targher, 2015; Martin-Rodriguez *et al.*, 2017). The increase in the incidence of NAFLD is not only associated with liver-related morbidity and mortality, but evidence shows NAFLD to be a multisystem disease, affecting numerous organs and other pathways (Albhansi, Issa and Alkhouri, 2018).

2.6.2 Hepatic *de novo* lipogenesis

Hepatic *de novo* lipogenesis (DNL) is an enzymatic pathway for the production of fatty acids from acetyl-CoA within the liver, driving lipid synthesis and storage by hepatocytes. In this context, DNL plays a role in a variety of metabolism-centered diseases and the most common of these is the link between NAFLD and the metabolic syndrome (Kawano and Cohen, 2013).

2.6.3 The biochemical processes of *de novo* lipogenesis

Energy homeostasis is primarily sustained by the liver, regardless of the nutritional state. In a well-fed state, glucose is converted to pyruvate through the process of glycolysis, which then enters the Krebs cycle to produce energy (Koo, 2013). In the Krebs cycle, citrate is produced and taken to cytosol where it is converted to acetyl-CoA by an enzymatic reaction facilitated by ATP citrate lyase. Acetyl-CoA is formed into malonyl CoA by acetyl-CoA carboxylase 1 (ACC1). Malonyl CoA is a negative regulator of fatty acid catabolism and can be recycled to acetyl-CoA and carbon dioxide by malonyl CoA decarboxylase (MCD). ACC is inhibited by glucagon, epinephrine, palmitoyl-CoA as well as AMP, while activated by insulin, citrate and SREBP (Sanders and Griffin, 2015).

Fatty acid synthesis occurs in a protein complex called fatty acid synthase, composed of different moieties, one being acyl carrier protein (ACP) which has a vitamin B5 derived component called phosphopantetheine (Berlanga *et al.*, 2014). Another important binding point is through cysteine residue. Both acetyl-CoA and malonyl-CoA bind to the fatty acid synthase protein complex. The acetyl group from acetyl-CoA undergoes an enzymatic reaction and takes two carbons from malonyl-CoA to form butyryl-CoA (four carbon

molecule), releasing the remaining carbons from malonyl-CoA as CO_2 (Sanders *et al*., 2018) i.e. malonyl CoA acts as a two-carbon donor for the elongation of the substrate acyl chain.

Two carbons from malonyl-CoA are added to butyryl-CoA in a condensation reaction (Von Wettstein-Knowles *et al.*, 2006) which results in the addition of a ketone group to the growing carbon chain. This chain undergoes reduction using NADPH to reduce the ketone group to a hydroxyl group and is removed by the dehydration reaction (Ameer *et al*., 2014). Further reduction occurs to form a six carbon molecule which then undergoes another cycle, extending the acyl chain by two carbons each cycle and producing a fatty acid such as palmitate (C16:0) (Solinas, Borén, and Dulloo, 2015). Palmitic acid is either desaturated to palmitoleic, which can also form oleic acid, or elongated to stearic acid (C18:0). All these fatty acids are important intermediaries for triglycerides. In hepatic steatosis, the additional oleic acid is a product of *de novo* fatty acid synthesis (Harada *et al*., 2007).

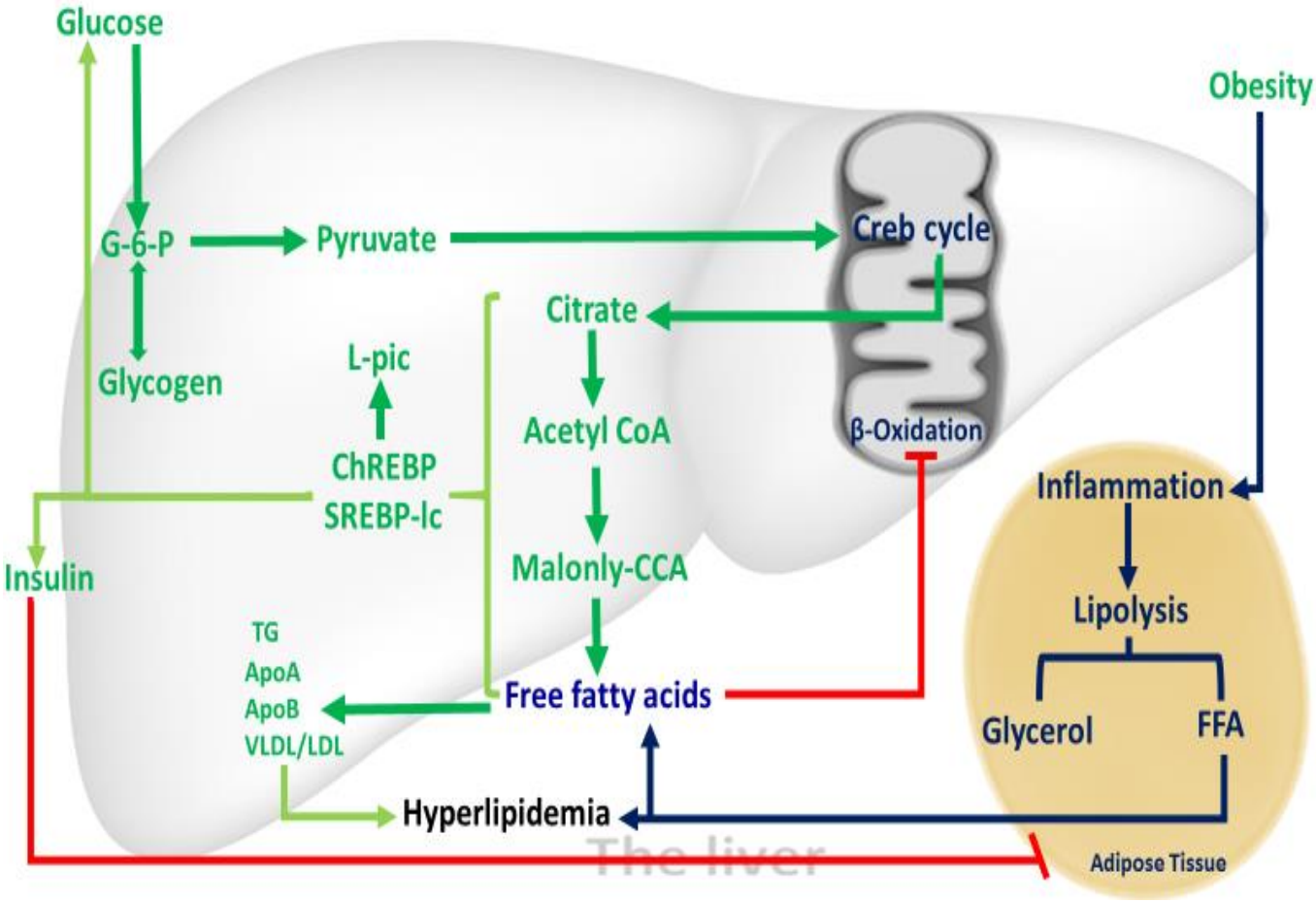

Figure 2.6 The biochemical process of *de novo* lipogenesis.

The process begins with glycolysis producing pyruvate. Pyruvate then moves into the mitochondria of the cell where it is acted on by another enzyme and converted to acetyl-CoA. Acetyl-CoA moves into a second metabolic pathway, TCA, producing intermediate molecule citrate. Citrate is transferred into cytosol by citrate transport protein that is then acted on by ATP acetyl-CoA lipase (ACL) which uses energy and biotin to convert citrate back to acetyl-CoA. ACC converts acetyl-CoA to malonyl-CoA, which has 2 primary reactions i.e. to propagate the synthesis of lipids and to inhibit a protein gate called CPT1, supressing beta oxidation. Three fatty acyl-CoAs are bound to glycerol backbone to form one TG. TG combines with apoB and back into VLDL for secretion into blood stream.

2.7 Regulation of hepatic *de novo* lipogenesis

In the liver, DNL is provoked by high levels of insulin and glucose (Linden et al., 2018). The mechanism whereby lipogenesis is activated in the liver, is by transcription factors including sterol regulatory element-binding protein (SREBP), carbohydrate response element-binding protein (ChREBP) and peroxisome proliferators-activated receptor-gamma (PPAR-γ) (Ma, Robinson, and Towle, 2006). These three bHLH-Zip transcription

factors all participate in the progression of hepatic steatosis (Ayisi, Yamei, and Zhao, 2017).

2.7.1 Sterol regulatory element-binding protein (SREBP)

Srebp is transcriptionally activated by insulin (Bhatt *et al.*, 2011). Hence, high levels of insulin activate SREBP which in turn activates the other lipogenic genes to trigger lipogenesis (Wang *et al.*, 2015). SREBP is one of three isomers under the transcription factors classified as basic-helix-loop-helix-leucine zipper (bHLH-ZipZ) (Song, Xiaoli, and Yang, 2018). *De novo* lipogenesis commences through enzymatic activation of acetyl-CoA carboxylase 2 (ACC2), an isomer of acetyl-CoA carboxylase (ACC), which generates malonyl-CoA at the mitochondrial membrane. Elevated levels of malonyl-CoA result in reduced beta-oxidation caused by inhibition of carnitine palmitoyltransferase-1 (CPT-1), an enzyme that delivers fatty acids into the mitochondria to be oxidized (Yanqiao Zhang, Yin, and Hillgartner, 2003). SREBP-1c is the principle gene in triglyceride synthesis. Therefore, upregulation of SREBP is concomitant with the occurrence of NAFLD (Zang 2016). The stimulatory effects of insulin on SREBP-1c is facilitated by the phosphoinositide 3-kinase (PI3K)-dependent pathway (Yang *et al*., 2018).

2.7.2 Carbohydrate response element-binding protein (ChREBP)

In contrast to SREBP1, ChREBP is activated by high levels of glucose in hepatocytes (Linden *et al*., 2018). This is achieved by the binding of ChREBP to an E-box motif located on the promoter of the liver type pyruvate kinase (L-PK) (Uyeda and Repa, 2006). Liver type pyruvate kinase regulates glycolysis by converting phosphoenolpyruvate to pyruvate, which is then integrated into the Krebs cycle producing citrate, an intermediate of acetyl-CoA used for fatty acid synthesis (Linden *et al.*, 2018; Uyeda and Repa, 2006). Thus, activation of L-PK promotes both glycolysis and lipogenesis (Benhamed *et al*., 2004).

2.7.3 Peroxisome proliferators-activated receptor-gamma PPAR-γ

A third transcriptional factor is peroxisome proliferator-activated receptor-gamma (PPAR-γ) which is a member of the nuclear hormone receptor superfamily essential for normal adipocyte differentiation (Han *et al*., 2017). In the presence of insulin resistance and hepatic steatosis, PPAR-γ levels in the liver are elevated (Ables, 2012). In comparison with other transcriptional factors, the exact molecular role of PPAR-γ in stimulating triglycerides deposition in the liver is not fully elucidated (Cave *et al.*, 2018). Despite this, various studies demonstrate that SREBP-1 activates PPAR-γ by stimulating the production of an activating ligand for the nuclear receptor (Browning and Horton, 2004).

2.7.4 The role of AMP-activated protein kinase in hepatic steatosis

Activated protein kinase (AMPK) is a heterotrimeric, fuel-sensing and energy detector enzyme found abundantly in all mammalian cells (Son *et al*., 2013). In the presence of high energy levels, AMPK promotes catabolic pathways for energy expenditure such as glucose uptake and β-oxidation while reducing lipogenesis (Woods *et al*., 2017).

2.8 Epidemiology of NAFLD

Non-alcoholic fatty liver disease constitutes a fast increasing burden to society (Chalasani *et al*., 2018). Statistics for NAFLD prevalence is lacking as confirmatory diagnosis methods are invasive and expensive. It has been estimated that the incidence of NAFLD worldwide is approximately 24-25%. However, South America exhibited the highest incidents of NAFLD with 31% (Araújo *et al*., 2018). According to Araújo et al., (2018), these statistics are likely to accelerate as NAFLD prevalence is parallel to obesity incidence. NAFLD was initially dominant in adults. In contrast, recent studies show that children are also affected by NAFLD (Takahashi and Fukusato, 2014). A detailed and better understanding of NAFLD epidemiology has drawn researchers' attention in identifying approaches to NAFLD prevention and treatment.

2.9 Risk factors for developing the non-alcoholic fatty disease (NAFLD)

Obese individuals are more prone to develop steatosis as excess body weight and liver fat content exhibits a close direct relationship, linked by impaired insulin action (Huh *et al.*, 2017). NAFLD is experienced more commonly in the elderly i.e. people over 50 years. People suffering from hypertension also have an increased risk of developing NAFLD (Alam *et al*., 2018). Lastly, medical conditions such as rapid weight loss, undernourishment and medications like tamoxifen (solt amox) and methotrexate (trexall) (Adams, Angulo, and Lindor, 2005) also contribute.

2.10 Progression and stages of NAFLD

The full spectrum of NAFLD ranges from simple reversible fat deposits to more severe irreversible stages (Jiang, Robson and Yao, 2012). In hepatic steatosis, there is abnormally large amounts of fats that build up in hepatocytes and at this stage the majority of patients experience no problems. However, if the deposit of fats becomes severe, non-alcoholic steatohepatitis (NASH) occurs, which is an inflamed state (Dyson, Anstee and Mcpherson, 2014). Over time, when this inflammatory condition continues, liver cells die and fibrosis scar tissue gradually forms, leading to dysfunction of the liver, an irreversible liver stage called cirrhosis. (Dyson, Anstee and Mcpherson, 2014). Representation of NAFLD progression to NASH is shown in Figure 2.7.

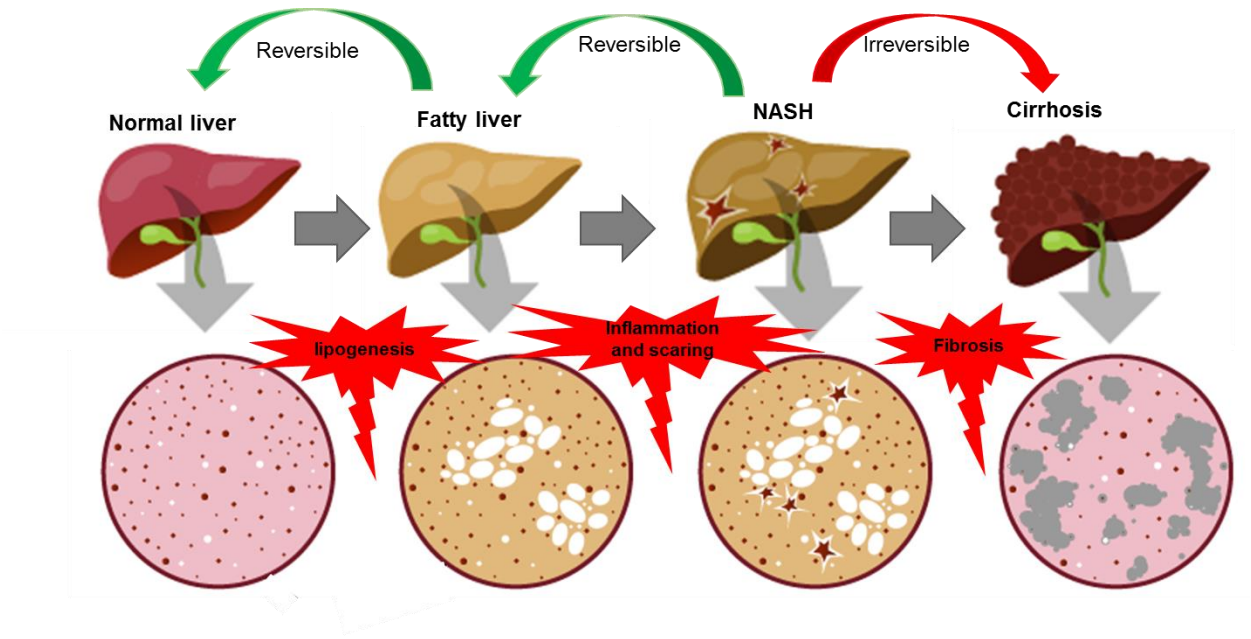

Figure 2.7 Disease progression of NAFLD showing how this disease progresses.
The disease progress from simple steatosis which is benign, to a serious life-threatening hepatocellular carcinoma (HCC). Both NASH and simple steatosis are reversible. However, if left untreated, NASH can progress to irreversible fibrosis, leading to cirrhosis and high risk of hepatocellular carcinoma.

For NAFLD to progress to NASH, Day. (2002) proposed a dual hit mechanism. He proposes that unaccompanied fat deposit is harmless to liver cells, however, the secondary insults such as inflammation and hormonal inequity are potent drivers for the "second hit" phenomenon theory (Dowman, Tomlinson and Newsome, 2009). NAFLD patients remain asymptomatic for years as long as a sufficient number of liver cells remain for the liver continue to function and this character has added to an under-appreciation of its potential dangers.

2.11 Development of non-alcoholic steatohepatitis

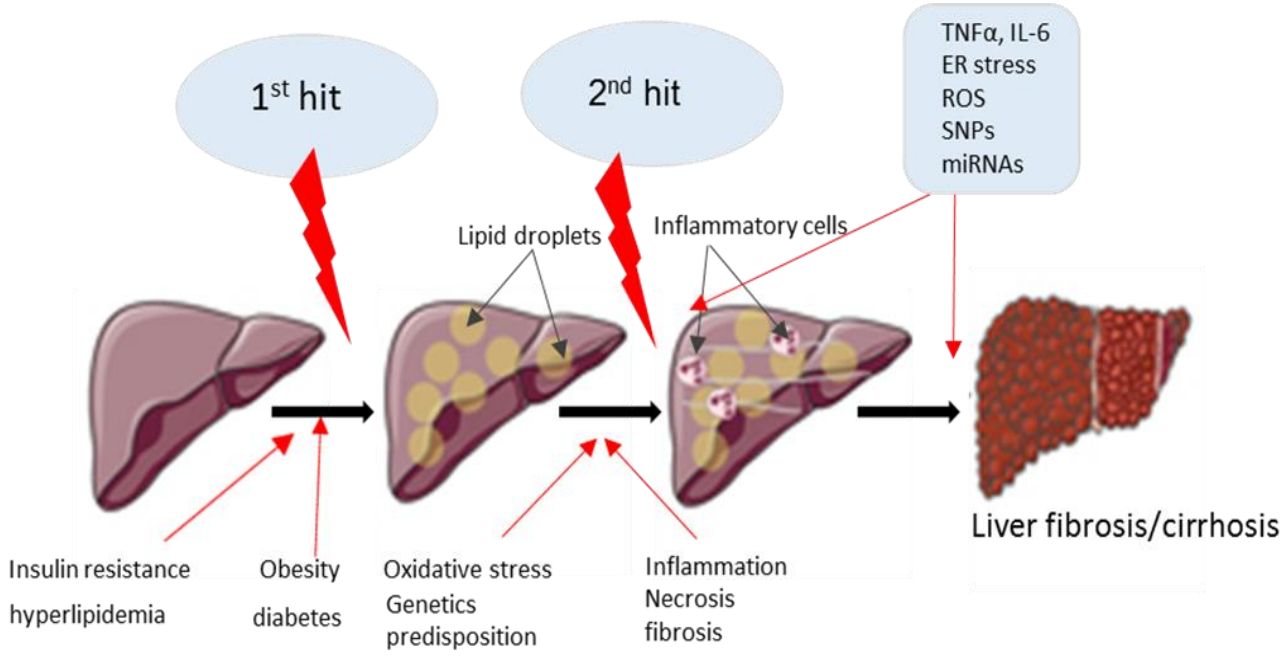

Figure 2.8 Proposed mechanism for the development of non-alcoholic steatohepatitis

adapted from (Kitade and Chen, 2017).

The pathophysiology of NAFLD is complex and multifactorial. However, the specific mechanism of NAFLD development is not clear. Insulin resistance, T2D and obesity, oxidative stress as well as inflammation appear to play a significant role (Takahashi and Fukusato, 2010), while in the adipose tissue, an enzyme hydrolyzing triglycerides is significant.

Under normal conditions, when insulin binds to its receptors, the activity of hormone sensitive lipase (HSL) is reduced. With insulin resistance, the intracellular signal is attenuated and as a result of this, HSL is not suppressed, leading to its increased activity and hydrolysis of triglycerides and increasing glycerol and free fatty acid release from the adipocytes into the circulation towards the liver. Free fatty acids are then taken up by the

liver where hepatocytes channel free fatty acids into secretory pathways. In the presence of hyperinsulinemia, increased synthesis of TG (esterification) in the liver with a decrease in beta oxidation occurs (Kitade and Chen, 2017).

Over time, fat deposits in the hepatocytes are degraded by reactive oxygen species (Azam *et al*., 2016). This pairing of radical species leads to cell death, an event that produces inflammation leading to a stage of NAFLD called steatohepatitis.(Hijona *et al*., 2010).

2.12 Diagnosis

2.12.1 Signs and symptoms of non-alcoholic fatty liver disease

Normally, the majority of patients with NAFLD encounter no symptoms as initially the disease is asymptomatic. However jaundice, ascites, nail changes (e.g. clubbing) splenomegaly and abdominal pain may occur at a later date (Adams, Angulo, and Lindor 2005; Khoonsari *et al*. 2017; Tian *et al*., 2016).

2.12.2 Imaging studies

Diagnosis of NAFLD can be made with imaging studies using non-invasive imaging techniques, including ultrasonography (least expensive), computed tomography and magnetic resonance imaging. These techniques are used to look for fatty infiltrates (Sass, Chang, and Chopra, 2005).

2.12.3 Liver Biopsy

A liver biopsy is a procedure where a small piece from the liver is removed and examined histologically (Nalbantoglu and Brunt, 2014). However, given the lack of effective medical treatment for patients with NAFLD, there has been a reasonable hesitation to perform a liver biopsy with the simple purpose of confirming the diagnosis (Rinella *et al*., 2014). Nevertheless, the liver biopsy remains not only the best diagnostic tool for confirming

NAFLD, but also the most sensitive and specific means of providing important prognostic information (Gunn and Shiffman, 2018).

2.13 *In vivo* models used for NAFLD

Animal models play a significant role in expounding the mechanism of NAFLD and are used to study possible treatments for NAFLD (Oligschlaeger, 2017). Commonly C57BL/6 mice and Wistar and Sprague Dawley rat strains are used because they are more prone to developing obesity and its related metabolic disorders (Kim *et al.*, 2017; Fengler, Macheiner and Sargsyan, 2016). Various models, including nutritional and chemically induced NAFLD, as well as genetic models of NAFLD are used (Van Herck, Vonghia and Francque, 2017).

2.13.1 Dietary models

A study conducted in the United States by Anderson et al. (2011) demonstrated a strong link between obesity and fast food consumption. Obesity and diet consequently leads to the development of hepatic steatosis in that most scenarios resemble NAFLD. The C57BL/6 mice appear to be more responsive to obesogenic diets, hence they are the most frequently used strain in NAFLD experiments (Hansen *et al*., 2017). These dietary mouse models are designed to mimic hepatic and metabolic conditions occurring during the development of human NAFLD.

2.13.1.1 Fructose

Foods rich in fructose have been related to the development of obesity and NAFLD (Kohli *et al.*, 2010). Fructose is a ketonic monosaccharide present in various fruits. Metabolism of fructose predominantly takes place in the liver and excessive intake leads to lipogenesis, fatty liver as well as insulin resistance (Ter Horst and Serlie, 2017). Hence, fructose is often supplemented in drinking water (10%) for animal models of steatosis (Kohli *et al.*, 2010). Studies conducted by Takahashi, Soejima and Fukusato, (2012) on hepatocytes of Wistar rats fed a diet enriched with 70% fructose for five weeks, found that

the rats developed macrovesicular steatosis (Figure 9A) and intralobular inflammation (Figure 2.9B) when contrasted to rats fed a normal diet. Based on this pathological observation, fructose-induced models can be considered as good models of NAFLD.

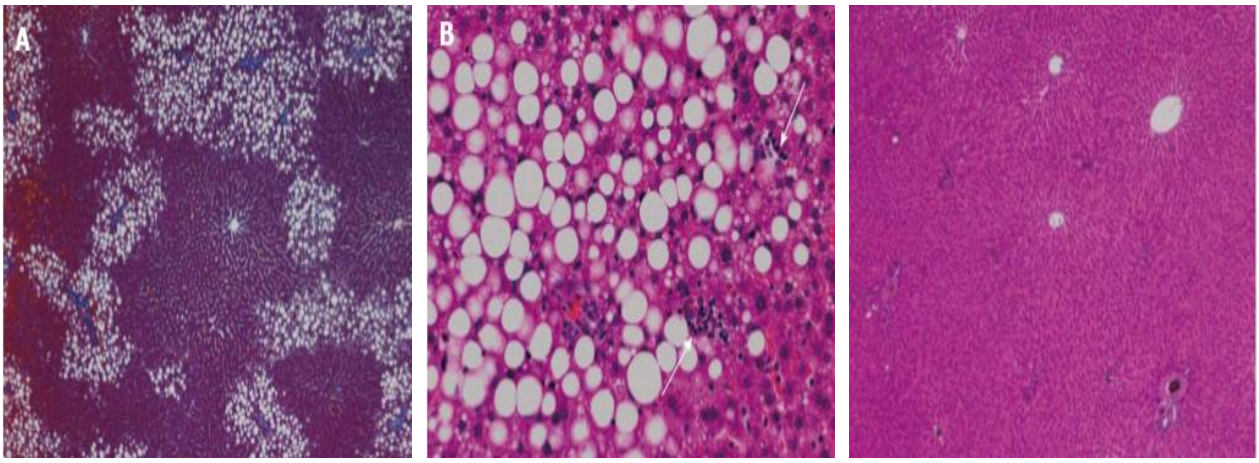

Figure 2.9 Liver histology of untreated Wistar rats fed a 70% fructose-enriched diet for 5 weeks
Images Stained by aza stain at 40x magnification (A), representation of microvacuolar and macrovesicular changes stained by haematoxylin and eosin (H&E) at 200x magnification and (B) after treatment with plant leaf extract (H&E) at 40x magnification.

2.13.1.2 Methionine and Choline Deficient Diet

An approach to induce hepatic steatosis is to provide the additional second hit to the hepatic metabolism. The methionine and choline-deficient diet contains high sucrose and 10-20% fat content (kcal) but lacks certain amino acids, essentially methyl donor and choline, which are crucial for hepatic beta oxidation and exportation of triglycerides through very low-density lipoproteins. The impairment of beta oxidation and VLDL production results in hepatic fat deposits (Fengler, Macheiner and Sargsyan, 2016; Van Heck,Vanghia and Francque, 2017).

In the liver, under normal conditions, triglycerides are exported by very low-density lipoproteins facilitated by phosphatidylcholine. Deficiency of choline (a precursor for the *de novo* synthesis of phosphatidylcholine) favors fatty liver as triglycerides are not

exported from the hepatocytes (Ramadori *et al*., 2015). MCD does not only impair VLDL secretion but also suppresses β-oxidation (Lau, Zhang and Yu, 2017). This approach is preferable to the obesogenic diets specifically when studying the late stages of NAFLD such as fibrosis (Hansen *et al*., 2017). The disadvantage of this model is the resultant hypophagia and hypercatabolism resulting in weight loss which is usually 20-40% (Koppe and Green, 2003; Takahashi, Soejima and Fukusato, 2012).

2.13.1.3 High-Fat Diet

The free fatty acids derived from a high-fat diet lead to increased accumulation of hepatic triglycerides which contribute to the development of obesity (Lau, Zhang and Yu, 2017). In rodents, a high-fat diet consisting of 45-75% of its calories derived from fat, was compared to a standard diet with less than 10% of its calories as fat (Van Heck,Vanghia and Francque, 2017). Using this diet, induction of hepatic steatosis resulted in histopathological changes resembling human NASH (Ramadori *et al.*, 2015; Lau, Zhang and Yu, 2017). Feeding with HFD diet renders the species predisposed to metabolic alterations which could be the result of the altered mRNA gene expression (Chiu et al. 2017). Based on this, the diet closely resembles pathogenesis of human NAFLD rather than genetic models and methionine and choline-deficient diet (Chiu *et al.*, 2017; Takahashi, Soejima and Fukusato, 2012).

A study conducted by Buettner et al. (2006) investigated the effects of four different high-fat diets (lard, olive oil, coconut oil and fish oil) on male Wistar rats. Liver histology was similar for the different fat diets, revealing only microvesicular steatosis with no inflammation or fibrosis. Similar effects were also noted on mRNA expression, which showed up-regulation of lipogenic genes such as SREBP-1c

2.13.2 Chemical models

Chemically-induced models are usually utilized for exploring hepatic fibrosis advancement and regression. Several chemicals have been used to induce hepatic

steatosis, including streptozotocin and carbon tetrachloride (CCl_4) (Castro and Diehl, 2018). Streptozotocin (STZ) is generally regarded as a pancreatic beta cell specific toxin, used to induce diabetes in various rodent models. However, STZ also affects other cells expressing the Glut-2 glucose transporter, such as hepatocytes, and therefore inadvertently causes liver damage in a dose and time-dependent manner (Eleazu *et al.*, 2013; Meagher *et al.*, 2007; Castro and Diehl, 2018).

Another chemical hepatotoxic model includes oral administration of carbon tetrachloride (CCl_4) which causes excessive oxidative stress in the hepatocytes through cytochrome P450 2E1 facilitated conversion of CCl_4 to CCl_3 (carbon tri chloride) which is a free radical and triggers oxidative necroinflammation. CCl_3 enters the mitochondria and causes lipid peroxidation as it steals electrons from the lipids which results in the breakdown of the cell walls of the endoplasmic reticulum. (Tsai *et al.*, 2015; Van Heck,Vanghia and Francque, 2017). It's also blocks apolipoprotein production which is required for binding triglycerides with lipids. In the absence of apolipoproteins, this binding does not occur, leading to hepatic steatosis.

2.13.3 Genetic models of obesity and diabetes

2.13.3.1 Ob/ob mice

Lepob/Lepob (*ob/ob*) mice are leptin deficient caused by a spontaneous mutation of the leptin gene *Ob* (*Lep*). Leptin is also identified as the *Ob* gene positioned at chromosome number 7. The leptin resistant mice are called *ob/ob* mice. Leptin is an adipocyte-derived satiety, anorexigenic as well as peptide hormone secreted in relative amounts to body fat mass (Facey, Dilworth, and Irving, 2017).

Leptin inhibits fat synthesis and stimulates beta-oxidation of fat in adipose tissue and reduces appetite and increases energy expenditure by activating its receptors in various regions of the central nervous system (CNS), especially in the hypothalamus and brainstem (Pocai *et al*., 2005). A deficiency in leptin leads to morbid early-onset obesity

(Fatima et al. 2011), due to hyperphagia, hyperlipidemia, and reduced energy expenditure (Francisco *et al*., 2018). This model does not develop steatohepatitis unless secondary insults are activated such as manipulating their diet (Ansteen and Goldin, 2006).

A. Lean B. Obese

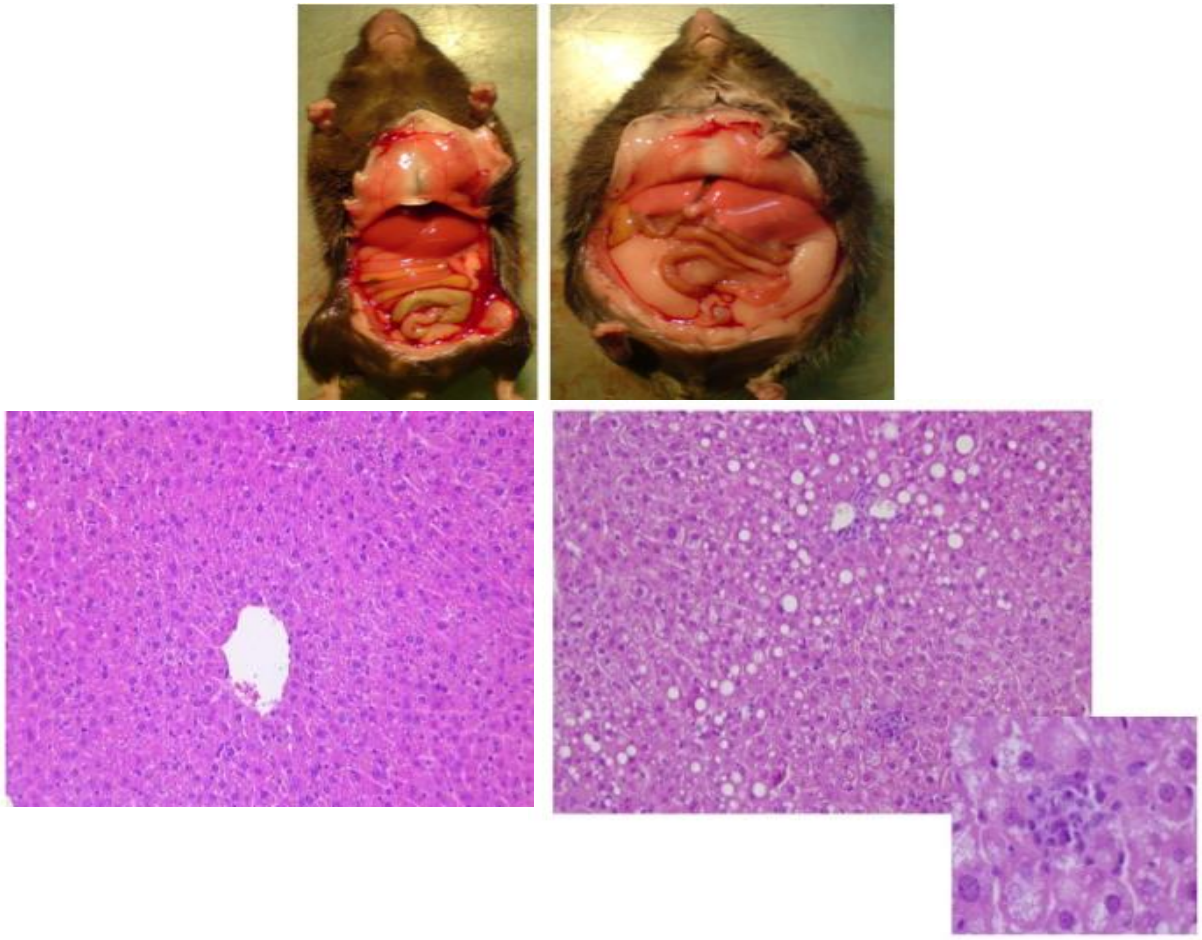

Figure 2.10 Illustrative images of a lean (C57BL/6) and an obese *ob/ob* mouse.
Hepatosteatotic changes in their liver histology is demonstrated by haematoxylin and eosin (200×) (Kanuri and Bergheim, 2013).

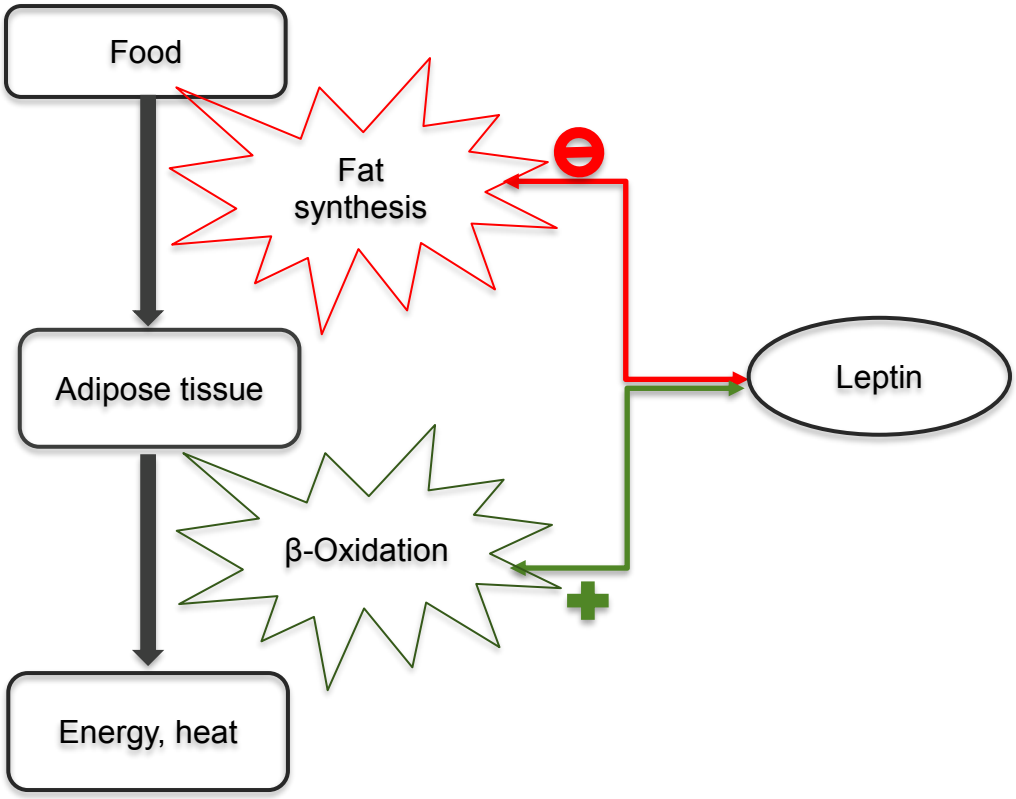

Figure 2.11 Role of leptin in energy homeostasis.
Leptin secretion is proportionate to body fat mass, as it regulates energy balance by limiting fat mass, and by controlling food intake while promoting energy expenditure (beta oxidation). Deficiency of leptin activity enhances food intake, lessens energy expenditure and fat storage.

2.13.3.1.2 *Db/db* mice

The *db/db* mice have spontaneous mutations in the *LEPR* gene encoding for the leptin receptor (*LEPR*) (Anstee and Goldin, 2006; Wang, Chandrasekera and Pippin, 2014). Leptin receptors are predominantly located in the hypothalamus of the brain. Therefore, although leptin is available in abundance in *db/db* mice, due to the mutation of the receptor, its signal is not translated into the cells, and particularly in the hypothalamus, the deficiency in leptin receptor leads to unrestrained feeding and excessive fat storage (Ortiga-Carvalho, Oliveira, and Pazos-Moura, 2002). As a result, this strain is characterised by hyperphagia, obesity and become spontaneously diabetic. The *db/db*

mice are good research models for studying NAFLD. Late stages of NAFLD can be induced by provoking secondary insults using the MCD or high-fat diet (Ka *et al.,* 2017).

2.13.3.2 Atherosclerosis Models

Atherosclerosis models consist of apolipoprotein deficient (*ApoE*$^{-/-}$) mice and low-density lipoprotein receptor deficient (*Ldlr*$^{-/-}$) mice (Van Herck, Vonghia and Francque, 2017). These models lack the LDL receptor gene which is required for the normal regulation of cholesterol (Mailleux *et al*., 2017). Its core function is to eliminate excess cholesterol present in low density lipoproteins from plasma. Therefore, low-density lipoprotein receptor-knockout mice are predisposed to develop hypercholesterolaemia, atherosclerosis and obesity, which are risk factors for NAFLD development (Ma *et al*., 2012).

2.14 *In vitro* models for fatty acid metabolism

Over the past decades, cell lines have gained growing attention as models for studying animal and human biology. Numerous cell models/types have been employed to study liver metabolism (Brandon *et al*., 2003). Fully characterized *in vitro* models are required to ascertain a suitable environment to assess the development of the disease (Poteser, 2017). Therefore, this section of the thesis focuses on the different types of models that could be used to study liver fatty acid metabolism depending on the objectives of the study.

2.14.1 Primary cell culture

Cells that are directly isolated from tissues or organs are referred to as primary cells (Van de Bovenkamp *et al*., 2007). This approach was discovered in the 1960s (Howard *et al*., 1967). Due to the complexity of its methodology, it was only applied in the 1970s. The downfall about this model is its availability, phenotypic instabilities, cryopreservation techniques and its lifespan, which is generally only 4 hours after isolation. The use of special culture methods such as embedding in matrix can extend the primary cell lifespan

and its phenotype stability up to a number of days (Mathijs *et al.*, 2009; Brandon *et al.*, 2003).

In vitro hepatocytes exhibit normal *de novo* pathways based on their response to external stimulus, such as fatty acid supplementation, leading to excessive triglyceride accumulation and secretion (Parafati *et al*., 2018). The cells used include hepatocytes isolated directly from NAFLD patients as well as Kupffer cells, stellate cells and iNKT cells. They are usually used as they imitate the *in vivo* setting (Kanuri *et al*., 2013). Hepatocytes have also been isolated from rodents and have similar limitations to human hepatocytes (Guillouzo, 1998). However isolation problems, ethical issues and limited culture time are major challenges as mentioned above (Howard *et al*., 1967).

2.14.2 Immortalized cell line

Immortalized cells, in contrast to primary cells, have been manipulated to grow and sustain a steady phenotype in culture. They can be cultured over several generations and are easy to cultivate and standardize (Green *et al*., 2017). Immortality is introduced by genetic manipulation of the primary cells. Some of these cells have been immortalized using 3T3 protocol where specific immortalized genes are transferred to induce clearly defined alterations. The disadvantage of this method is alteration of the cellular processes which might affect the pathways to be experimented. However, immortalization using gene SV40 virus large T-antigen (TAg) overcomes the downfalls of 3T3 protocol. Cell lines immortalized using this method have been shown to be advantageous (May, Hauser, and Wirth 2004).

2.14.2.1 Liver tumour cell line

Hepatoma cells are spontaneously immortalized having undergone genetic manipulation to resist senescence. These are the most commonly used hepatic cell lines used to investigate the effects of extracts and anti-cancer drugs due to their stability (Kaur *et al*., 2018). HepG2 cells are differentiated from a cell line derived from 15-year adolescent

liver tissue expressing hepatic carcinoma and are commonly used as they exhibit several liver-specific characteristics without any alterations.

Wang et al., (1988) demonstrated that HepG2 cells' secretion of dense triglycerides more closely resemble LDL, instead of VLDL, lipoproteins seen in human hepatocytes, and this accounts for the high susceptibility for fat accumulation in HepG2 cells. C3As are a sub-clonal derivative of the HepG2 cell line and mostly share its characteristics. Vendel Nielsen et al., (2013) demonstrated that genes participating in cholesterol metabolism were highly upregulated in HepG2 cells by elaidic acid

2.14.3 Co-culture models

Many *in vitro* approaches have been established where multiple cell types are cultured simultaneously to imitate *in vivo* settings. Kupffer cells, macrophages found in the sinusoids of the liver, play a major role in hepatic injury and the sepsis response. However, there have been difficulties encountered regarding their adherence during culturing (Alabraba *et al*., 2007). Kupffer cells have been shown to be involved in improving lipid metabolism. Hence, simultaneous incubation of Kupffer cells with hepatocytes might be of great use to reduce triglyceride accumulation (Nishikawa *et al*., 2008). Endothelial cells play a vital role in regeneration and inflammation. Their core function is to exchange lipids between blood and sinusoidal regions of the liver and, as a result, their co-culture aids in retaining the differentiated role of hepatocytes (Bale *et al.*, 2014).

2.15 Therapeutic interventions for non-alcoholic fatty liver disease

2.15.1 Diet and lifestyle modification

Presently no medication is available to cure NAFLD. However, proper guidance and lifestyle changes contribute significantly to reversing early stages of fatty liver (Takahashi *et al.*, 2015; Sumida and Yoneda, 2017). Based on studies conducted by Bril and Cusi, (2017), this approach (diet and lifestyle modification) is considered as the primary

treatment in the management of hepatic steatosis. For this reason, it is of paramount importance to moderate lifestyle risk factors (Romero-gómez, Zelber-sagi, and Trenell, 2017).

2.15.2 Pharmacological agents

Various therapeutic agents have been intensively studied for the treatment of NAFLD. However, most of the therapeutic research focuses on treating NAFLD indirectly i.e. treating risks factors for NAFLD as listed below. (Bril and Cusi, 2017; Lomonaco *et al.*, 2013).

2.15.2.1 Insulin sensitizers

Insulin resistance is a major contributor to the pathogenesis of NAFLD (Takahashi *et al*., 2015) hence insulin sensitizers have been studied as potential therapeutic agents to target NAFLD. Among those insulin sensitizers are thiazolidinediones (TZDs) including rosiglitazone and pioglitazone. TZDs are ligands for PPAR-γ, a transcriptional factor that plays a significant role in the regulation of glucose and lipid metabolism, as well as in inflammation (Soccio, Chen and Lazar, 2014).

PPAR-γ regulates metabolic pathways in various tissues. Pioglitazone binds and activates the receptor leading to activation of the RXR receptor in the nucleus of adipocytes. This regulates gene transcription by binding to a specific DNA site, leading to an increase in tissue sensitivity to insulin and consequently increases glucose uptake in muscle and adipose tissue (Soccio, Chen and Lazar, 2014). Pioglitazone also causes a decrease in hepatic glucose production and an increase in hepatic glucose uptake (Chang, Park, and Park, 2013).

Considering the study relationship between insulin-resistance and NAFLD, any attempt to improve insulin sensitivity might be of therapeutic importance in NAFLD patients

(Mazza *et al*., 2012). Metformin is a first line anti-hypoglycaemic drug that acts by reducing energy stores of ATP, which increases the activity of the AMP-dependent protein kinase (AMPK) enzyme (Rouabhia, Milic, and Abenavoli, 2014). Activated AMPK stimulates glycogen storage in skeletal muscle, decreases hepatic glucose production, decreases blood glucose levels and finally increases tissue sensitivity to insulin (Inzucchi *et al*., 2015).

2.15.2.2 Antioxidants

Due to the existing correlation between oxidative stress and the progression of NAFLD, pharmacological agents aiming to ameliorate oxidative stress have been extensively studied. Vitamin E is a potent fat-soluble antioxidant that moderates oxidative stress in NAFLD patients. It donates a hydrogen atom from its hydroxyl group to counterbalance free radicals (Hadi, Vettor, and Rossato, 2018). A study conducted by Sanyal et al*.,* (2010) showed that vitamin E improved histological features by 37% in patients receiving vitamin E. However, it had no effect on portal inflammation.

2.15.2.3 Lipid-lowering drugs

Altered hepatic cholesterol metabolism plays a crucial role in the pathogenesis of NAFLD (Arguello *et al*., 2015). Hence this has been another targeted approach for treating NAFLD. The production of cholesterol is facilitated by HMG-CoA reductase, an enzyme which converts HMG-CoA to mevalonate. Statins are lipid-lowering agents that inhibit HMG-CoA reductase, lowering the production of cholesterol by the liver. Due to the absence of persuasive histological data, statins have not been fully considered as a therapeutic agent to treat NAFLD (Cioboată *et al*., 2017). Based on this, statins are not recommended as a treatment for NAFLD. Additionally, side effects have been noted with consumption of statins including liver and muscle injury (Pappachan *et al*., 2017).

2.15.2.4 Pentoxifylline

Obesity and insulin resistance are the leading causes of NAFLD. Pro-inflammatory cytokines such as TNF-α play a critical role in both obesity and insulin resistance (Kang *et al*., 2016). Pentoxifylline is a methylxanthine compound and a non-selective phosphodiesterase inhibitor that produces vasodilatory effects (Ye *et al*., 2016). Pentoxifylline exhibits its pharmacological role by inhibiting the synthesis of TNF-α. A study conducted by Du et al. (2014) shows that pentoxifylline reduces plasma TNF-α and IL-6 levels. It also significantly reduces ALT and AST in patients with NASH compared to the placebo or UDCA groups.

2.15.2.5 Medicinal herb/natural products (polyphenols)

Plant-based or natural therapies are generally perceived to be safe and effective in managing metabolic disease (Malviya, Jain, and Malviya, 2010). The efficacy of herbal medicine has been extensively studied as potential therapeutic agents to ameliorate and protect against NAFLD. Generally natural products are deemed to be effective and exhibit a low risk for side effects (Ferramosca *et al*., 2017). Polyphenols, that are the plant's secondary metabolites, are frequently explored for their anti-oxidant and anti-inflammatory potential (Takahashi *et al*., 2015).

Herbal medicines, especially flavonoid-containing/centered therapeutic agents such as silybin, green tea and the isoflavones, quercetin and rutin, have antioxidant, anti-inflammatory and weight regulation properties (Van De Wier *et al.*, 2017). These properties have drawn attention to herbal medicines as potential therapeutic agents for treating NAFLD. Green rooibos has demonstrated similar properties as discussed in section 2.16.1. Hence the motivation of this study originated from the findings on herbal medicines properties.

2.16 Rooibos (*Aspalathus linearis*)

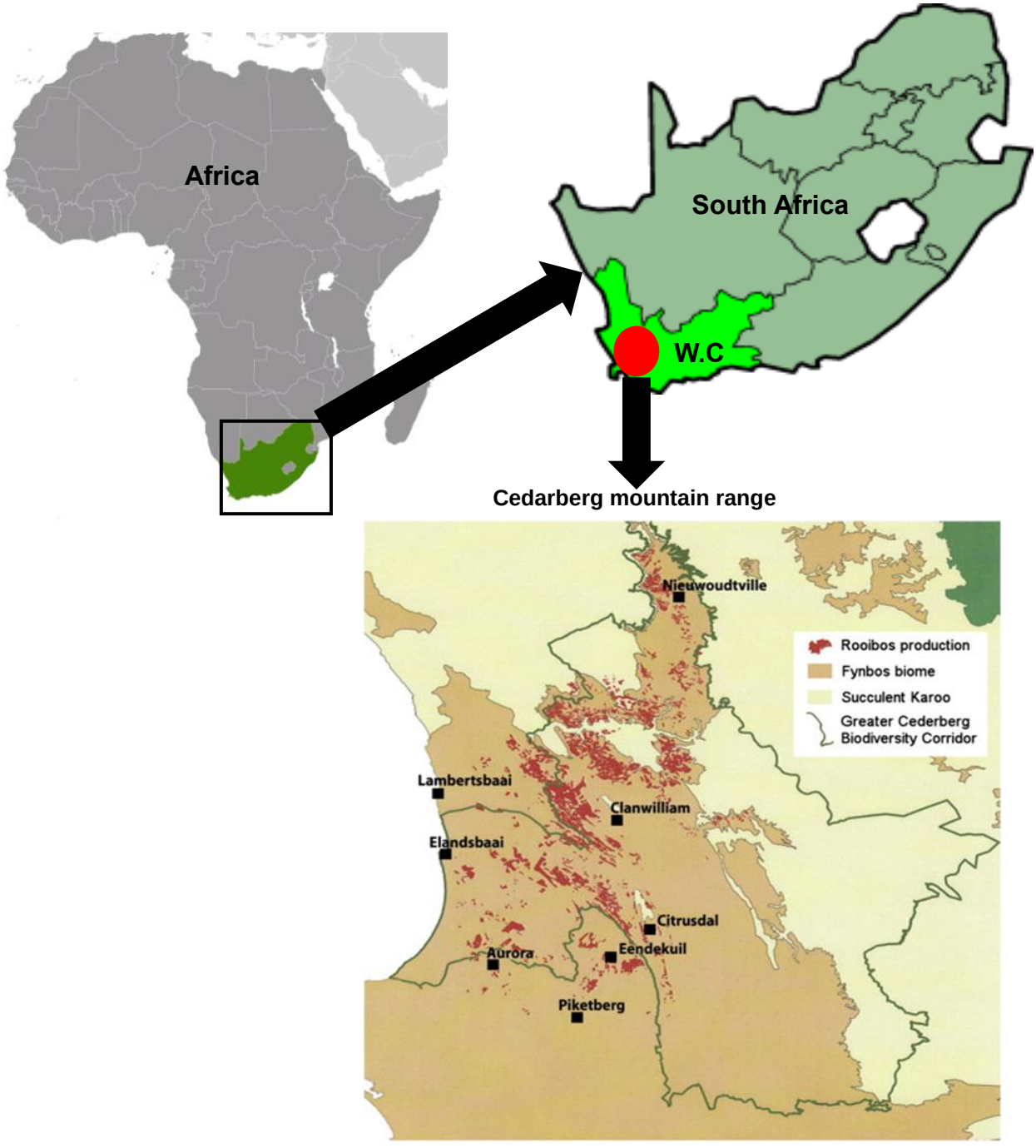

Figure 2.12 Distribution of rooibos.
A geographical map illustrating the production and distribution areas of *Aspalathus linearis* in the Western Cape Province of South Africa (Johnson et al. 2018).

2.16.1 Overview of *Aspalathus linearis* (Rooibos)

Aspalathus linearis (Botanical name; *Aspalathus linearis* (Burm.f.) R.Dahlgren), also known as rooibos, is a fynbos shrub that grows naturally in the Cederberg Mountain area, of the Western and Northern Cape Provinces of South Africa (Joubert and De Beer, 2011). Rooibos is commercially cultivated and widely consumed as a hot beverage lacking caffeine and having low quantities of tannins. It is a rich source of health promoting phenolic compounds such as the *C*-*C*-linked dihydrochalcone glucoside, aspalathin (Joubert *et al*., 2016), that is unique to the *Aspalathus* species.

Aspalathus linearis, primarily cultivated as a herbal tea, has a growing worldwide market share, that has been boosted by its health promoting properties (Mahomoodally, 2013; Van De Merwe, Beer and Joubert, 2015). Traditional rooibos tea (a fermented rooibos tea) is produced by oxidation of the cut and bruised leaves and stems to obtain the classical red-brown rooibos herbal tea. In contrast, unfermented rooibos tea (green rooibos) is rapidly dried to avoid oxidation and retain the antioxidant properties of its phenolic compounds (Joubert and De Beer, 2011) Apart from aspalathin which is the major polyphenol, *A. linearis* also contains nothofagin, a structural analogue of aspalathin, and their flavone derivatives orientin, isoorientin, vitexin and isovitexin; as well as several other relevant bioactive polyphenolic sub-groups, such as the flavonols quercetin, isoquercetin and rutin and the flavanones chrysoeriol and luteolin (McKay and Blumberg, 2006). Other bioactive compounds of interest include phenylpropenoic acid Z-2-(*β-D*-glucopyranosyloxy)-3-phenylpropenoic acid (PPAG) and several other phenolic acids such as p-coumaric acid, caffeic acid, ferulic acid and chlorogenic acid (Muller *et al*., 2013).

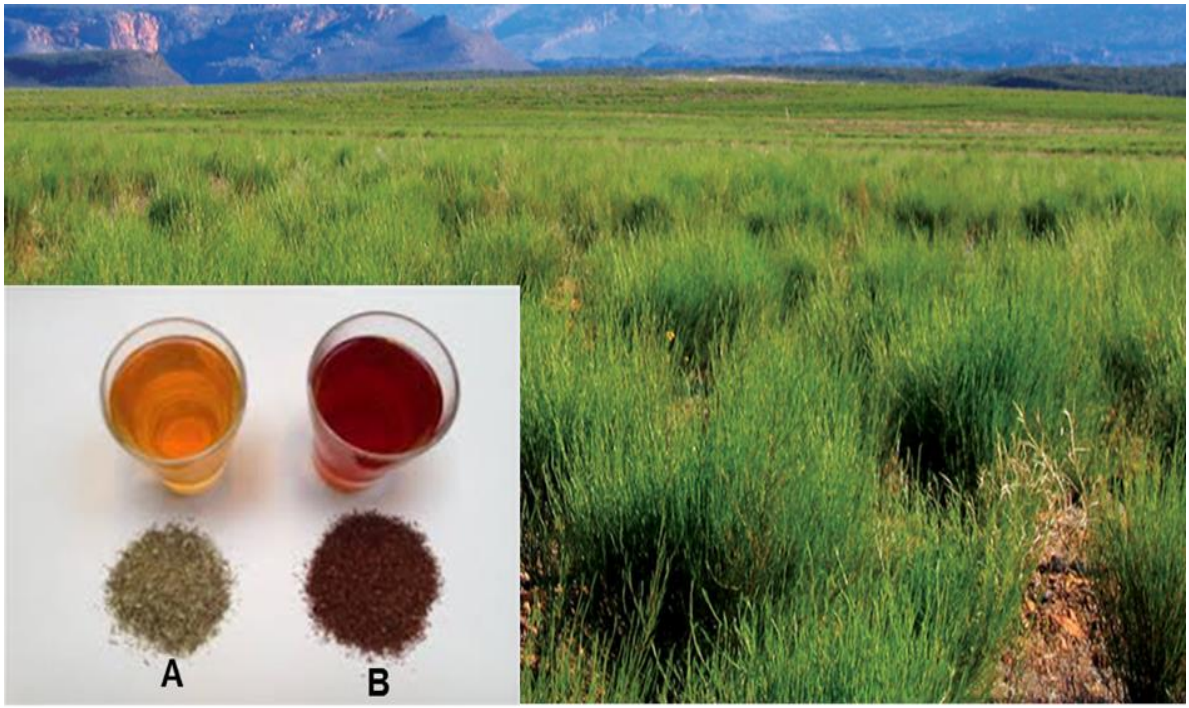

Figure 2.13 The picture showing cultivation of Rooibos plant.
Agro-processing of rooibos (*Aspalathus linearis*) produces two forms of rooibos tea. Unfermented rooibos (A) and fermented rooibos (B) differ in taste and their polyphenolic composition (Johnson *et al*., 2018).

2.16.2 Aspalathin

The dihydrochalcone *C*-glycoside, aspalathin (Figure 2.13) is the most abundant polyphenol present in *Aspalathus linearis*. Although the aspalathin content varies greatly, in rooibos material the mean content was shown to be ca. 3.6 g/100 g dried green plant material (Johnson *et al*., 2018). Aspalathin is a strong antioxidant and therefore is quickly broken down during the fermentation process. Fermented rooibos only contains about 7% of the original aspalathin content (Joubert, 1996). During the oxidation process aspalathin is oxidized to its flavone derivatives orientin and isoorientin via their respective flavanone precursors (Koeppen, 1965).

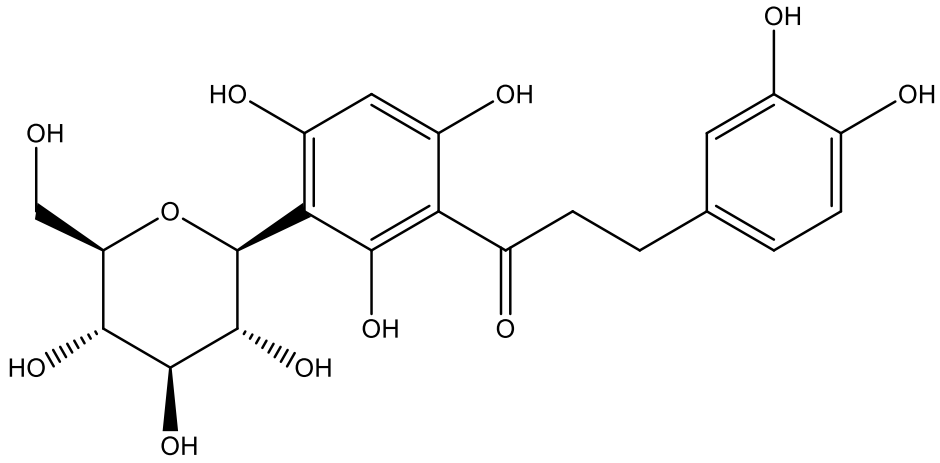

Figure 2.14 Chemical Structure of Aspalathin.
Aspalathin (formula $C_{21}H_{24}O_{11}$) is a member of 2'-hydroxy-dihydrochalcones described that is the 2-*C*-beta-*D*-glucopyranide of phloroglucinol and which is substituted at position 4 by a 3-(3,4-dihydroxyphenyl) propanoyl group.

2.16.3 Therapeutic effects of aspalathin

Apart from its antioxidant effects, aspalathin has been shown to have anti-diabetic (Kawano *et al.*, 2009; Muller *et al.*, 2012), hypolipidemic (Johnson *et al*., 2018; Najafian, Najafian and Najafian, 2016; Van der Merwe *et al*., 2015; Beltrãn-Debãn *et al*., 2011; Orlando *et al*., 2017) and anti-inflammatory activities (Canda, Oguntibeju, and Marnewick 2014). At a molecular level, aspalathin was shown to enhance PI3K-mediated AKT insulin signalling, suppressed by palmitate, and the activation of AMPK, that increased glucose uptake via GLUT 4 (Mazibuko *et al.*, 2015; Son *et al*., 2013). In addition, Son et al. (2013) demonstrated that aspalathin protected pancreatic beta cells against oxidative stress induced by artificial advanced glycation end (AGE) products. Aspalathin has also been shown to modulate the activation of pro-inflammatory transcription factor NF-κB by palmitate (Mazibuko *et al*., 2015) and lipopolysaccharide (LPS) (Lee *et al*., 2015). In addition, aspalathin was able to suppress TNF-α and IL-6 production induced by LPS in HUVEC cells and in mice (Lee *et al.,* 2015).

Activation of NF-κB promotes the production of pro-inflammatory cytokines which promote metabolic dysfunction and play a central role in the pathogenesis of NAFLD (Reddy and Rao, 2006). The increased inflammatory cytokines, FFAs and associated ROS perpetuates NF-κB activation and leads to further liver damage (Ponmari *et al*., 2014). Flavonoids, including aspalathin, enhance endogenous intracellular antioxidant defences by increasing the expression and binding of the stress response transcription factor Nrf2 to the anti-oxidant response elements (ARE), promoting the transcription of antioxidant enzymes, such as GSH, SOD and UCP-2 (Son *et al*., 2013; Johnson *et al*., 2018; Yang, Gadi and Thomson, 2010)

Aspalathin positively effects lipid metabolism in the liver. Aspalathin enhances CPT-1 expression, thereby increasing beta oxidation and, by activating AMPK *de novo,* reducing lipid synthesis. (Van De Wier *et al*., 2015). Activating AMPK inhibits liver X-receptor-α (LXRα) and sterol regulatory element-binding protein-1c (SREBP-1c) transcription, suppressing the expression of the lipogenic enzymes fatty acid synthase (FAS), glucokinase (gk) and acetyl-coenzyme A carboxylase (ACC) (Ferre and Foufelle, 2010).

2.16.4 Hepatoprotective role of Rooibos and aspalathin

Several studies, using different modalities to induce liver damage, have been conducted to demonstrate the hepatoprotective potential of rooibos. A study conducted by Uličná et al., (2003) looked at the hepatoprotective role of green rooibos tea against liver injury induced by carbon tetrachloride (CCl_4) in male Wistar rats. The results revealed that rats which had free access to rooibos tea decreased CCl_4-induced steatosis up to 73%. The effect of rooibos was comparable to the N-acetyl-L-cysteine used as a positive control.

A study by Ajuwon et al. (2013) used tert-butyl-hydroperoxide (t-BHP) to induce oxidative hepatotoxicity. Fermented rooibos extract decreased liver marker enzymes, prevented lipid peroxidation and improved antioxidant enzymes (Ajuwon *et al.,* 2013). Another study by the same group in 2014 demonstrated the protective role of fermented rooibos

against lipopolysaccharide (LPS) induced liver injury in male Wistar rats. Rooibos treatment reduced liver injury by modulating oxidative stress and suppressing pro-inflammatory cytokines (Ajuwon, Oguntibeju and Marnewick,2014).

A study conducted by Van der Merwe et al. (2015) investigated the role of unfermented rooibos on the antioxidant homeostasis in the liver of male Fischer rats. The results demonstrated that rooibos can alter glutathione homeostasis in a time and dose related manner. The authors speculated that the protective responses by rooibos against oxidative stress in the liver could be mediated by increasing the expression of Nqo1 and Gpx2, both targets for Nrf2 (Van der Merwe *et al*., 2015).

2.16.5 Hepatotoxicity role of Rooibos

Most studies have focused on the protective and beneficial roles of rooibos. However, recently, Sinisalo, Enkovaara and Kivistö. (2010) presented a case study reporting possible hepatotoxicity of rooibos. A 42-year-old woman treated for low-grade β -cell malignancy presented with minor steatosis on ultrasound. The steatosis could not be attributed to alcohol or other medication; however, she had started drinking rooibos for the two weeks before her medical examination. She was instructed to abstain from drinking rooibos and her liver enzymes normalized within a week. The authors concluded that causality could either be attributed to herb-drug interaction of rooibos or by rooibos contaminated with another hepatotoxic compound.

A poster presentation in San Francisco 15-18 June, (2013) at the 95th Endocrinology Society conference presented a second case study related to hepatoxicity and rooibos. A 52-year old male patient with hyperlipidemia on treatment with atorvastatin presented with jaundice and elevated liver enzymes. The patient confessed to have been consuming rooibos for three months. As the jaundice and liver enzymes normalized, after the patient stopped drinking rooibos, the authors concluded that high consumption of rooibos was responsible for the observed hepatotoxicity.

In our group, a study conducted by Buthelezi (2017) (unpublished M.Sc. thesis) investigated the potential hepatotoxicity of GRT in a sub-chronic toxicity study using Sprague Dawley rats and *in vitro* using C3A cells. The results demonstrated that at a high concentration (1 mg/mL), GRT extract was cytotoxic *in vitro*. Similar results were observed *in vivo* where a high dose (300 mg/kg BW) showed mild toxicity of the liver by histology.

As mentioned above, the beneficial versus harmful effects of rooibos on the liver is related to dose and time. At therapeutic doses, rooibos has positive effects that enhance the endogenous anti-oxidant defenses. However, at high doses over extended periods, it elicits a pro-oxidant effect that depletes the endogenous anti-oxidants. These assumptions are supported by Buthelezi, (2017) and the Van der Merwe et al. (2015) study that showed that after 28 days of treatment with a green rooibos extract, liver GSH levels were increased and after 90 days the levels were decreased (Van der Merwe, De Beer and Joubert, 2015).

CHAPTER THREE

MATERIALS AND METHODS

The chapter comprises of two sections: A and B.

Section A is *in-vitro* work.

Section B is *in-vivo* work.

3.0 METHODS

3.1. Cell Culture

3.1.1 Materials

The human derived hepatoma C3A cell line (Cat No: CRL-10741) was purchased from the American Type Culture Collection (ATCC) (UA, USA). All cells used for this study were derived from the original stock of passage 12 and further experiments were limited to less than 5 additional passages. Afriplex GRT™ green rooibos extract (GRT), containing approximately 12% aspalathin, was kindly provided by Afriplex (Pty) Ltd, Paarl, South Africa. All other materials, suppliers and product numbers are listed in Appendix A.

3.1.2 Thawing of cells

Cryopreserved C3A cells, stored under nitrogen, were thawed at 37 °C in a preheated water bath. Once thawed, the cells were transferred to a 50 ml tube containing 16 ml of pre-warmed Eagle's Minimum Essential Medium (EMEM) complete growth media supplemented with 100 mM sodium pyruvate, 1 % non-essential amino acids (NEAAs), 10 % foetal bovine serum (FBS) and 2 ml glutamine; then gently mixed by repeated pipetting. Thereafter, cells were transferred to a 75 cm^2 cell culture flask and incubated in humidified air with 5 % CO_2 at 37°C. The cell media was refreshed every second day and the cells cultured until 70-80 % confluency.

3.1.3 Trypsinization

Upon reaching 70-80 % confluency, cells were rinsed with 8 ml of pre-warmed Dulbecco's phosphate buffered saline (DPBS) and incubated with 2 ml of trypsin/versene under standard tissue culture conditions (37°C, 5 % CO_2 in humidified air) until the cells were dislodged from the cell culture flask (5-7 min). Dislodgement of cells was confirmed through visual observation under an inverted light microscope (CKX 41, Olympus; Melville, NY, USA). Thereafter, trypsinization was ended with the addition of 8 ml of pre-warmed EMEM growth media supplemented with 10% FBS. A single cell suspension was achieved by repeated pipetting and the cell suspension centrifuged at 800 × g (SL 16R

Thermo Fisher Scientific, Waltham, MA, USA) for 5 min. After centrifugation, the supernatant was removed and the cell pellet was re-suspended in 10 ml of pre-warmed EMEM growth media. Prior to seeding, cell density was determined and adjusted as described in section 3.1.4.

3.1.4 Counting of cells

The number of viable cells was determined by a manual counting technique using an improved Neubauer haemocytometer, containing two identical cover slipped counting chambers into which a small volume of cell suspension is added and viewed under an inverted microscope. Briefly, 10 µl of cell suspension was transferred into a micro centrifuge tube and trypan blue solution was added. The cells/trypan blue mixture was placed into the chamber, viewed and counted using an inverted light microscope at 100 x magnification. Each counting chamber is divided into a grid pader consisting of nine squares. The rules of counting cells differ from lab to lab, however in our lab we counted four corner squares as shown in Figure 3.1. The number of cells were calculated using the following formula:

No. of cells = number of cells counted/number of squares × 2 × 10 000.

Dead cells were distinguished from the live cells using trypan blue. In dead cells, the dye passes through the cell membrane and the cells appear blue under the microscope. For this study only the culture yielding >95% cell viability was used for further culturing.

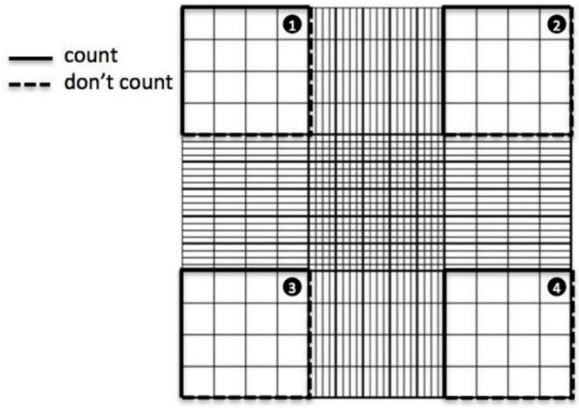

Figure 3.1 : Cell counting chamber.
Squares labelled 1-4 represents designated sites on which cells were counted.

3.1.5 Freezing cells

After obtaining the number of viable cells, cells were harvested by centrifugation at 800 × g for 5 min. The supernatant was discarded, and the cells were re-suspended in sterile freezing cold EMEM with 7% DMSO, at a volume ratio required to achieve 1×10^6 cells/ml. The cell suspension (1 ml) was aliquoted per cryotube and kept on ice. Cells were then kept at -80 °C overnight and transferred to liquid nitrogen the following day for long-term storage.

3.1.6 Sub-culturing of cells

C3A cells were seeded in 75 cm^2 culture flasks at a density of 5.5×10^4 cells/ml. A total volume of 18 ml of pre-warmed growth media was added to the cells. Cells were then incubated at 37 °C in 5% CO_2 and humidified air for three days until the cells were approximately 70-80% confluent. Media was refreshed every 48 hrs.

3.1.7 Seeding in multi-well plates

After establishing the number of viable cells, as described in section 3.1.4. C3A hepatocytes were seeded at the respective seeding densities as indicated in Table 3.1 for further experimental purposes, followed by incubation at 37 °C for four days.

Table 3.1: Seeding of C3A hepatocytes in multi-well plates

Multi-well plate	Seeding density (cells/well)	Volume (µl)
96	11x10^3	100
6	2x10^4	3000

3.1.8 Preparation of treatments and treating of cells

3.1.8.1 10 mM oleic acid (Stock solution)

3 488,3 µl BSA in EMEM (0.9 g BSA was weighed and dissolved in 45 ml of pre-warmed EMEM) was added to 11,7 µl (3M) oleic acid to make up a 10 mM stock solution. The BSA/oleic acid stock was allowed to conjugate in a water bath at 37°C for 2 hrs before treating.

3.1.8.2 Preparations of working concentrations of oleic acid (for dose-response)

Different concentrations of the conjugated oleic acid (0.125, 0.25, 0.5, 0.75, 1 and 2 mM) used in this study were prepared using the dilution equation below:

$$C_1V_1=C_2V_2$$

where C1 is concentration of oleic acid stock solution (10 mM), V1 unknown volume of oleic acid, C2 desired concentration of oleic acid and V2 is the desired final volume of medium.

3.1.8.3 1 mM oleic acid (for inducing steatosis)

After conducting dose response experiments, a suitable concentration of oleic acid was selected to induce steatosis, and prepared for two of three treatment conditions as follows: 1600 µl of 10 mM stock solution was added to 14,400 µl (EMEM without BSA) to make up 1 mM oleic acid, and kept in a water bath (37°C) until further use. For the second condition (oleic acid and treatment), the same method was followed using half the volume of EMEM.

3.1.8.4 Afriplex GRT™ green rooibos extract (GRT)

Two milligrams of GRT was dissolved in 2 ml of medium (EMEM) to make up a stock solution (1000 µg/ml), followed by serial dilutions as shown in Figure 3.2 for the first and third condition (controls and post-treatments). For the second condition (simultaneous

treatments), incubating both oleic acid and the treatments, the same method was followed but with half the volume of EMEM.

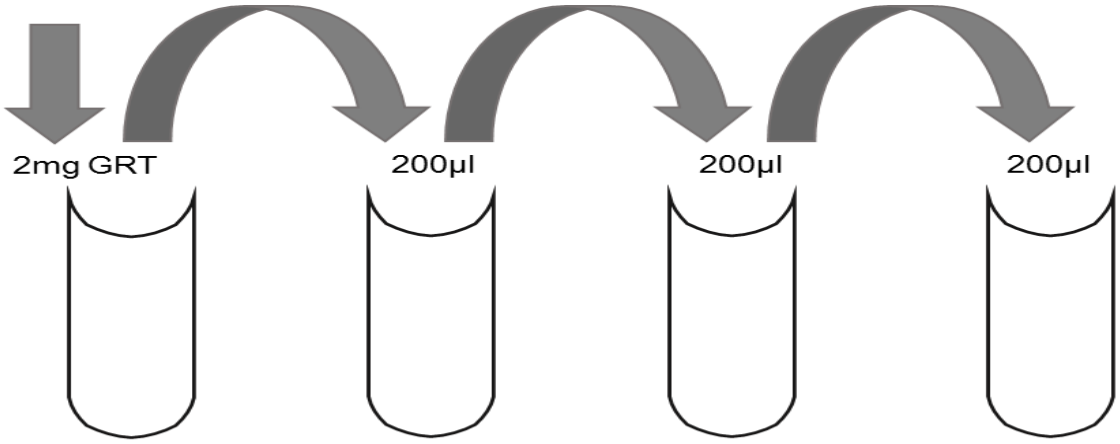

2 ml Stock solution	1800 µl EMEM	1800 µl EMEM	1800 µl EMEM
1000 µg/ml GRT	100 µg/ml GRT	10 µg/ml GRT	1 µg/ml GRT

Figure 3.2: A graphical representation of the preparation of 10-fold serial dilutions of GRT for experiments.

3.1.8.5 Pioglitazone

A volume of 12,5 µl of 10 mM pioglitazone stock solution was diluted with 4 987,5 µl EMEM to make up 25 µM pioglitazone working solution.

3.1.9 Steatosis induction in C3A cells

3.1.9.1 Establishing in vitro steatosis model

The C3A liver cells ($11x10^3$ cells/well) were incubated with increasing concentrations of oleic acid (0.125, 0.25, 0.5, 0.75 1 and 2 mM) for 24 and 48 hrs respectively in 96 multi-well plates. After incubation, an Oil Red O (ORO) assay was performed to visualize intracellular lipid content induced by oleic acid. Based on this dose and time response, the most suitable non-toxic concentration and time for steatosis induction was selected, for further treatment with respective concentrations of GRT as well as pioglitazone as

described below.

Six plates were subjected to different treatments depending on the three conditions as described below

3.1.9.2 Afriplex GRT treatment of normal cells

According to the experimental plate layout in Figure 3.2, two 96 multi-well plates (one for MTT assay and the second one for ORO) were treated for 24 hrs with three different concentrations of GRT (low, middle and high dose) as well as pioglitazone which was used as a reference known to modulate fat accumulation. The vehicle control was left untreated.

3.1.9.3 Steatotic groups with treatment (Simultaneous and Post-treatment groups)

Treatment of cells, exposed to oleic acid for 24 hrs, was preformed either in the presence of the oleic acid (simultaneous treatment group) or treated after the induction of steatosis with oleic acid for 24 hours, followed by various treatments in the absence of oleic acid for 24 hrs (post-treatment group). Simultaneous and post-treatments were prepared and applied according to the plate layout illustrated in Figure 3.3

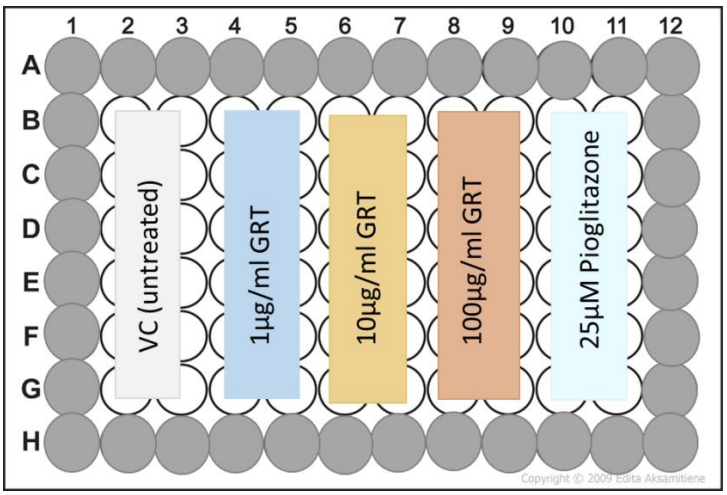

Figure 3.3: Plate layout.

The outer wells (grey) contain DPBS to maintain the rate of evaporation in the plate. Treatments were applied to the inner wells as per the illustration.

3.1.10 In vitro bioassays

The assays conducted include determination of cell viability using MTT assay and lipid content evaluation using Oil Red O assay as described in the following sections.

3.1.10.1 Oil Red O Assay

To quantify intracellular lipid content, cells were stained with Oil Red O (ORO) after treatment. Oil Red O is a hydrophobic dye that is more soluble in lipids than the solvent, resulting in the uptake of the dye by fats and lipids (Lillie *et al*., 1943). For the assay, the culture media was removed, and the cells were rinsed with pre-warmed PBS and then fixed with 10% (v/v) neutral buffered formalin for 15 min at room temperature. The formalin was removed by rinsing twice with PBS and the cells were then stained with 0.7% (v/v) ORO staining solution (prepared as shown in appendix 6.5) for 30 min at room temperature.

After staining, cells were washed three times with double distilled water and visualized using an inverted light microscope at 40X magnification and images were taken to quantify intracellular lipid accumulation. Quantitative estimation of lipid accumulation was performed by adding 50 µl of isopropanol to the cells of the dye elution retained by cells for 2 min. Thereafter, the eluted ORO stain was transferred to a micro assay plate and the optical density measured at 490nm using a BioTek® ELx800 plate reader.

To normalize cell numbers to lipid content, crystal violet staining was measured according to the method described by Sanderson *et al*. (2014). Briefly, after performing the ORO assay, the cells were washed with 70% (v/v) ethanol and the cells were stained with 0.5% (v/v) crystal violet (CV) working solution for 5 min. After staining, CV was aspirated completely, and the cells washed thrice with PBS. To extract CV stain from cells, 70%

ethanol was added, and optical density was measured at 570 nm using a BioTek® ELx800 plate reader. ORO was normalized to CV values and expressed as a percentage relative to the vehicle control.

3.1.10.2 The 3-[4, 5-Dimethylthiazol-2-yl]-2, 5 diphenyltetrazolium bromide (MTT) assay

The effects of oleic acid (used to induce steatosis) and GRT on cell viability was determined using 3-[4, 5-dimethylthiazol-2-yl]-2, 5-diphenyltetrazolium (MTT) colorimetric assay. The MTT method described by Mosmann (1983) is based on the production of a purple formazan by enzymatic action of mitochondrial dehydrogenase of viable cells. The product is insoluble in aqueous solutions (Weyermann *et al*., 2005).

Briefly, $2x10^4$ cells/well were seeded in 96 multi-well plates and treated with GRT extract in the presence or absence of oleic acid for 24 and 48 hrs. Briefly, after aspirating the media and washing the cells with 100 µl pre-warmed DPBS, 100 µl of 2 mg/ml MTT solution (prepared as shown in appendix 6.5) was added to each well and incubated at 37 °C in humidified air with 5% CO_2 for 30 min. Thereafter the MTT solution was aspirated and a mixture of 200 µl of 100% DMSO and 25 µl of Sorenson's glycine buffer were added to dissolve the formazan product. Optical density was measured at 570 nm using the BioTek® plate reader ELx800 and the Gen 5 software. Results were expressed as a mean percentage relative to the control set at 100%.

3.1.11 RNA isolation and Real-time quantitative reverse transcription polymerase chain reaction

The effect of aspalathin enriched green rooibos extract was evaluated on the mRNA expression of genes involved in inflammation, glucose and lipid metabolism.

3.1.11.1 Harvesting of cells

After treatment as described above in subsection 3.1.9**,** cells were washed with 0.5 ml DPBS and lysed by adding 1 ml Qiazol lysis reagent for 5 min. The cells were scraped from the plate using cell scrapers and wells were pooled in triplicates in 2 ml Eppendorf tubes and stored at -80 ºC until analysis.

3.1.11.2 RNA extraction

Sterile stainless-steel beads were added to 2 ml Eppendorf tubes containing the cells and homogenized using the Qiagen tissue lyser for 1 min at 25 Hz. This was repeated 4 times and samples were alternated between 1 min in the Tissue Lyser and 1 min on ice. The homogenate was then centrifuged at 15 000 x g at 4 ºC for 1 min and the supernatant was transferred to a 1.5 ml tube. A volume of 0.2 ml chloroform was added per ml of Qiazol initially added for harvesting, followed by brisk shaking for 15 min on a shaker and then re-centrifuged at 15 000 x g at 4ºC for 15 min. While avoiding destruction of phases, the upper aqueous phase was transferred into a new 1.5 ml microcentrifuge tube, 0.5 ml of isopropanol was then added before mixing and overnight incubation at -20ºC.

On the following day, the samples were centrifuged at 15 000 x g for 30 min at 4 ºC, the supernatant discarded and 1 ml of 70 % ethanol added to the pellet before re-centrifuging at 15 000 x g for 10 min at 4 ºC. The supernatant was removed and the tubes were blotted on a paper towel. The ethanol step was repeated. However, this time the RNA pellet was left to air dry in a pre-cleaned hood for 30 min. After the pellet was completely dry, it was then dissolved in 100 µl RNase-free water, mixed and then incubated for 10 min at 55 ºC on a heating block.

3.1.11.3 RNA integrity

RNA quantification and purity were assessed using Nanodrop ND-100 which usually determines both RNA and DNA concentrations within 1 µl samples with high accuracy in a 260/280 nm ratio format. A ratio of 2.0 is considered pure for RNA and 1.8 for DNA. If the ratio is lower, that indicates contamination (e.g. protein, phenol or other contaminants)

(Nanodrop Technologies, Wilmington, DE, USA). The quantification was initiated by cleaning the pedestal, followed by blanking with RNase-free water. RNA was then measured by loading 1 µl of the sample onto the pedestal and the absorbance measured. Each sample aliquot was read in duplicate and the average of the two readings was used.

3.1.11.4 DNase treatment

This step was performed to eradicate contaminating genomic DNA to preclude its interference with gene expression. RNA samples were DNase treated using TURBO DNA-free kit (Ambion by life technologies) as per manufacturer's instruction. Briefly, 5 µl of DNase buffer and 1 µl of DNase were added to the RNA sample making up a final volume of 50 µl, mixed and incubated at 37ºC for 30 min. After the incubation period, another 1µl of DNase was added and reincubated for another 30 min. A volume of 10 µl of inactivation reagent was added and the tubes were then placed on an orbital shaker for 5 min at room temperature (25 ºC), followed by centrifugation at 10 000 x g for 1.5 min. After centrifuging, RNA was transferred into a new tube and RNA concentrations were determined using nanodrop as described 3.1.11.3

3.1.11.5 Reverse transcription/cDNA synthesis

Total RNA was reverse transcribed into a single-stranded complementary DNA (cDNA) using the High-Capacity cDNA kit (Applied Biosystems, Foster City, CA, USA), according to the manufacturer's instructions. Briefly, nuclease-free water was added to DNase treated samples to make a volume of 10 µl. Thereafter a high-capacity cDNA reverse transcription kit (Applied Biosystem) was used to generate cDNA as per manufacturer's instructions. Negative and positive reverse transcriptions were prepared as shown in Table 3.2

Table 3.2: components of reverse transcription

Component	Volume/reaction(µl)	
	RT Positive	RT Negative

10x RT buffer	2	2
25x dNTP mix	0.8	0.8
10x random primers	2	2
RNase inhibitor	1	1
Nuclease-free water	3.2	4.2
Reverse Transcriptase	1	0
Total volume	**10**	

3.1.11.6 Testing cDNA

To test cDNA for genomic DNA contamination, cDNA generated from positive and negative RT were amplified using both reverse and forward primers. A reaction mix, containing 12.5 µl SYBR Green master mix (Applied Biosystems), 1 µl ActB reverse and forward primers (10 µM) and 9.5 µl nuclease free waterwas added to a final volume of 24 µl as shown in Table 3.3. The reaction mix was upscaled according to the number of samples to be analyzed.

Twenty-four microliters of the reaction mix was pipetted into a 96 well PCR plate (Applied Biosystems) and topped up with 1 µl of undiluted cDNA (RT positive or negative). The plate was covered with a plate cover, centrifuged and mixed on a plate shaker for 5 min. The PCR reaction was conducted using Sequence Detection System Instrument ABI 7500 (Applied Biosystems)

Table 3.3: Reaction mix components to determine genomic DNA contamination.

PCR reaction	Volume (µl)
2x master mix	12.5
Beta Actin forward primer (10 µM)	1
Beta Actin reverse primer (10 µM)	1
Nuclease-free water	9.5

Cdna	1
Final volume	**25**

3.1.11.7 Quantitative real-time PCR

TaqMan® gene expression assays, as shown in Table 3.4, were used in this study to assess the effects of aspalathin enriched green rooibos extract on the expression of genes involved in inflammation, glucose and lipid metabolism. The PCR master mix consisted of 5 µl of TaqMan® universal PCR master mix from Applied Biosystems, 0.5 µl TaqMan® gene expression assay and 3.5 µl of nuclease-free water, to a final volume of 9 µl. The mix was scaled up according to the samples to be analyzed. Thereafter, 9 µl of PCR master mix was added in a 96 well PCR plate (Applied Biosystems) followed by 1 µl of cDNA as shown in Table 3.5. This was then covered with a plate cover (Applied Biosystems) and centrifuged on a microplate centrifuge. Thereafter, the plate was placed on an orbital shaker for 5 min to allow for mixing.

A standard curve was prepared from cDNA samples (control groups) diluted with nuclease-free water (1:5 ratio). Real Time PCR was performed using ABI 7500 on cDNA and housekeeping genes were used for normalization. The relative change in gene expression was determined using the ΔΔCT method. All kits in this study were used as per manufacturer's instruction. Gene expression was analyzed in duplicate.

Table 3.4: TaqMan® gene expression assays used for Quantitative real-time PCR in C3A cells

Assay name	Assay number	Species
Peroxisome proliferators-activated receptor-Alpha (PPARα)	Hs01115513_m1	Human
Fatty acid synthase (FASN)	Hs001204974_m1	Human
Sterol regulatory element binding protein (SREBP-1)	Hs00550338_m1	Human

Carnitine palmitoyl transferase-1 (CPT-1)	Hs00912671_m1	Human
Tumor necrosis factor (TNF)	Hs00174128_m1	Human
Glucokinase (GCK)	Hs00386984_m1	Human
Housekeeping genes	**Assay number**	**Species**
Beta Actin	Hs01060665_m1	Human
glyceraldehyde-3-phosphate dehydrogenase (GAPDH)	Hs02758991_m1	Human

Table 3.5: PCR master mix for RT PCR reaction

PCR reaction	Volume (µl)
2x Master mix	5
Probe assay	0.5
Nuclease-free water	3.5
cDNA	1
Final Volume	10

3.1.12 Statistical analysis

The quantitative results were presented as mean + SEM of triplicate experiments. Statistically significant values were compared using one-way analysis of variance (ANOVA) followed by Dunnett's post hoc analysis, and $p<0.05$ was considered significant using pro-graph GraphPad Prism 5.0.

Section B

3.2 *In vivo*

The *in vivo* effects of GRT on liver steatosis were assessed using male C57BLKS *db/db* mice as an animal model of NAFLD. The *db/db* mice have a leptin receptor deficiency. They become obese due to persistent hyperphagia and spontaneously develop diabetes and associated liver steatosis similar to patients with NAFLD.

Animals were treated with two different GRT extracts and pioglitazone was used as a positive control. After treatment, liver tissue was harvested for histology, and key steatogenic genes and proteins were accessed by RT-PCR and Western blot, respectively.

3.2.1 Ethical approval

Ethics Committee for Research in Animals at the Medical Research Council of South Africa (SAMRC-ECRA REF.05/17, see appendix 6.2) approved the animal study protocols. This study was performed in accordance with the guidelines of the South African Medical Research Council as defined in Guidelines on Ethics for Medical Research. Additionally, ethical clearance was obtained from the University of Zululand Committee on Animal Research and Ethics (UZREC 171110-030, see appendix 6.1).

3.2.2 *In vivo* model of NAFLD

Our study used 64 C57BLKS *db/db* mice obtained and housed at the SAMRC Primate Unit & Delft Animal Centre. At approximately four weeks of age, the mice prone to obesity were identified as mice homozygously expressing the diabetes spontaneous mutation (*Leprdb*). The identified mice were housed in pairs with free access to water and food, a controlled temperature (23-24℃) and a relative humidity of 50 % with 12 hrs light/dark cycle.

All animals were acclimatized to the experimental environment for 6 weeks with body weights assessed weekly. After the acclimatization period, mice were randomised into four treatments groups (n = 8/ group). Lean C57BLKS *db/+* litter mates were included as controls. GRT was administered with food at doses of 70 mg/kg BW/day and 740 mg/kg BW/day.

Treatment dosages used in this study stemmed from previously published data and/or unpublished studies at the South African Medical Research Council's Biomedical Research and Innovation Platform (SAMRC-BRIP) (Muller *et al*., 2012). Body weight and fasting plasma glucose were measured weekly during the 10-week treatment period.

GRT doses as described previously by Arakawa. (2001) were calculated from the food intake as recorded three times per week. Daily treatment dosages were administered in proportion to the average daily food intake. e.g. if mice consumed 5 g food /day, pioglitazone was mixed in a ratio of 15 mg/ 5 g of powdered food.

The ratio of treatment: food was recalculated every three days according to the most recent food intake data. The selected doses of pioglitazone are in accordance with the literature (Kanda *et al*., 2010; Ishida *et al*., 2004). The dose of GRT extract was based on a previous study by Muller et al. (2012) in rats and converted to the mouse equivalent dose according to conversion formula described by Reagan-Shaw et al. (2008).

Table 3.6: Treatments dosages used in this study

Group	Lean control mice	Group	Obese diabetic mice	Treatment
A	Control	E	Control	Food equivalent daily
B	Pioglitazone	F	Pioglitazone	15 mg/kg BW/day
C	GRT 1	G	GRT 1	74 mg/kg BW/day
D	GRT 2	H	GRT 2	740 mg/kg BW/day

3.2.3 Food intake monitoring

Food consumed was calculated by subtracting the remaining food in the feeder together with spillage from amount of food initially given to animals.

3.2.4 Body weight monitoring

Body weights were measured weekly for the 10-week treatment period, using a weighing balance. Average weight per treatment group was calculated on an MS Excel sheet.

3.2.5 Blood glucose monitoring

Blood glucose concentrations were recorded on MS Excel weekly for the period of the study. Prior to pricking tails for the blood sample, water and 70% ethanol were used to clean and sterilize the tail. Blood glucose levels were measured by loading the sample onto a glucose strip inserted in a glucometer (OneTouch Select®, LifeScan Inc., Milipitas, CA). Thereafter, average per treatment group was calculated using MS Excel.

3.2.6 Oral Glucose Tolerance Test (OGTT)

A week before terminations, the mice were subjected to an oral glucose tolerance test. Briefly, mice were fasted for 16 hrs and a baseline glucose determined. For the OGTT mice were given 1 g/kg glucose bolus via oral gavage. Blood glucose levels were measured from a tail prick at 0, 15, 30, 60, 120 min. The glucose concentrations over time were used to construct glucose tolerance test curves and to calculate the area under the curve (AUC) with the trapezoidal rule using Graphpad Prism version 5.00.

3.2.7 Animal termination and tissue harvesting

Mice were anaesthetized using 2% fluothane and 98% oxygen inhalation. Once deep anaesthesia was established by pinching the toe, blood was collected from the abdominal

vena cava and the liver harvested, weighed and cut into pieces that were either snap frozen, preserved in RNAlater or fixed in 10% buffered formalin for histology.

3.2.8 Histological examination of liver tissue

Histology examination was performed to assess for the presence of specific histological abnormalities related to NAFLD and liver steatosis (Brunt *et al*., 2011).

3.2.8.1 Processing of liver tissue for histology

Liver samples were fixed overnight in 10% phosphate buffered formalin pH 7.4. Thereafter the liver tissue was processed on a Leica TP 1020 automatic tissue processor (Nussloch, Germany) through ascending concentrations of ethanol (70% for 1.5 h, 2 x 96% for 1 h each and 3x 100% for 1 h each), then xylene before being impregnated with heated paraffin wax. After processing, the liver tissue was embedded in paraffin wax and 5-7 µm sections cut using a Leica RM 2125 RM rotary microtome (Nussloch, Germany). Sections were floated out on a water bath set at ± 40 °C and mounted on 3-aminopropyltriethoxysilane (APES) coated slides.

3.2.8.2 Haematoxylin and Eosin staining of liver sections

Slides were heated at 60 ºC for 45 min to allow the sections to adhere and melt the wax. Slide were then dewaxed with two changes of xylene for 10 min each before rehydrating the sections through descending concentrations of ethanol (100% and 95 %). Slides were rinsed with distilled water and stained with Mayer's haematoxylin stain for 12 min followed by washing with running water to "blue". They were counterstained with 1% aqueous eosin stain for 2 min and washed with distilled water. For mounting, slides were dehydrated through ascending concentrations of ethanol 95% and 100%, before clearing the slides with xylene.

3.2.8.3 Mounting

Entellan (Merck) was used to mount the stained sections with coverslips (24x40mm). Slides were left to air dry at room temperature for a couple of hours before being viewed under the Nikon Eclipse Ti inverted light microscope equipped with a camera and images were captured using NIS elements software (Nikon, Kanagawa, Japan) at 200x magnification.

3.2.8.4 NAFLD scoring

Liver sections were assessed using the NAFLD severity scoring defined by Trak-Smayra *et al*., 2011. This scoring system scores the intensity, distribution and type of lipid accumulation in the *db/db* liver lobules. The intensity of steatosis was scored as the percentage of hepatocytes containing lipid vacuoles assessed at 200x magnification in 10 non-overlapping random chosen fields. Further, lipid accumulation was scored by its zonal distribution within the lobules i.e. centrilobular, mediolobular or periportal. The steatotic type was also classified into microvesicular, mediovacuolar or microvacuolar, based on the size of the lipid vacuoles present in the hepatocytes, ranging from very small to a single large vacuole that displaces the nucleus.

3.2.9 Real time PCR

50 mg of liver samples were weighed, and the total cellular RNA was extracted using a RNA extraction kit (QIAGEN RNeasy Mini kit) as per manufacturer's instruction. The cDNA was synthesized using a cDNA Synthesis High-Capacity cDNA kit (Applied Biosystems, Foster City, CA, USA) according to manufacturer's instructions. Real Time PCR was performed using primers for selected genes involved in NAFLD listed in Table 3.7. Gene expression was analyzed in duplicate and normalized to the housekeeping genes (ActB and HPRT1) listed in Table 3.7. A fully detailed PCR methodology is previously described under subsection 3.1.11.

Table 3.7: TaqMan® gene expression assays used for Quantitative real-time PCR in liver tissues

Assay name	Assay number	Species
Peroxisome proliferators-activated receptor-Alpha (PPARα)	Mm00440940_m1	Mouse
Fatty acid synthase (FASN)	Mm01204974_m1	Mouse
Hydroxymethylglutaryl-CoA synthase-1 (HMGCS1)	Mm01304569_m1	Mouse
Sterol regulatory element binding protein (SREBP-1)	Mm01088679_m1	Mouse
Apolipoprotein AI (APO AI)	Mm00437569_m1	Mouse
Apolipoprotein AI (APO AIV)	Mm00431814_m1	Mouse
Carnitine palmitoyl transferase-1 (CPT-1)	Mm01231183_m1	Mouse
Acetyl CoA carboxylase (ACACA)	Mm01304257_m1	Mouse
Hydroxymethylglutaryl-CoA reductase (HMGCr)		
Housekeeping genes		
β-Actin	Mm02619580_g1	Mouse
Hydroxanthine phosporibosyltransferaserase 1 (HPRT 1)	Mm01545399_m1	Mouse

3.2.10 Western blot analysis

Western blot analysis was performed to assess the effect of GRT on proteins associated with inflammation, lipid and glucose metabolism in NAFLD.

3.2.11 Protein isolation from liver tissue

50 mg of liver samples were weighed in 2 ml tube and 500 µl of cold Tissue Extraction Reagent I (Invitrogen Corporation, Camarillo, CA) and stainless-steel beads were added. The tubes were transferred to pre-cooled tissue lyser blocks and the tissue was homogenized at 25 Hz for 60 seconds using a Qiagen Tissue Lyser (Qiagen, Hilden, Germany) alternating by cooling the tissue in the ice for 60 seconds. This step was repeated five times and the protein lysate transferred into a fresh 1.5 ml tube and kept at -20ºC.

3.2.12 Protein concentration determination

The concentrations of proteins were determined using the Bicinchoninic (BCA) protein

assay. BCA is a detergent-compatible formulation centered on bicinchoninic acid (BCA) for the colorimetric detection and quantitation of total protein (Smith *et al*., 1985; Bainor *et al*., 2011). The assessment of total proteins was conducted using the BCA Protein Assay Kit (ThermoFisher) as per manufacturer's instruction. Briefly, an albumin standard (BSA) and working solution were prepared as specified in the product instruction sheet. Thereafter, 20 µl of each standard and sample replicate were added to a 96 well plate and 200 µl of the working solution was added to each well and mixed well on microplate shaker for 10 min. The plate was covered with foil to prevent light interference and incubated at 37°C for 30 min.

After the incubation, the plate was allowed to cool to room temperature and the absorbance read at 562 nm using a BioTek® ELX800 plate reader with Gen 5® software. The average 562 nm absorbance measurements for blank replicates were then subtracted from the absorbance measurement of all other individual standards and samples replicates. From this, a standard curve was plotted to determine the protein concentration of each sample.

3.2.13 Protein gel electrophoresis

This technique uses the phenomenon of protein separation and characterization based on their size or molecular weight. Thirty micrograms of protein sample was diluted using equal amounts of 2 X Sample buffer (Bio-Rad) i.e. 1:1 ratio. Subsequently, proteins were denatured by heating at 95°C for 5 min. Protein samples were then loaded onto 12% SDS-polyacrylamide gel electrophoresis (SDS-PAGE) pre-cast gels (Bio-Rad). Blue marker (4 µl) was also added to the 1st well (for gel profiling) while 4 µl of Precision Plus Protein Western C standard was added to the other wells for western blot analysis. Gel electrophoresis was started at 150 V for 60 min. Stain-free profile gels were then captured using Bio-Rad Chemidoc image analysis (Bio-Rad, Hercules, CA, USA).

3.2.14 Assemble of sandwich and transfer of gel to a membrane

PVDF membranes were immersed in 99.99% methanol for 1 min followed by equilibrating both PVDF membrane and Whatman filter paper in transfer buffer with shaking for 5 min. This was used to assemble the transfer sandwich as illustrated in Figure 3.5 The cassette was placed between the electrodes as per manufacturer's instructions. After the transferring step, the sandwich was removed from the cassette, the membrane labeled and the stain-free image captured using Bio-Rad Chemidoc MP (Bio-Rad, Hercules, CA, USA).

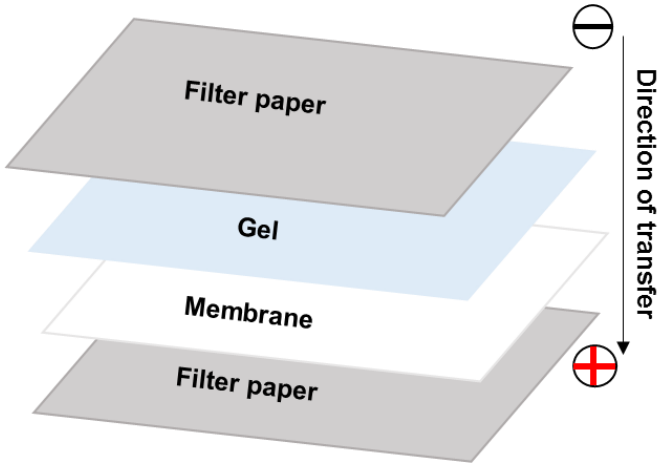

Figure 3.4: Diagrammatic representation of the transfer sandwich used for proteins transfer in western blotting.
Illustration adapted from Mahmood and Yang, 2012.

3.2.15 Blocking and labelling with antibodies

Membranes were blocked using 5% (w/v) fat-free milk (Clover, South Africa) in Tris-buffered saline with Tween 20 (TBST) for 2 hrs on a shaker. Blocked membranes were immunoblotted using selected primary antibodies diluted in 1 x TBST overnight on a shaker at 4°C, using either manufacturers recommended, or laboratory optimized antibody dilutions as listed in Table 3.8. After overnight incubation, the membranes were washed 3 times for 10 min with 1 x TBST. Thereafter, they were incubated with the secondary antibody in 2.5% fat-free milk in 1 x TBST at room temperature for 90 minutes. After incubation with the secondary antibody, the wash step was repeated three times.

Table 3.8: List of antibodies and their dilution factor

Antibody	Dilution	Gel	Cat no	Company
Primary antibody				
Acety-CoA Carboxylase (ACC)	1:1500	12%	3662S	Cell signaling
Fatty acid synthase (FASN)	1:1500	12%	3180	Cell signaling
Carnitine palmitoyl transferase-1(CPT)	1:1500	12%	28568	Abcam
Sterol regulatory element binding protein (SREBP-1)	1:1500	12%	30682	Abcam
Peroxisome proliferators-activated receptor-Alpha (PPARα)	1:1500	12%	24509	Abcam
β-Actin	1:1000	12%		
Secondary antibody				
Donkey anti-rabbit IgG-HRP	1:400	12%	Sc-23181	Santa Cruz
Donkey anti-mouse IgG-HRP	1:400	12%	Sc-23181	Santa Cruz

3.2.16 Detection

The immunoblots were detected using a chemiluminescence detection kit. Quantity one software (Bio-Rad, Hercules, CA, USA) was used for densitometric analysis of the bands. Images were captured using chemidoc (Bio-Rad, Hercules, CA, USA).

3.2.17 Stripping of Western blot

The membrane was washed once with 1 x TBST and stripped using Restore Plus Western Blot Stripping Buffer (Thermo Scientific 46430) for 13 min at room temperature. Thereafter the blot was reused for another analysis.

3.2.18 Statistical analysis

The quantitative results were presented as mean + SEM of eight mice per group. Statistically significant values were compared using one-way analysis of variance (ANOVA) followed by Dunnett's *post hoc* analysis, and $p< 0.05$ was considered significant carried out using pro-graph GraphPad Prism 5

CHAPTER FOUR

RESULTS

4.0 RESULTS

4.1 Section A- *In vitro*

4.1.1 Establishing the C3A liver model for hepatic steatosis

In vitro cell models are widely used for the screening of extracts and compounds for toxicity and biological efficacy. Cell models are also useful to study pathophysiological processes such as NAFLD. NAFLD is characterized by excessive accumulation of lipid droplets in hepatocytes. *In vitro,* NAFLD can be induced in liver cells using oleic acid. In this study, C3A liver cells were selected as the hepatocyte cell line and oleic acid was used to induce steatosis. The first approach of this study was to establish a suitable concentration of oleic acid to induce steatosis that was non-toxic. Cytotoxicity was evaluated using 3-(4,5-dimethylthiazol-2-yl)-2,5-diphenyltetrazolium bromide (MTT). Oil red O (ORO) staining, normalized to cell number by crystal violet staining, was used to assess lipid accumulation.

4.1.1.1 Concentration-response effect of oleic acid in C3A liver cells

A concentration-response was conducted at six different concentrations of oleic acid for 24 and 48 hrs respectively. The results showed oleic acid had varying effects on cell viability, in a concentration and time related manner. At concentrations of 0.5, 0.75, 1 and 2 mM, oleic acid significantly reduced cell viability after 24 hrs of culture (Figure 4.1a). After 48 hrs, all concentrations tested reduced cell viability in a concentration- dependent manner, with 2 mM oleic acid reducing cell viability by ca. 50% (Figure 4.1b).

In terms of lipid accumulation at 24 hrs, 0.125 - and 0.25 mM oleic acid had no effect, while concentrations of 0.5, 0.75 - and 1 mM increased lipid accumulation in C3A liver cells compared to the vehicle control ($p< 0.05$, $p< 0.01$, $p< 0.05$) (Figure 4.2A and 4.3). After 48 hrs, 0.125, 0.25, 0.5 and 2 mM of oleic acid reduced lipid content compared to the control ($p< 0.001$; $p< 0.01$; $p< 0.01$; $p< 0.01$) (Figure 4.2b) and at the higher concentrations ≤ 1 mM the cells were starting to detach from the surface (Figure 4.4).

Based on these findings, a concentration of 1 mM oleic acid for 24 hrs was selected to induce steatosis for further experiments.

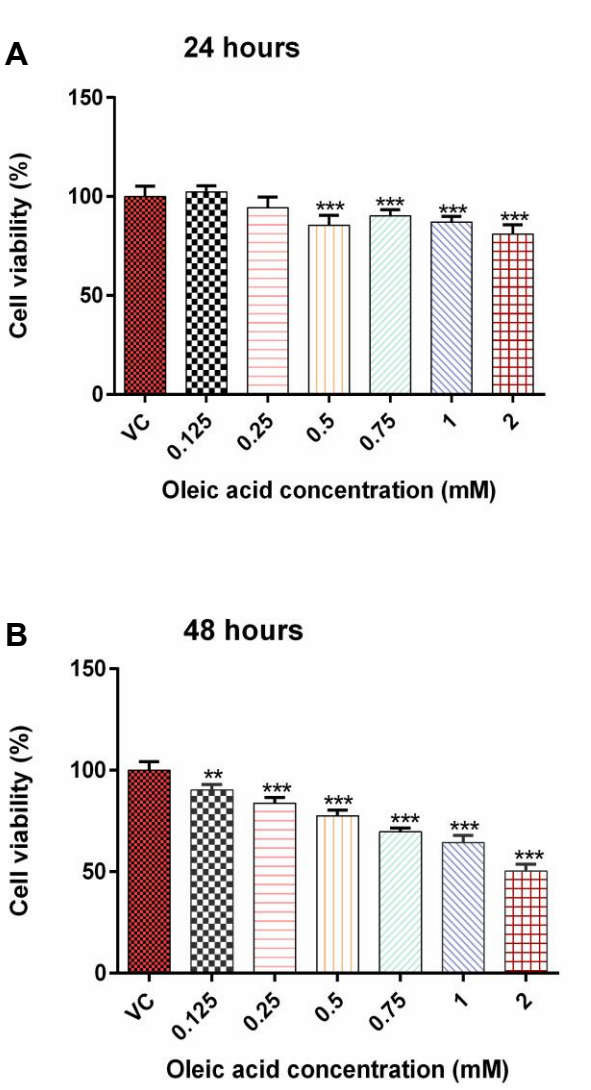

Figure 4.1: Oleic acid cytotoxicity in C3A liver cells.
Cells cultured in EMEM with 8 mM glucose supplemented with various concentrations (0.125, 0.25, 0.5, 0.75, 1 and 2 mM) of oleic acid for 24 (A) or 48 (B) hours, respectively. Cell viability was assessed by MTT activity. Absorbance was read on a microplate reader at 570 nm. The data is presented as mean ± SD of three independent experiments, expressed relative to the vehicle control (VC) set at 100%. P value, **p< 0.01, ***p< 0.001.

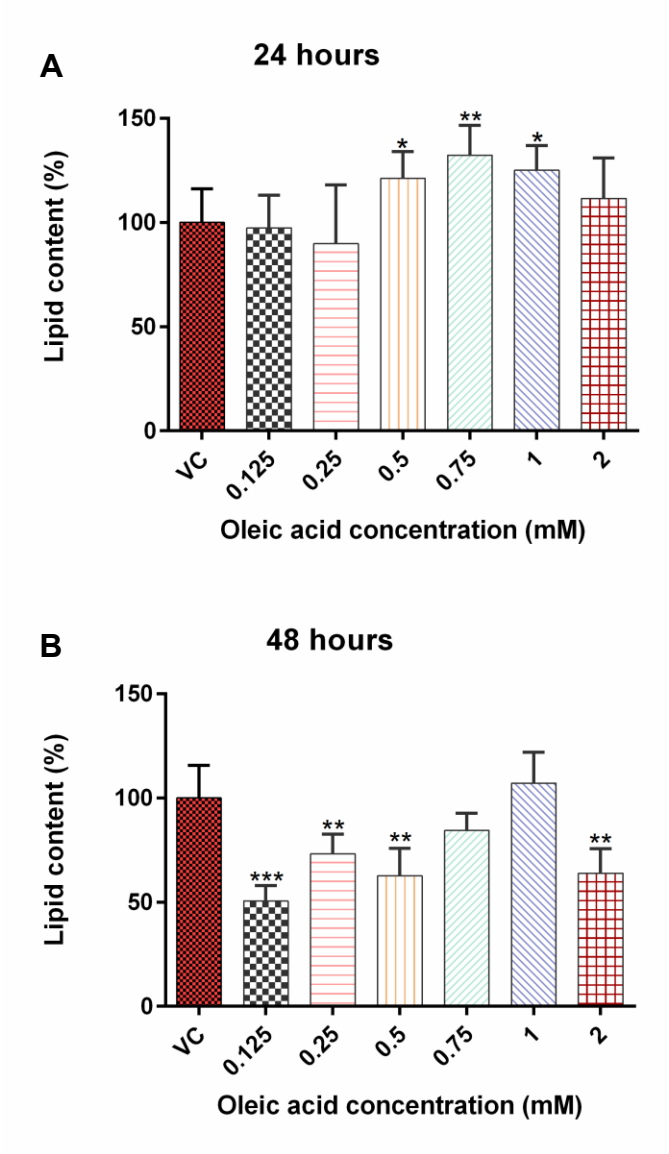

Figure 4.2 Oleic acid induced lipid accumulation in C3A liver cells.
Cells were cultured in EMEM with 8 mM glucose supplemented with various concentrations (0.125, 0.25, 0.5, 0.75, 1 and 2 mM) of oleic acid for 24 (A) or 48 (B) hours, respectively. Intracellular lipid accumulation was assessed using oil red O (ORO) staining followed by isopropanol extraction before the absorbance was read on a microplate reader at a wavelength of 490 nm for ORO and 570 nm for crystal violet. The data is presented as mean ± SD of three independent experiments, normalized to crystal violet and expressed relative the vehicle control (VC) set at 100%, P values *p< 0.05, **p<0.01, ***p< 0.001.

C3A STEATOSIS INDUCED BY OLEIC ACID FOR 24 HOURS

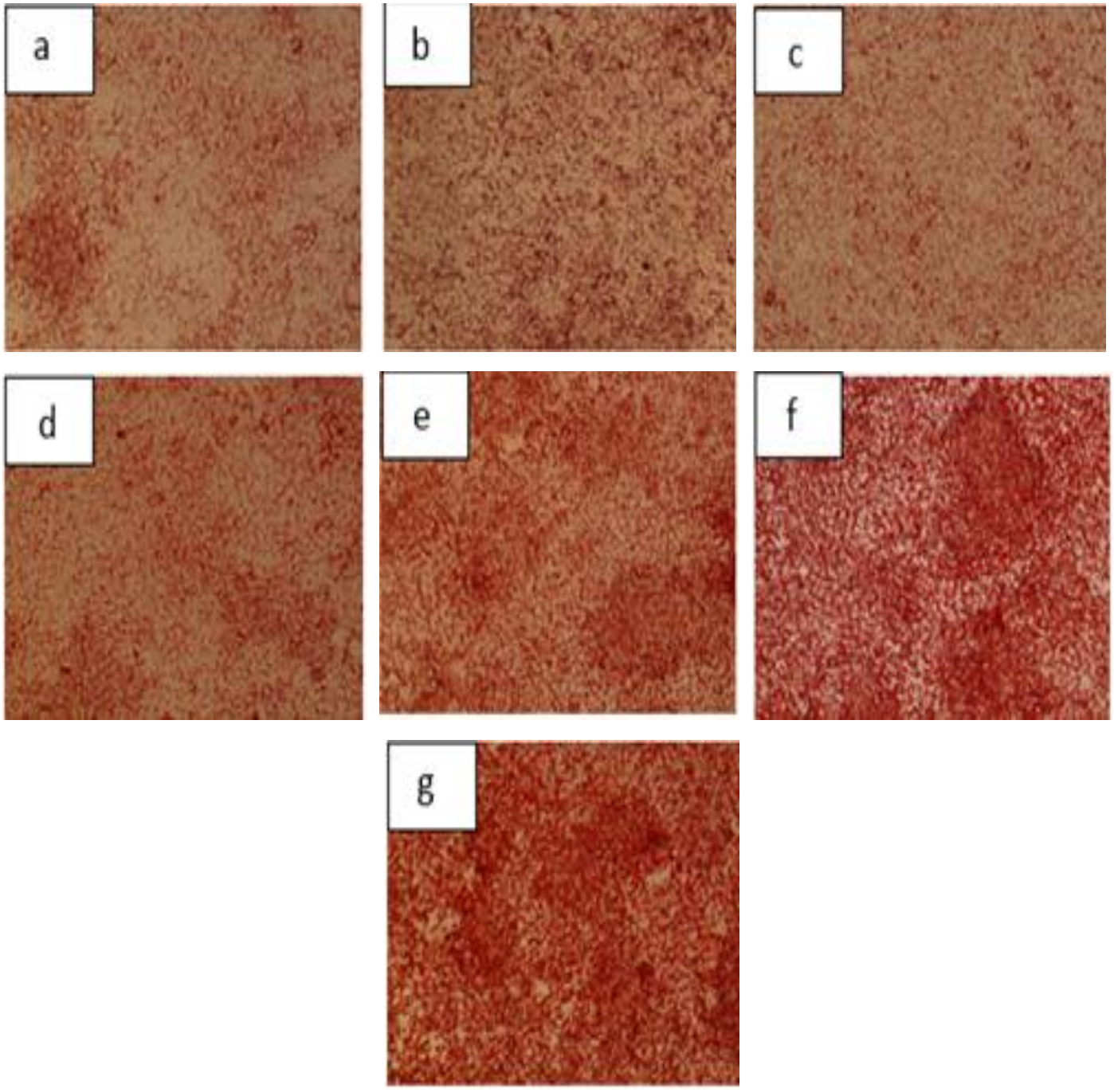

Figure 4.3: Induction of hepatic steatosis by oleic acid in C3A liver cells.
Cells were cultured in EMEM with 8 mM glucose supplemented with various concentrations (0.125, 0.25, 0.5, 0.75, 1 and 2 mM) oleic acid for 24 hours. Intracellular lipid accumulation was visually assessed using oil red O staining; (a) untreated, (b) 0.125 mM oleic acid, (c) 0.25 mM oleic acid, (d) 0.5 mM oleic acid, (e) 0.75 mM oleic acid, (f) 1 mM oleic acid and (g) 2 mM oleic acid. Photomicrographs taken at 400x magnification.

C3A STEATOSIS INDUCED BY OLEIC ACID FOR 48 HOURS

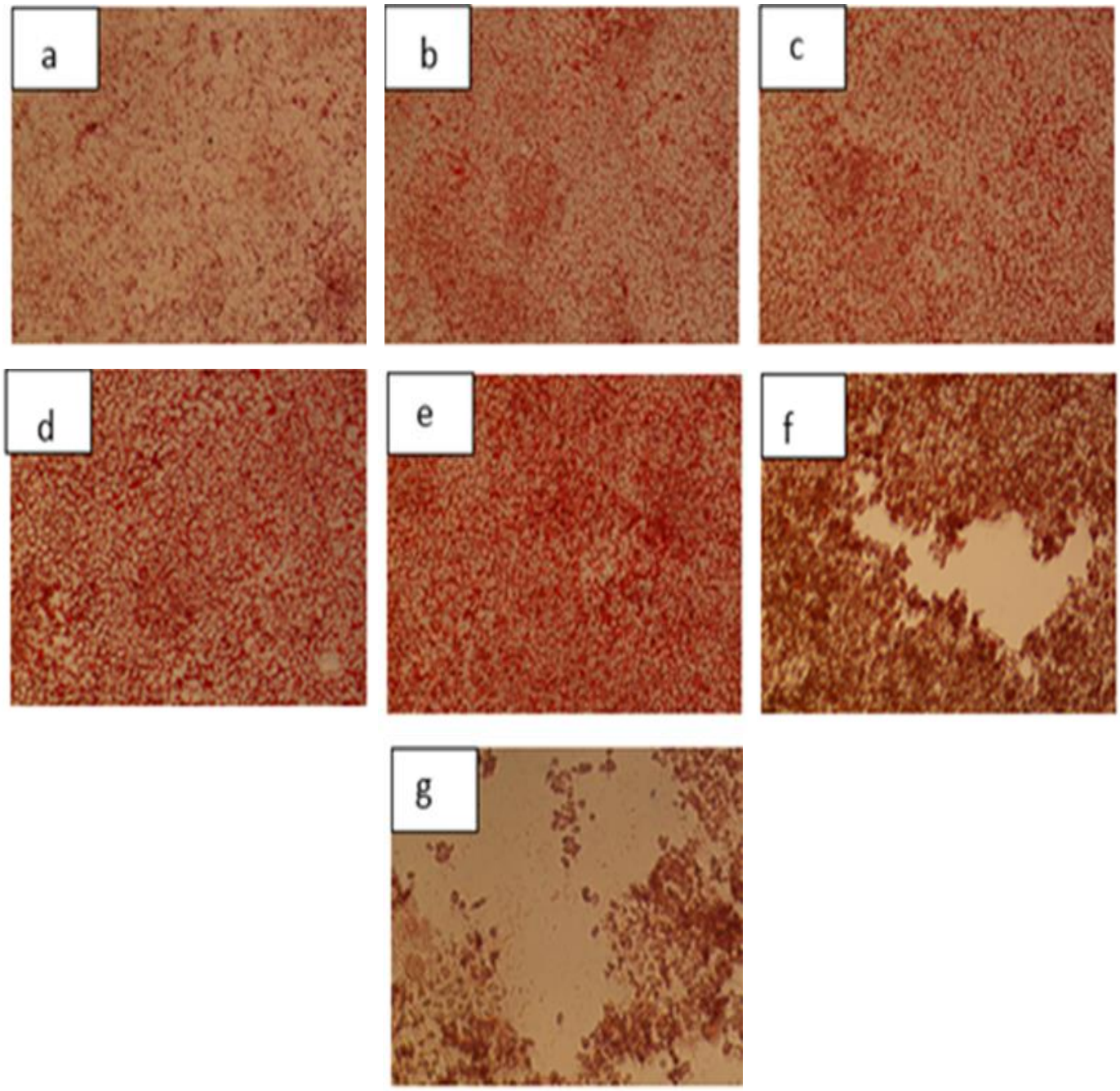

Figure 4.4: Induction of hepatic steatosis by oleic acid in C3A liver cells.
Cells were cultured in EMEM with 8 mM glucose supplemented with various concentrations (0.125, 0.25, 0.5, 0.75, 1 and 2 mM) oleic acid for 48 hours. Intracellular lipid accumulation was visually assessed using oil red O staining; (a) untreated, (b) 0.125 mM oleic acid, (c) 0.25 mM oleic acid, (d) 0.5 mM oleic acid, (e) 0.75 mM oleic acid, (f) 1 mM oleic acid and (g) 2 mM oleic acid. Photomicrographs taken at 400x magnification.

4.1.2. Effect of GRT extract on oleic acid induced cytotoxicity.

In terms of GRT extract cytotoxicity in C3A cells, no significant effect on cell viability was evident in C3A cells cultured for 24 hrs with GRT extract, as determined by the MTT assay, compared to the control (Figure 4.5A). C3A cells were treated with oleic acid for 24 hrs, and GRT extract at 1, 10 and 100 µg/ml either during oleic acid treatment (simultaneous group) or following oleic acid treatment for a further 24 hrs (post-treatment group). The GRT extract increased MTT activity under both treatment conditions ($p< 0.05$, $p< 0.001$ and $p< 0.001$), for simultaneous treatment and ($p< 0.05$, $p< 0.01$ and $p< 0.001$) for post treatments (Figure 4.5B and C). Pioglitazone (25 µM), used as a positive control, also increased MTT activity under both treatment conditions $p< 0.001$ for simultaneous treatments and $p< 0.05$ for post treatments, relative to the control group. The results demonstrated that GRT extract was non-toxic at all concentrations tested.

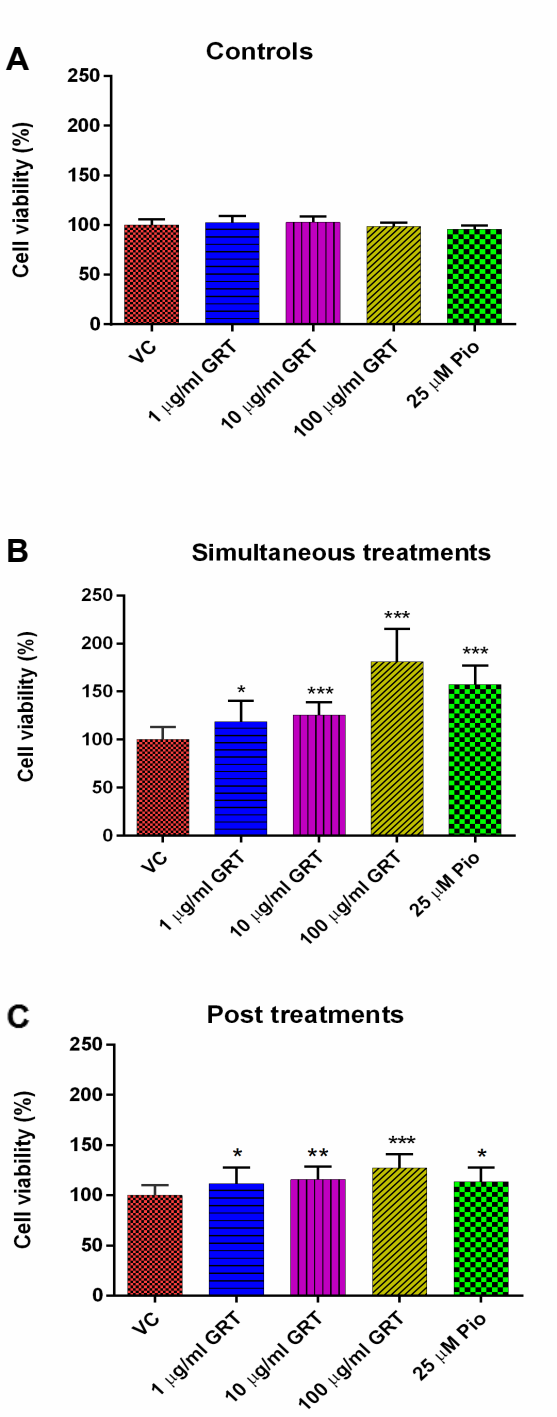

Figure 4.5: Evaluation of GRT extract cytotoxicity on oleic acid treated C3A liver cells.
C3A cells were cultured to confluence in EMEM media and treated with 1 mM oleic acid for 24 hours, then treated with different concentrations of GRT extract (1, 10 and 100 µg/ml) and pioglitazone (25 µM) for 24 hours. The GRT extract treatments were either performed on controls not exposed to oleic acid (A), during oleic acid induction (simultaneous group) (B) or after oleic acid induction (post treatment group) (C). Cell viability was assessed by MTT read at 570 nm. Data is presented as the mean ± SD of three independent experiments, expressed to the relative control set at 100%. *p< 0.05, **p< 0.01, ***p< 0.001.

4.1.3. The effect of GRT extract on oleic acid induced steatosis.

The effect of GRT extract on oleic acid induced steatotic C3A liver cells was assessed using various concentrations of GRT extract (1, 10 and 100 µg/ml) for a period of 24 hrs. Intracellular lipid content was determined using ORO staining. The effects of GRT on cellular lipid content varied according to the oleic acid treatment and concentration of GRT used. In the control group (cells not exposed to oleic acid) GRT extract reduced lipid content ($p < 0.05$, $p < 0.01$, $p < 0.01$) (Figure 4.6A).

In the presence of oleic acid (simultaneous treatment group) the high concentration of GRT (100 µg/ml) and pioglitazone (positive control) enhanced lipid accumulation ($p < 0.001$) (Figure 4.6B). In contrast, in the post-treatment group (cells treated with GRT extract after oleic acid induction), GRT extract appeared to non-significantly reduce lipid accumulation in a concentration-dependent manner (Figure 6C). A similar effect was observed for pioglitazone.

This effect was substantiated by visualizing intracellular lipid content stained with ORO using phase contrast microscopy. The control group displayed minimal lipid accumulation as indicated by negative staining of ORO (Figure 4.7). In the simultaneous treatment group, an increase in lipid content was observed for high dose GRT extract (100 µg/mL) and pioglitazone (Figure 4.8). In the post treatment group, GRT extract at a low concentration (1 µg/mL) visibly increased intracellular lipid content, whilst higher concentrations (10 and 100 µg/mL) decreased lipid content (Figure 4.9).

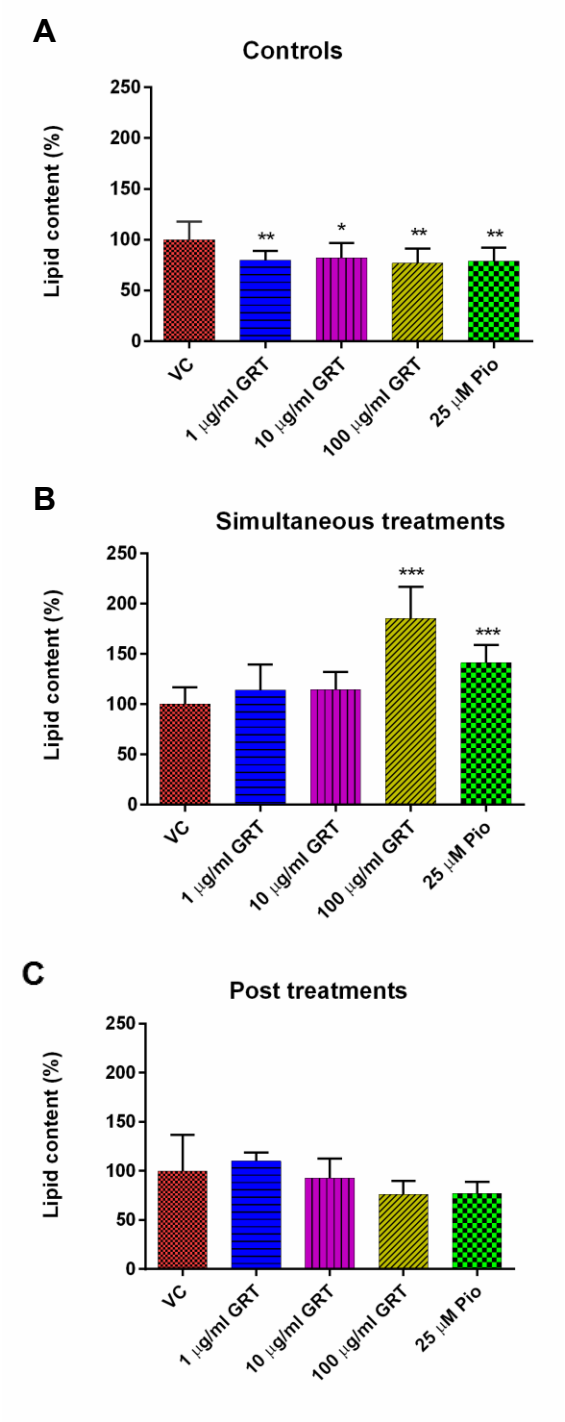

Figure 4.6: The effect of GRT extract on lipid content in oleic acid induced C3A liver cells.
C3A cells were cultured in EMEM with 8 mM glucose, induced with 1 mM of oleic acid for 24 hours. Oleic acid treated cells were then also treated with different concentrations of GRT extract (1, 10 and 100 µg/ml) and pioglitazone (25 µM) for 24 hours. The GRT extract treatments were either performed on controls not exposed to oleic acid (A), during oleic acid induction (simultaneous treatment group) (B) or after oleic acid induction (post treatment group) (C). Lipid content was assessed by ORO staining read at 490nm. Data presented as mean ± SD of three independent experiments, normalized to crystal violet and expressed to the relative control set at 100%. *p< 0.05, **p< 0.01, ***p< 0.001.

CONTROL

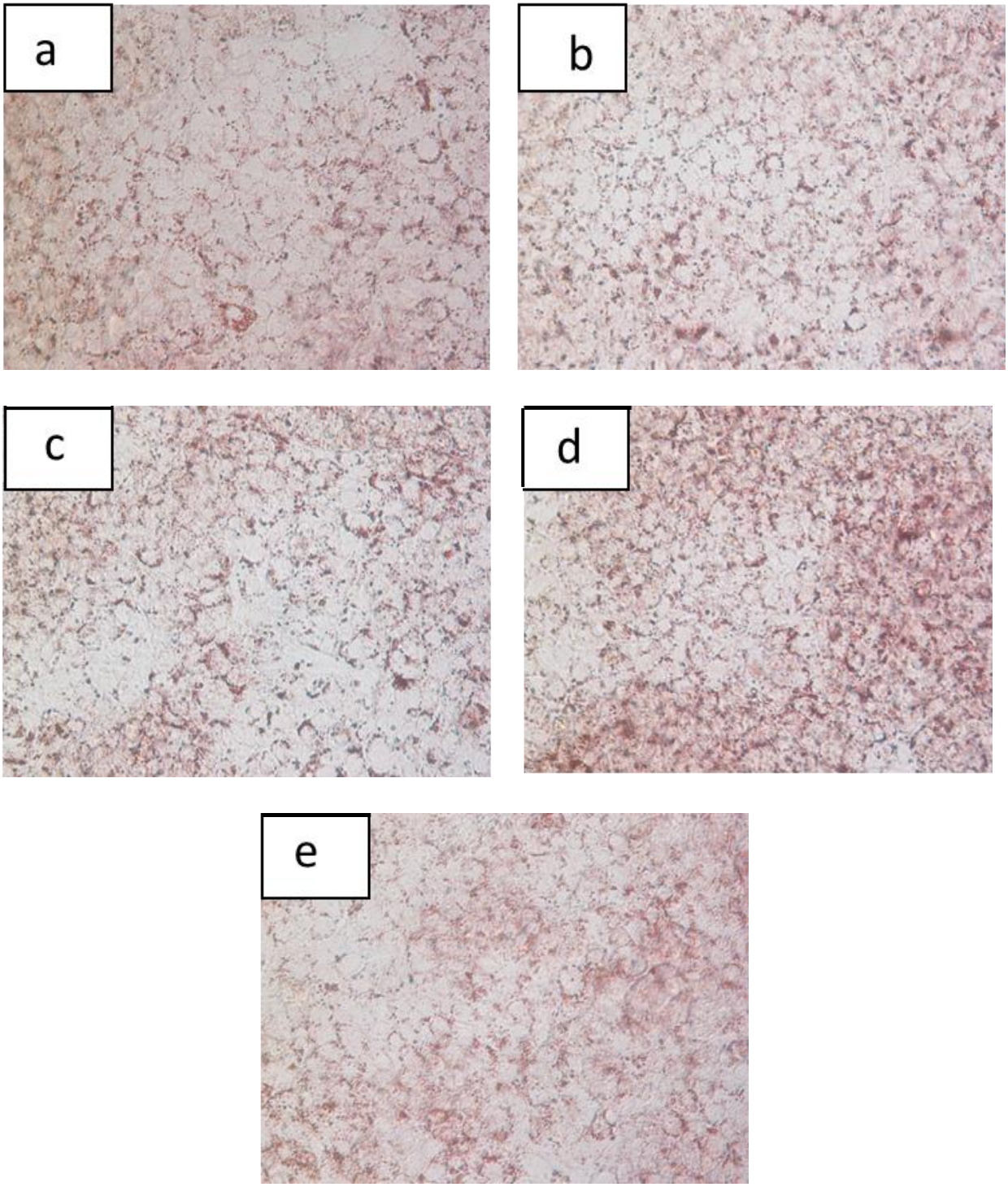

Figure 4.7: The effect of GRT extract in control C3A liver cells.
C3A cells were cultured in EMEM with 8 mM glucose, and (a) control (untreated), (b) 1 µg/ml of GRT, (c) 10 µg/ml, (d) 100 µg/ml of GRT and (e) 25 µM pioglitazone, respectively. Lipid accumulation was visualized by oil red O staining. Images were taken at 400x magnification.

STEATOTIC C3A LIVER CELLS TREATED WITH GRT EXTRACT

Simultaneous treatments (GRT extract treatment during oleic acid induction)

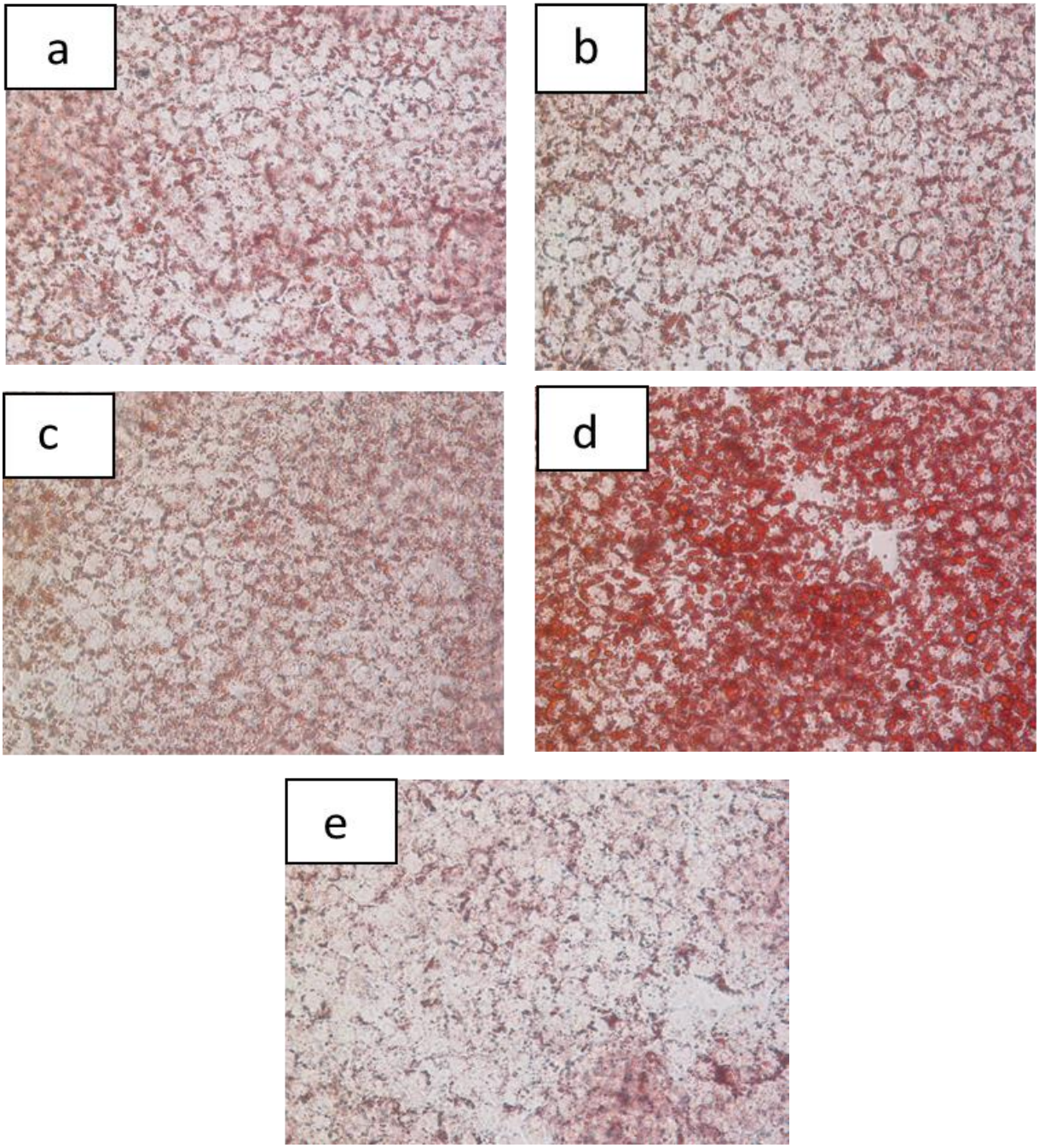

Figure 4.8: The effect of GRT extract on C3A liver cells treated with oleic acid.
C3A cells were cultured in EMEM with 8 mM glucose. GRT extract treatment was initiated during the induction of steatosis with oleic acid (simultaneous treatment group) for 24 hours. Photomicrographs of steatotic C3A cells treated with (a) control (untreated), (b) 1 µg/ml of GRT, (c) 10 µg/ml of GRT, (d) 100 µg/ml of GRT and (e) 25 µM pioglitazone, respectively. Lipid accumulation was visualized by oil red O staining. Images were taken at 400x magnification.

Post treatments (GRT extract treatment following oleic acid induction)

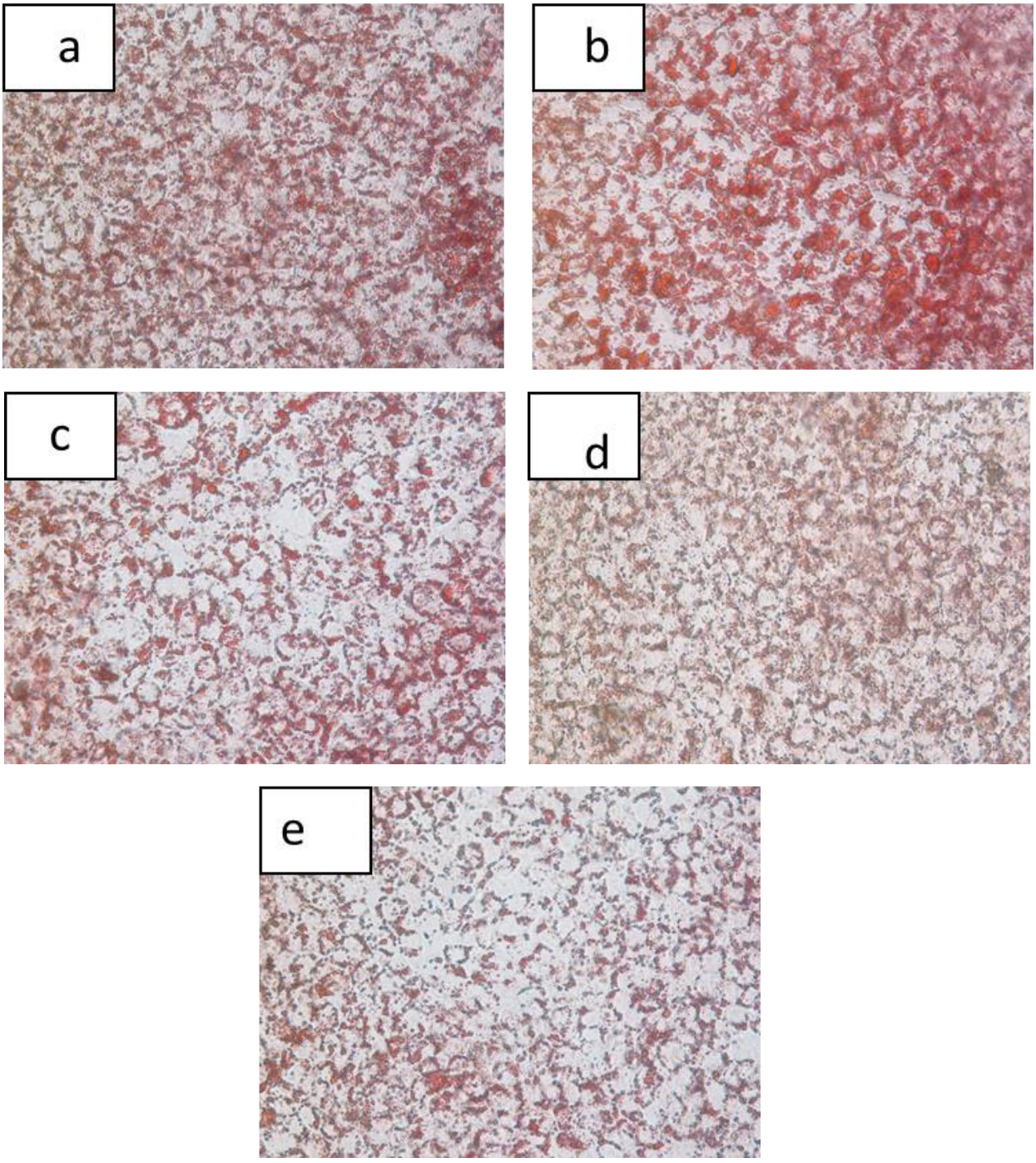

Figure 4.9: The effect of GRT extract on C3A liver cells after induction with oleic acid.
C3A cells were cultured in EMEM with 8 mM glucose and treated with oleic acid for 24 hours. GRT extract treatment was initiated after oleic acid induction for a further 24 hours (post-treatments group). Photomicrographs of steatotic C3A cells treated with (a) control (untreated), (b) 1 µg/ml of GRT, (c) 10 µg/ml of GRT, (d) 100 µg/ml of GRT and (e) 25 µM Pioglitazone, respectively. Lipid accumulation was visualized by oil red O staining. Images were taken at 400x magnification.

4.1.4 The effect of GRT extract on mRNA of oleic acid induced steatotic C3A liver cells

The effect of GRT extract on genes related to NAFLD was assessed in oleic acid induced steatotic C3A liver cells using qRT-PCR. Treating steatotic C3A liver cells with GRT extract decreased the relative mRNA expression levels of two key genes regulating glucose metabolism, namely carbohydrate responsive element binding protein (ChREBP) and glucokinase (GCK) (Figure 4.10).

GRT extract and pioglitazone appeared to have no effect on ChREBP expression in control cells (Figure 4.10A). In the simultaneous treatments group, 1 µg/ml and 10 µg/ml GRT significantly lowered mRNA levels of ChREBP ($p< 0.05$, $p< 0.01$) and at the higher concentration GRT (100 µg/ml) induced a slight but non-significant decrease compared to the vehicle control (18%) (Figure 4.10B). In the post treatment group, 10 and 100 µg/ml GRT extract decreased ChREBP expression ($p< 0.01$, $p< 0.05$) compared to the vehicle control (untreated) while pioglitazone (positive control) showed $p< 0.05$ decrease compared to vehicle control (Figure 4.10C).

GCK, an enzyme playing a key role in glycogen synthesis, was also decreased by GRT extract for both simultaneous and post treatments compared to the control group (untreated). Although GRT treatment had no effect on GCK expression in the control cells (Figure 4.10D), for cells in the simultaneous treatment group, treated with 1 µg/ml and 10 µg/ml GRT extract, the mRNA expression levels of GCK were decreased ($p< 0.01$, $p< 0.01$) (Figure 4.10E). In the post-treatment group, a decrease was observed for 10 and 100 µg/ml GRT ($p< 0.05$, $p< 0.01$), respectively (Figure 4.10F).

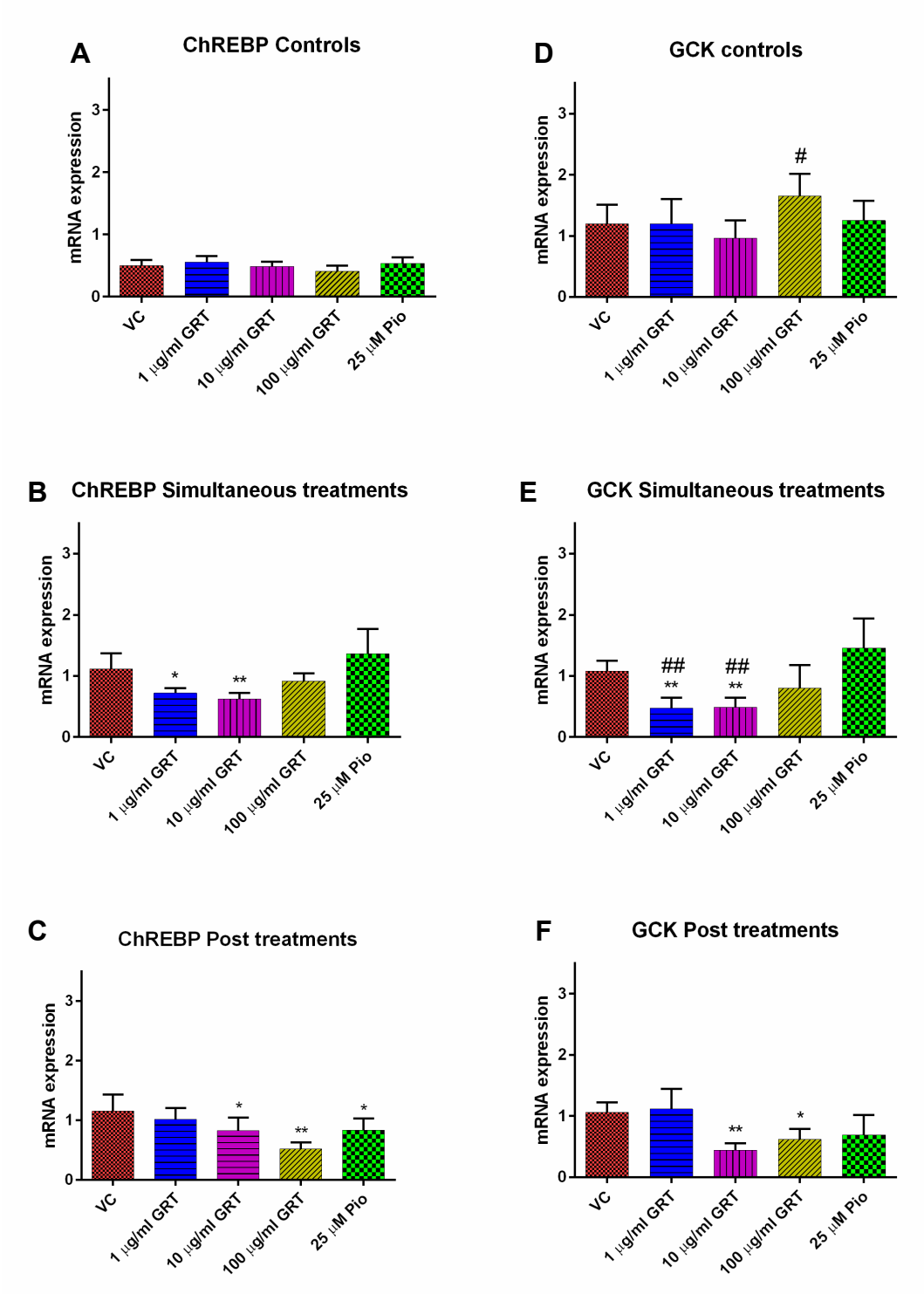

Figure 4.10: The effect of GRT extract on ChREBP and GCK mRNA expression in oleic acid induced C3A liver cells.
RT-qPCR analysis of carbohydrate responsive element binding protein (ChREBP) and glucokinase (GCK). The data is presented as the relative mRNA expression of the specific genes to the housekeeping genes β-actin and GAPDH. Data is presented as mean ± SD of three independent experiments. *p value < 0.05, **p< 0.01 compared to vehicle control #p< 0.05, ##p < 0.01 compared to pioglitazone.

4.1.5 The effect of GRT extract on mRNA expression of genes involved in lipid metabolism in oleic acid induced steatotic C3A cells

Synthesis of fats is essential for the body because of the role that fats play in the body homeostasis for energy storage and utilization. Hence, we investigated the effect of GRT on the expression of hepatic genes involved in lipid metabolism. An increase ($p< 0.05$), relative to the control in mRNA levels of SREBP 1c in the control group, was observed for 1 µg/ml GRT treated cells ($p< 0.01$) compared to the controls and relative to pioglitazone (Figure 4.11A). SREBP 1c expression was decreased by 1, 10 and 100 µg/ml GRT extract treatment of the simultaneous treatment group ($p< 0.05$, $p< 0.01$, $p< 0.05$) (Figure 4.11B) whilehile GRT extract had no effect on SREBP 1c expression following oleic acid treatment (post treatment group) (Figure 4.11C).

For PPAR-α, GRT extract treatment had no effect on control cells (Figure 4.11D). However, in the simultaneous treatment group, GRT extract treatment lowered PPAR-α mRNA expression at 10 and 100 µg/ml ($p< 0.05$ and $p< 0.01$) (Figure 4.11E). In the post-treatment group, GRT extract lowered PPAR-α expression at 1, 10 and 100 µg/ml ($p< 0.05$, $p< 0.05$, $p< 0.01$) in comparison to the vehicle control (Figure 4.11F).

GRT extract had no effect on FASN expression in the control group (Figure 4.12A). However, in the simultaneous and post-treatment groups, GRT extract reduced the relative expression of FASN in a concentration-dependent manner. In the simultaneous treatment group, GRT extract reduced the relative expression by 30%, 47% and 60%, respectively, with 100 µg/ml showing a significant difference to the control ($p< 0.05$) (Figure 4.12B).

In the post treatment group, GRT extract had a similar concentration dependent effect on mRNA expression for 1 ($p< 0.05$), 10 ($p< 0.01$) and 100 µg/ml ($p< 0.001$) of GRT extract treatments, respectively. Pioglitazone treatment also showed a decrease ($p< 0.05$)

compared to the vehicle control when post treated. In the post-treatment group, pioglitazone decreased FASN expression by 21% compared to the control (Figure 4.12C).

In the control cells, GRT extract treatment decreased CPT-1 expression at all concentrations (Figure 4.12D) whilst GRT extract had no effect on CPT-1 expression in the simultaneous and post treated cells. Pioglitazone increased CPT-1 expression relative to the control in both the simultaneous and post treatment groups (Figure 4.12E and F).

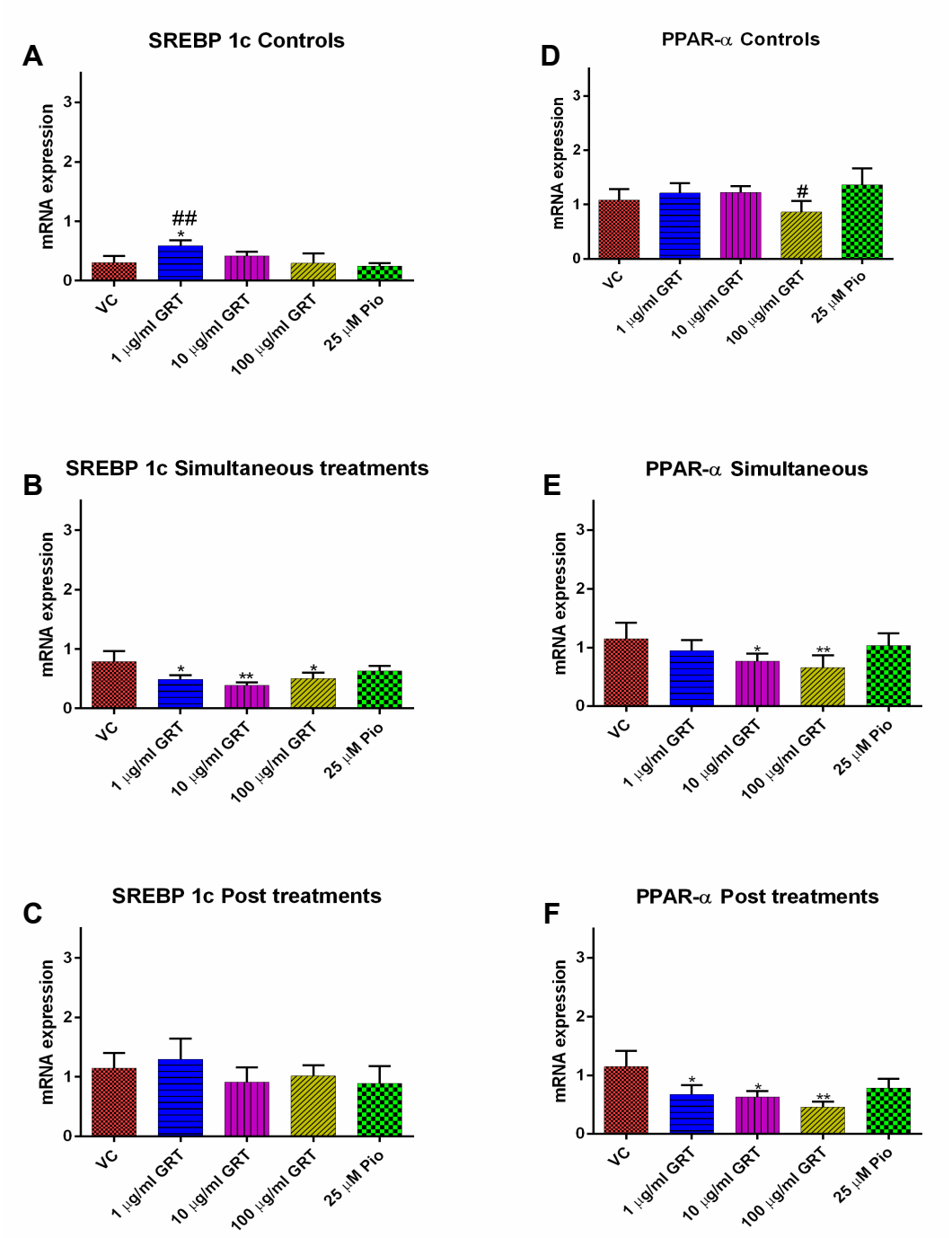

Figure 4 acid induced C3A liver cells.

RT-qPCR analysis of Sterol regulatory element binding protein (SREBP 1c) and peroxisome proliferator-activated receptor alpha (PPAR alpha) mRNA expression. The data is presented as mean ± SD of three independent experiments. Expressed relative to mRNA levels of β-actin and GAPDH *p value < 0.05, ** < 0.01 compared to vehicle control #p< 0.05, ##p < 0.01, ###p < 0.001 compared to pioglitazone.

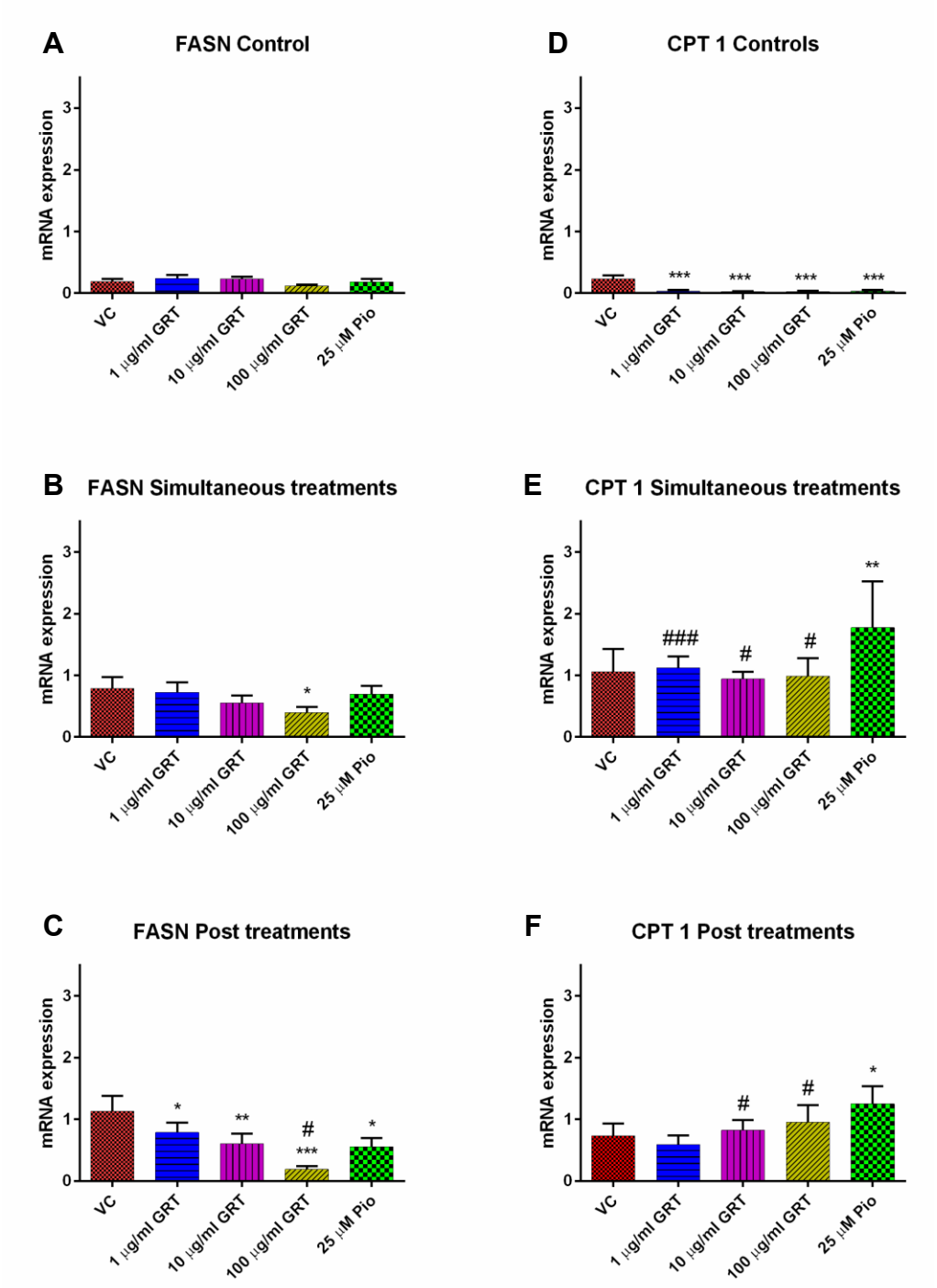

Figure 4.12: The effect of GRT extract on FASN and CPT-1 mRNA expression in oleic acid induced C3A liver cells.

RT-qPCR analysis of fatty acid synthase (FASN) and carnitine palmitoyltransferase I (CPT 1) mRNA expression. The data is presented as mean ± SD of three independent experiments. Expressed relative to mRNA levels of β-actin and GAPDH *p value <0.05, **p <0.01, ***p <0.001 compared to vehicle control #p<0.05, ###p <0.001 compared to pioglitazone.

4.1.6 The effect of GRT extract on inflammation

As liver injury occurs in response to inflammation, we used mRNA expression of the proinflammatory cytokine TNF-α as an inflammatory marker. In the controls, GRT extract at 1 µg/ml appeared to increase TNF-α mRNA expression (Figure 4.13A). In the simultaneous treatment group, GRT extract decreased TNF-α mRNA expression at 10 and 100 µg/ml ($p< 0.01$, $p< 0.01$) (Figure 4.13B) and in the post-treatment group, GRT extract concentration-dependently decreased TNF-α mRNA expression at 10 and 100 µg/ml ($p< 0.05$, $p< 0.01$). Treating with pioglitazone resulted in ($p< 0.01$) decrease in the post treatment group (Figure 4.13C).

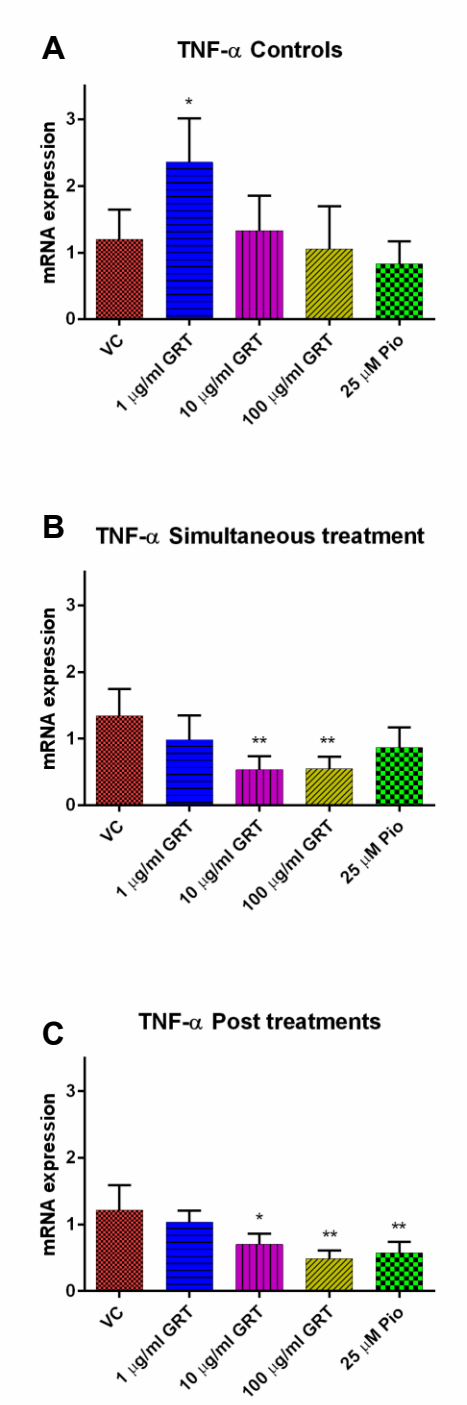

Figure 4.13: The effect of GRT extract on TNF-α mRNA expression in oleic acid induced C3A liver cells.

RT-qPCR analysis of tumor necrosis factor-alpha (TNF-α) expression was performed. The data is presented as mean ± SD of three independent experiments expressed relative to the housekeeping genes, β-actin and GAPDH. *p value < 0.05, **p< 0.01 compared to vehicle control.

4.2 Section B- *In vivo* study

In vivo studies are commonly utilized to validate *in vitro* results in appropriate living animal models, enabling the observation of *in vitro* pathophysiological mechanisms. One of the objectives of this study was to investigate the effect of GRT extract on hepatic steatosis in obese leptin resistant *db/db* mice and their lean *db/+* littermates. Different dosages of GRT extract and pioglitazone (used as a positive control) were administered to the mice to further investigate the effect of treatments *in vivo*.

4.2.1 Effects of GRT extract on food intake, body and liver weights of *db/db* mice

GRT administration for 10 weeks had no significant effect on food intake or body weights of the lean *db/+* and obese *db/db* mice (Figures 4.14 and 4.15). In terms of liver-to-body weight ratio, in the lean mice the ratio decreased slightly in mice that received 740 mg/kg BW for 10 weeks (Figure 4.16A). However, no effect on liver-to-body weight was observed in the obese *db/db* mice treated with GRT extract (Figure 4.16B).

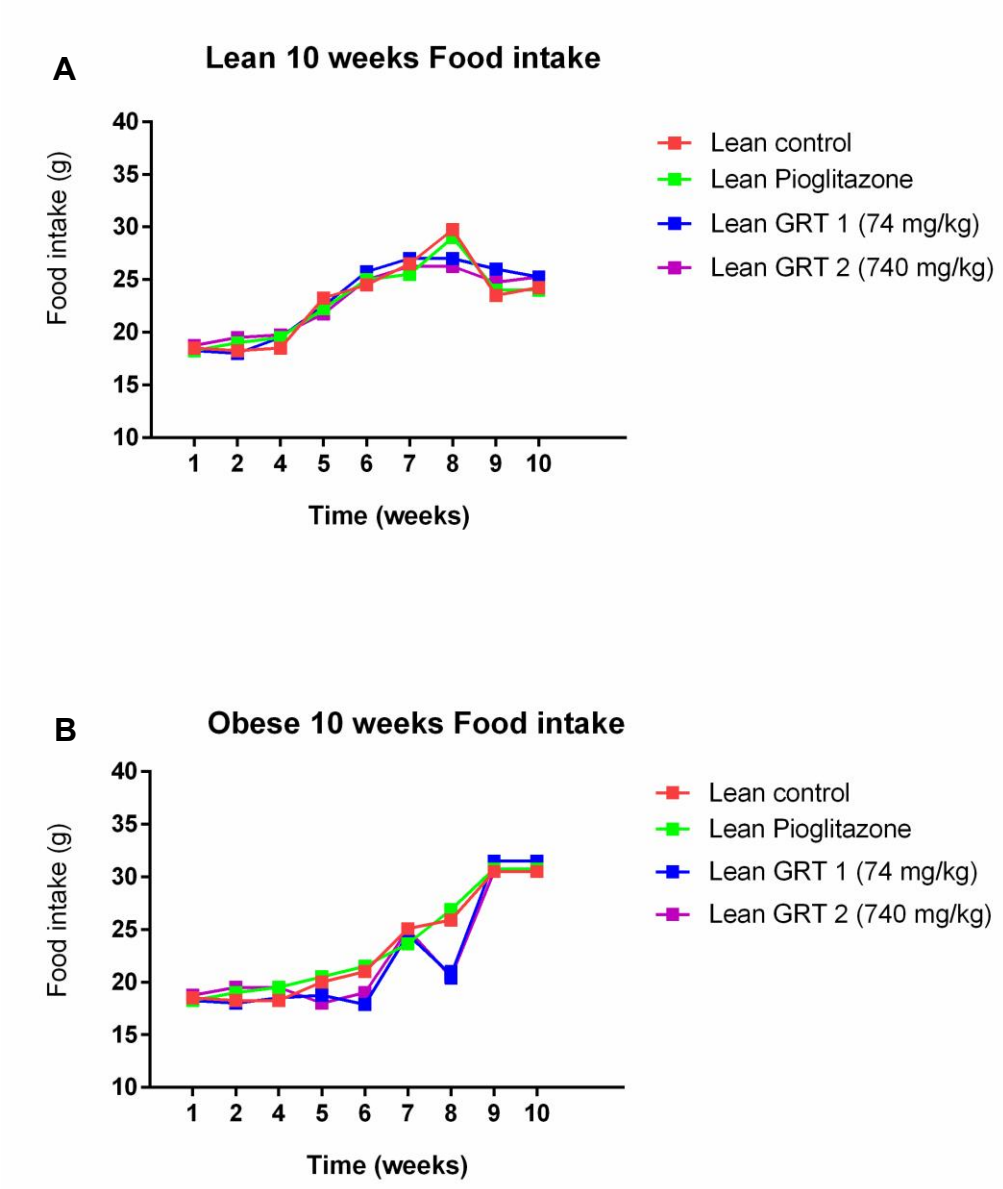

Figure 4.14: The effect of GRT extract on food intake in *db/db* and *db/+* mice.
Lean *db/+* (A) and obese *db/db* (B) mice received daily oral doses of GRT extract at 74 or 740 mg/kg body weight (BW) for 10 weeks. Controls receiving only water, and pioglitazone administrated orally at a dose of 10 mg/kg BW was included as a positive control. Data expressed as mean ± SD of eight mice per group.

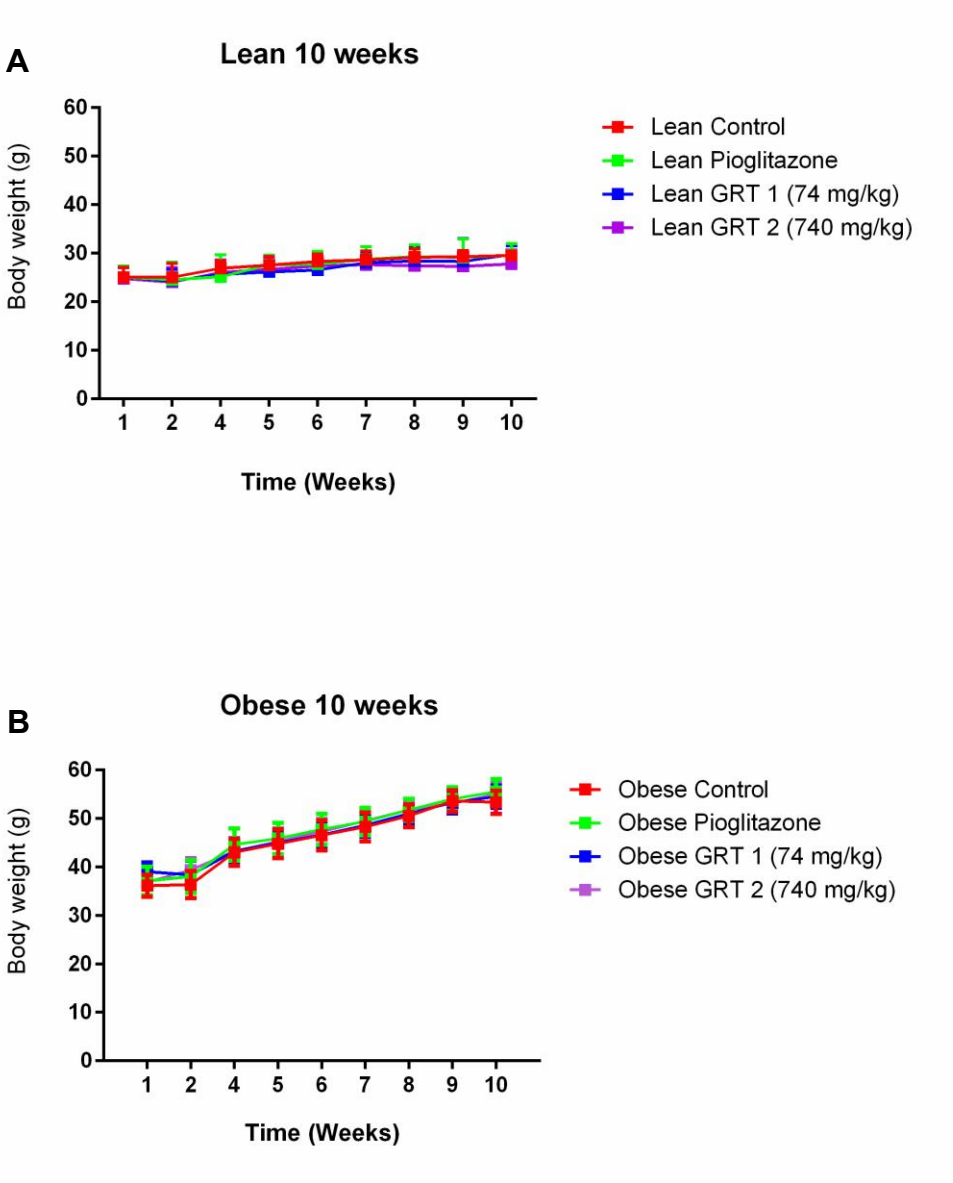

Figure 4.15: The effect of GRT extract on body weight gain of *db/db* and *db/+* mice.
Lean *db/+* (A) and obese *db/db* (B) mice received daily oral doses of GRT extract at 74 or 740 mg/kg body weight (BW) for 10 weeks. Controls receiving only water, and pioglitazone administrated orally at a dose of 10 mg/kg BW was included as a positive control. Data expressed as mean ± SD of eight mice per group.

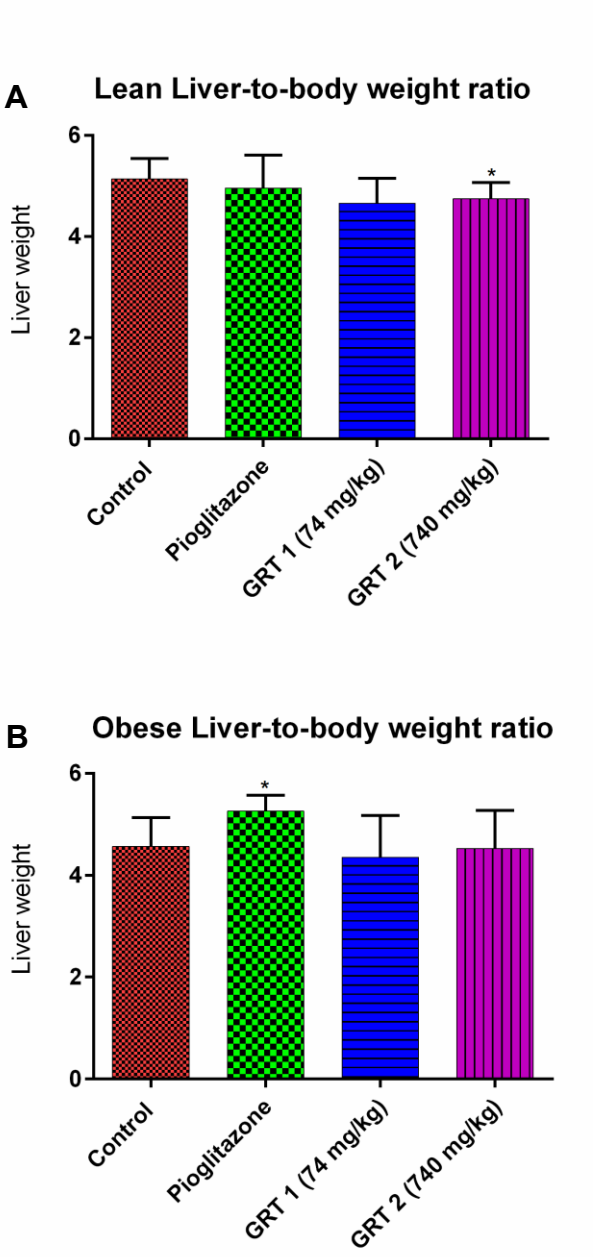

Figure 4.16: The effects of GRT extract on the liver-to-body weight ratio of *db/db* and *db/+* mice. Lean *db/+* (A) and obese *db/db* (B) mice received daily oral doses of GRT extract at 74 or 740 mg/kg body weight (BW) for 10 weeks. Control receiving only water, and pioglitazone administrated orally at a dose of 10 mg/kg BW was included as a positive control. Data expressed as mean ± SD of eight mice per group. *$p < 0.05$.

4.2.2 The effects of GRT extract on blood glucose parameters.

The effects of GRT extract on blood glucose levels in lean *db/+* and obese *db/db* mice were assessed. GRT had no effect on the fasting glucose levels of the lean mice (Figure 4.17A). In the obese *db/db* mice, GRT extract treatment at a dose of 740 mg/kg and pioglitazone, the positive control, reduced fasting glucose levels, however these effects were not significant (Figure 4.17B). Glucose tolerance was assessed using an oral glucose tolerance test (OGTT). No effect was observed in lean control mice however, pioglitazone appeared to improve glucose clearance ($p < 0.05$) (Figure 18A &19A). In the obese *db/db* mice, GRT extract lowered the OGTT AUC values however the effect was also not significant (Figure 18B & 19B). This data indicated that GRT extract has the potential role to ameliorate disorders of glucose in obese mice.

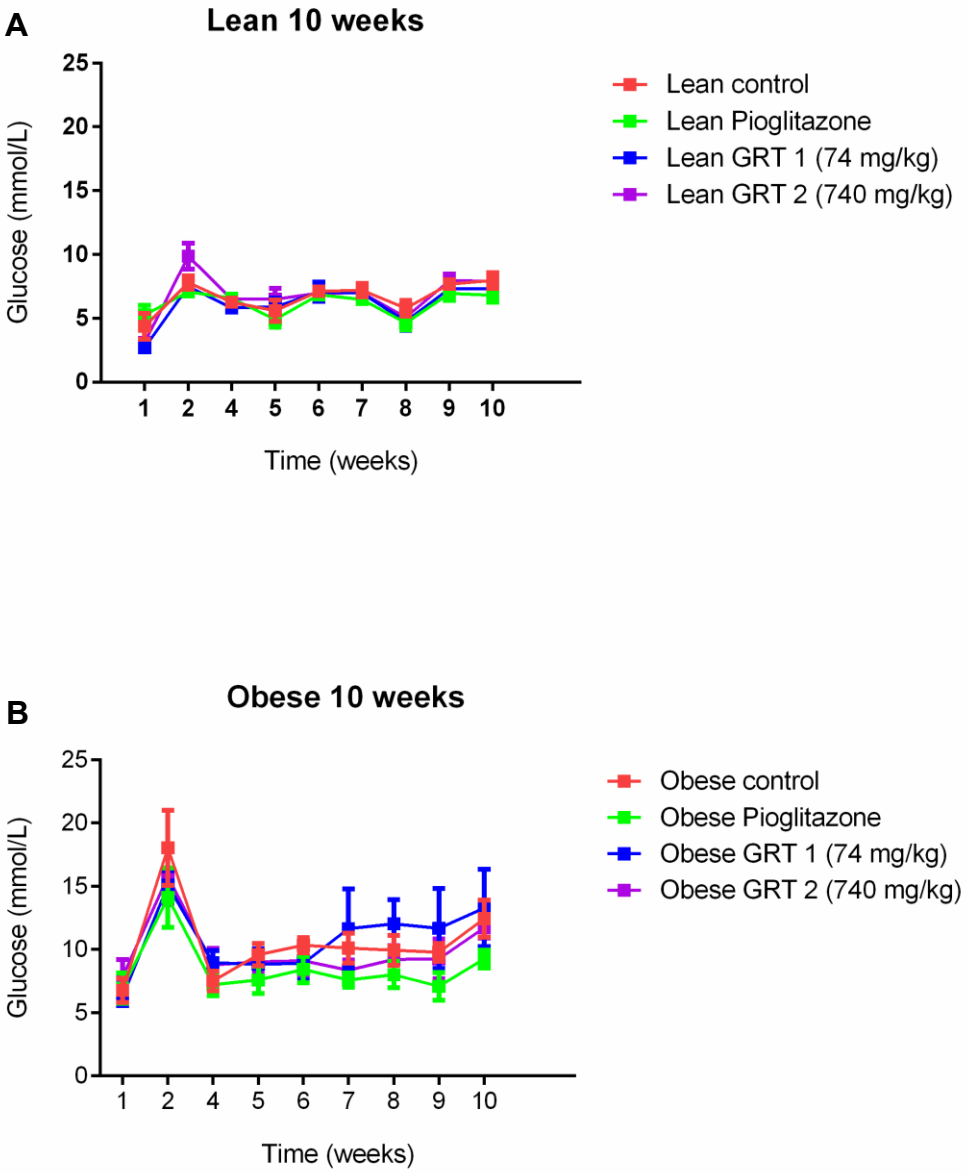

Figure 4.17: The effects of GRT extract on fasting blood glucose levels in *db/db* and *db/+* mice. Lean *db/+* (A) and obese *db/db* (B) mice received daily oral doses of GRT extract at 74 or 740 mg/kg body weight (BW) for 10 weeks. Controls receiving only water, and pioglitazone administrated orally at a dose of 10 mg/kg BW was included as a positive control. Data expressed as mean ± SD of eight mice per group.

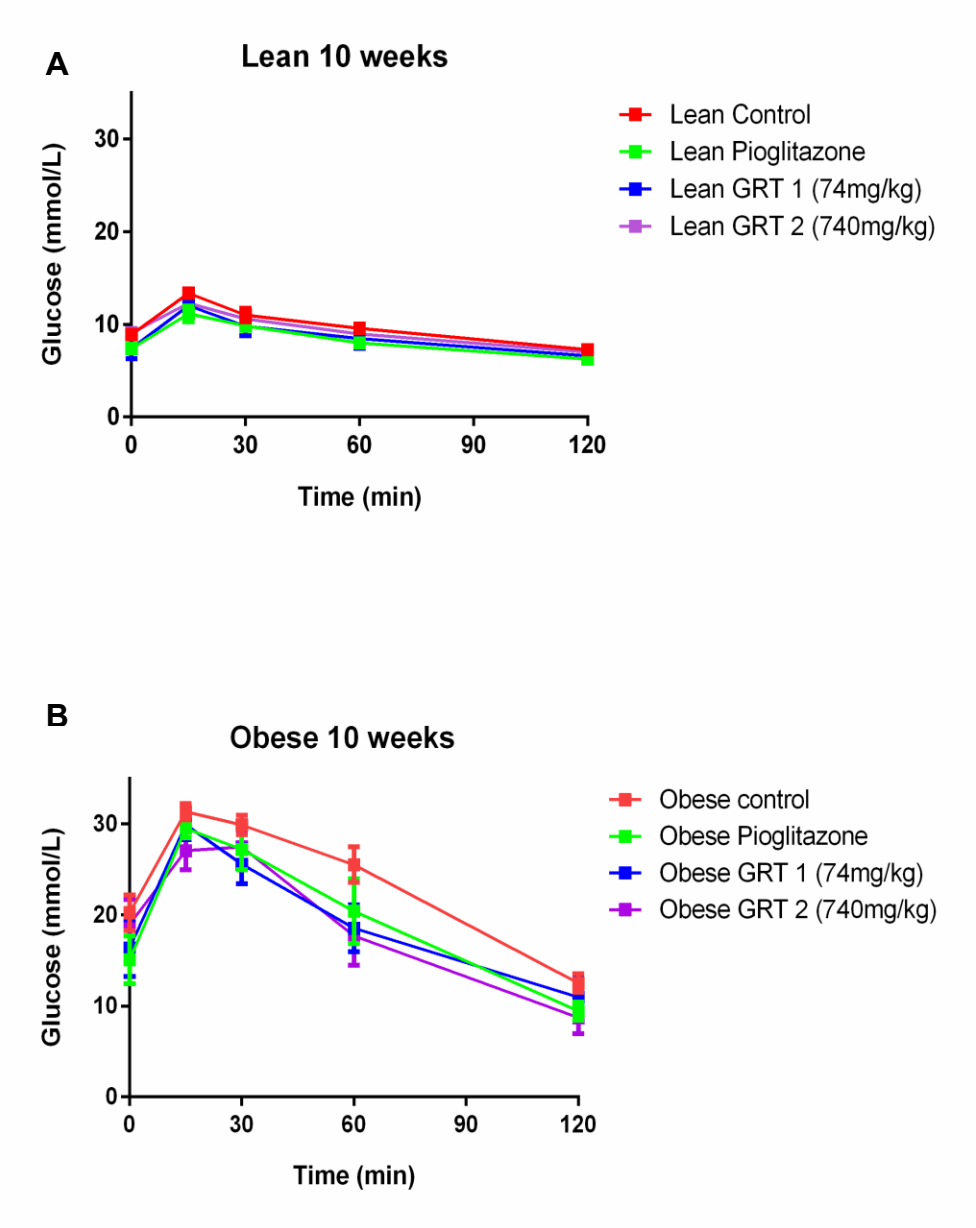

Figure 4.18: The effects of GRT extract on oral glucose tolerance for *db/db* and *db/+* mice.
Lean *db/+* (A) and obese *db/db* (B) mice received daily oral doses of GRT extract at 74 or 740 mg/kg body weight (BW) for 10 weeks. Controls receiving only water, and pioglitazone administrated orally at a dose of 10 mg/kg BW was included as a positive control. Data expressed as mean ± SD of eight mice per group.

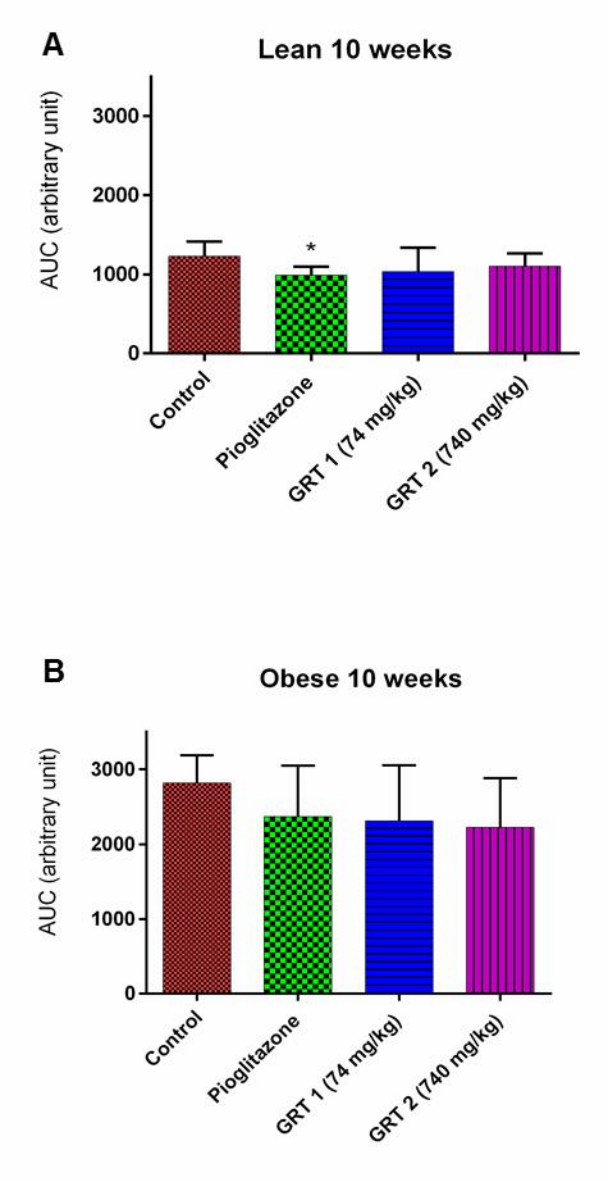

Figure 4.19: The effects of GRT extract on glucose tolerance (area under the curve) for *db/db* and *db/+* mice.
Lean *db/+* (A) and obese *db/db* (B) mice received daily oral doses of GRT extract at 74 or 740 mg/kg body weight (BW) for 10 weeks. Controls receiving only water, and pioglitazone administrated orally at a dose of 10 mg/kg BW was included as a positive control. Data expressed as mean ± SD of eight mice per group. *p< 0.05.

4.2.3 The effects of GRT extract on mRNA expression of obese *db/db* and lean *db/+* mice liver samples

The effect of GRT extract (74 and 740 mg/kg) was assessed on the mRNA expression of genes involved in cholesterol synthesis (APOA1, APOA4, HMGCR and HMGCS), lipid synthesis (SREBP 1c, PPAR α, ACACA and FASN) and glucose metabolism (ChREBP) in obese *db/db* and lean *db/+* mice following a 10-week treatment period.

4.2.4 The effect of GRT extract on carbohydrate responsive element binding protein (ChREBP) of obese *db/db* and lean *db/+* mice liver samples

GRT extract had no effect on ChREBP mRNA expression in the lean *db/+* and obese treated mice (Figure 4.20A and B). However, when compared to the *db/+* lean untreated group (control) in the obese *db/db* untreated mice, the relative expression of ChREBP appeared to be increased but the difference was not significant (Figure 4.20B).

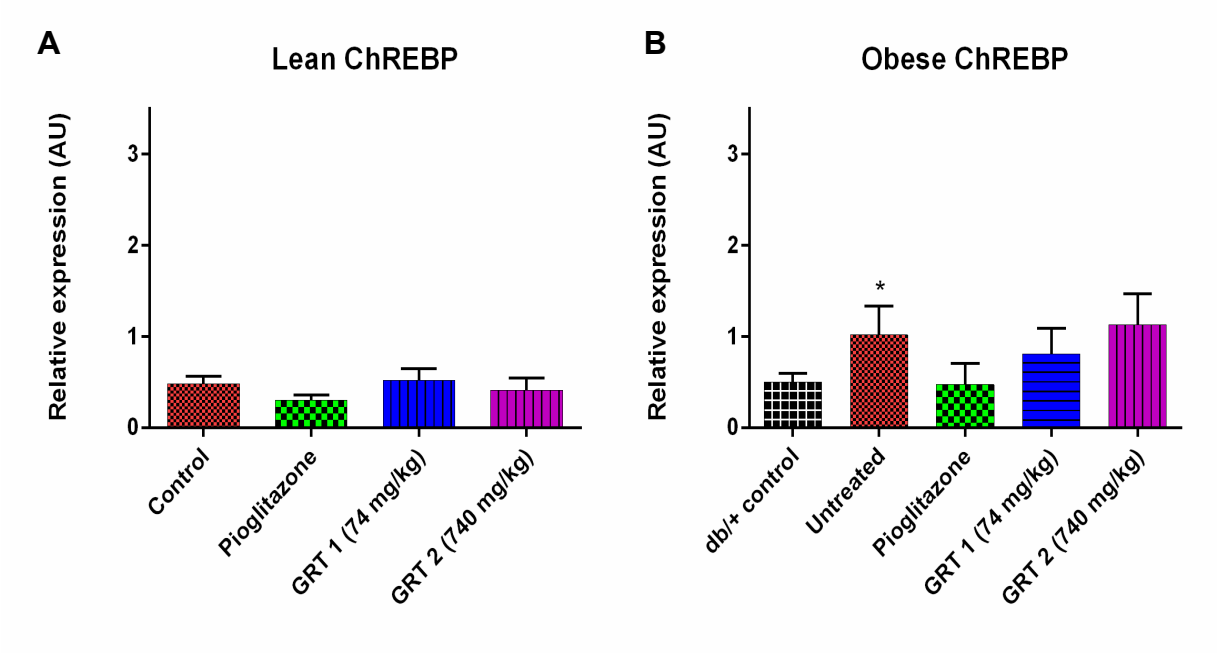

Figure 4.20: The relative mRNA expression of ChREBP in the liver of lean *db/+* and obese *db/db* mice treated with GRT extract.
Lean *db/+* (A) and obese *db/db* (B) mice received daily oral doses of GRT extract at 74 or 740 mg/kg body weight (BW) for 10 weeks. Controls receiving only water, and pioglitazone administrated orally at a dose of 10 mg/kg BW was included as a positive. Data expressed as mean ± SD of eight mice per group. *p< 0.05 compared to control.

4.2.5 The effects of GRT extract on lipid metabolism genes of obese *db/db* and lean *db/+* mice liver samples

The relative mRNA expression of ACACA in the obese *db/db* controls was increased relative to the lean *db/+* control mice ($p < 0.05$). GRT extract decreased ACACA mRNA expression in the *db/db* mice with 74 mg/kg the most effective ($p < 0.05$), compared to untreated *db/db*, in normalizing the increased expression in the obese *db/db* mice compared to the lean *db/+* control mice (Figure 4.21A and B). FASN mRNA expression was also increased in the obese *db/db mice* relative to the *db/+* controls and similar to ACACA, GRT extract reduced the increased FASN expression with the lower dose of 74 mg/kg the most effective ($p=0.01$) (Figure 4.21C and D).

GRT extract had no effect on the mRNA expression of the transcription factor SREBP 1c of lean *db/+* mice. In comparison to the lean mice, SREBP 1c expression was significantly increased in the obese *db/db* mice ($p < 0.01$). GRT and pioglitazone treatment appeared to modulate the increased expression, but the effect was not statistically significant (Figure 4.22B). The expression of PPARα was not affected by GRT treatment in either the lean *db/+* or the obese *db/db* mice (Figure 4.22C & D).

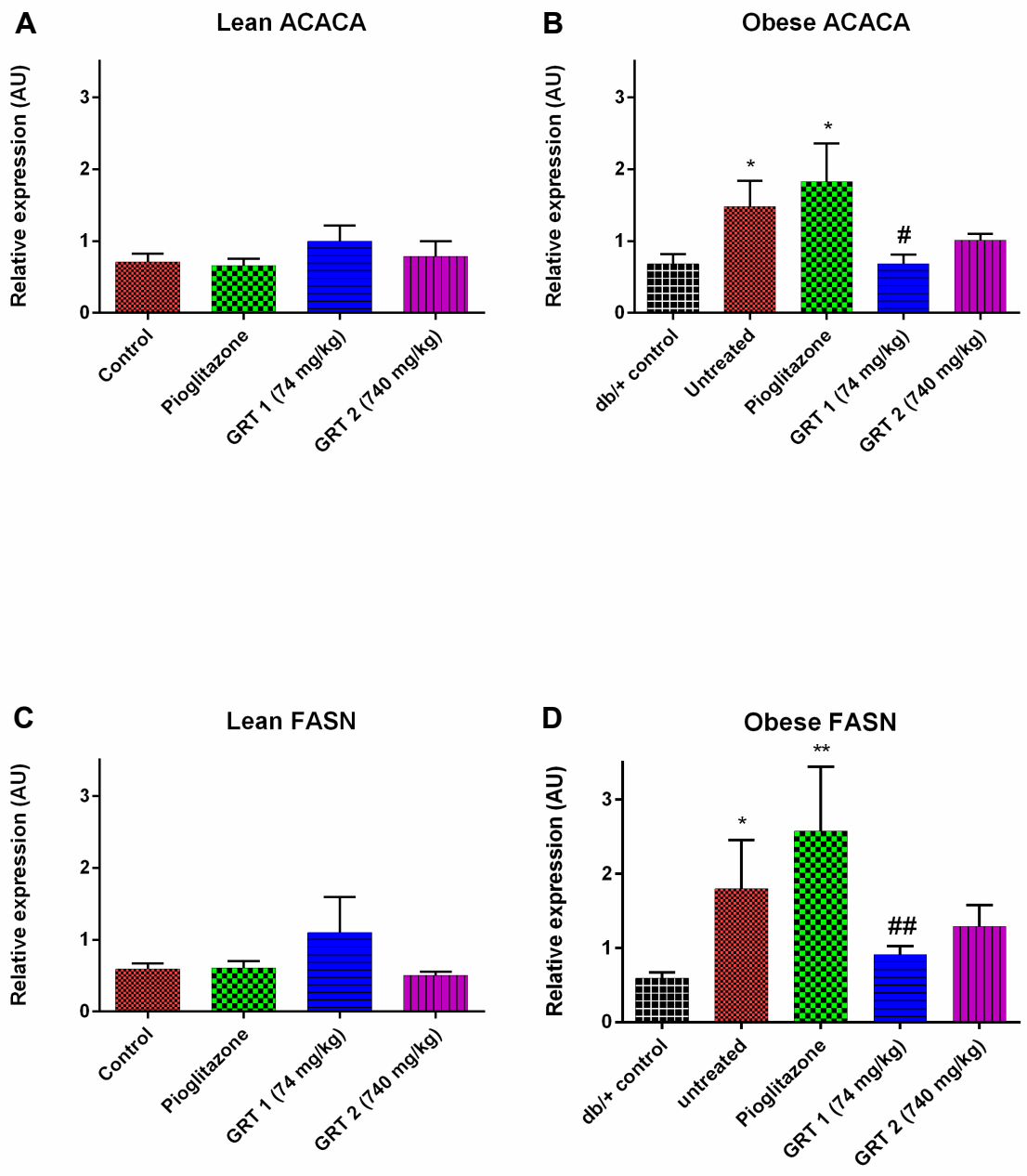

Figure 4.21: Relative mRNA expression of ACACA and FASN in the livers of lean *db*/+ and obese *db/db* mice treated with GRT extract.

Lean *db*/+ (A) and obese *db/db* (B) mice received daily oral doses of GRT extract at 74 or 740 mg/kg body weight (BW) for 10 weeks. Controls receiving only water, and pioglitazone administrated orally at a dose of 10 mg/kg BW was included as a positive. Data expressed as mean ± SD of eight mice per group. mRNA is expressed relative to that of β-actin. *p< 0.05, p< 0.01 compared to control and # p< 0.05, p< 0.01 compared to *db/db* untreated

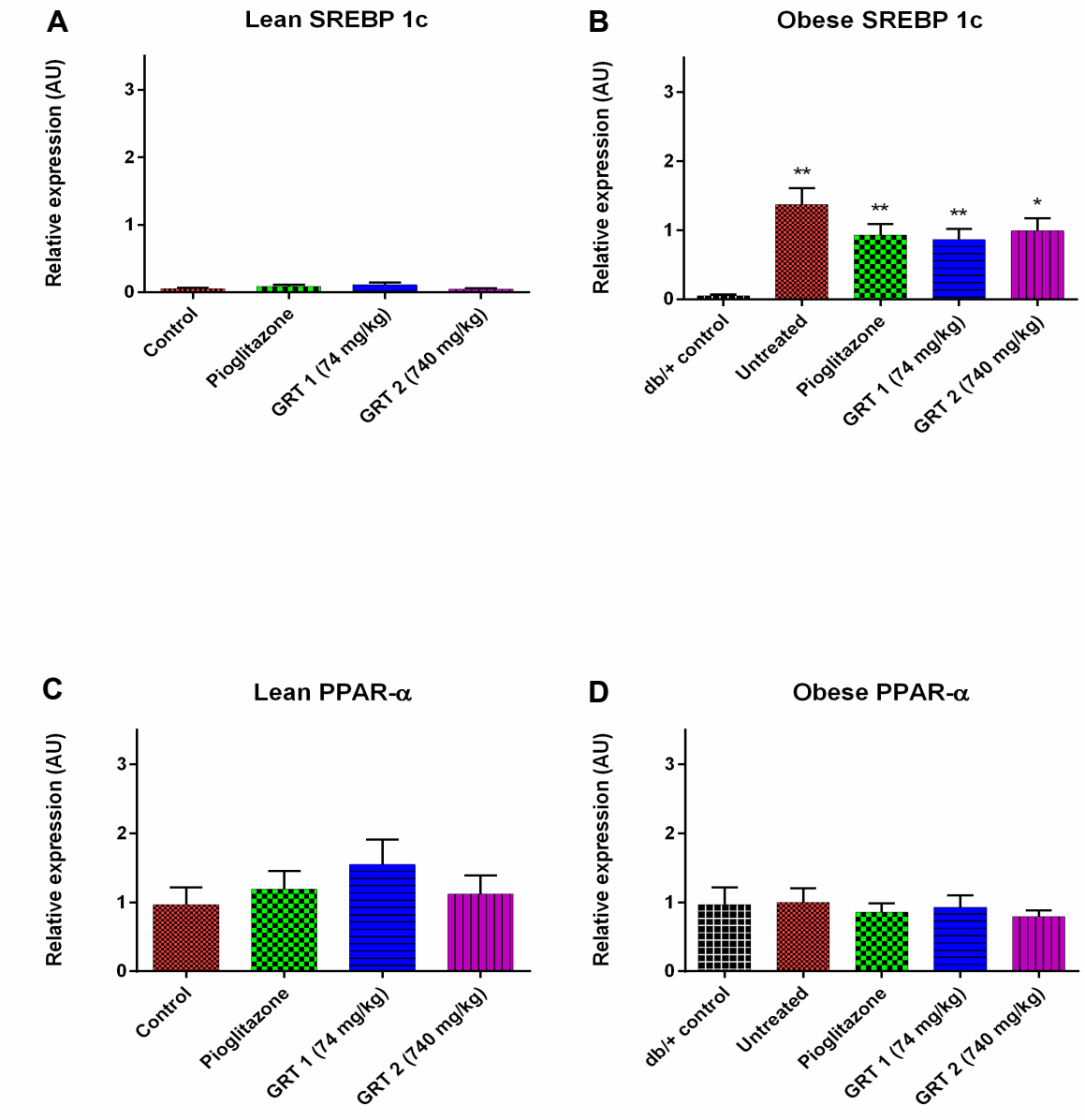

Figure 4.22: Relative mRNA expression of SREBP 1C and PPARα in the livers of lean *db*/+ and obese *db/db* mice treated with GRT extract.
Lean *db*/+ (A) and obese *db/db* (B) mice received daily oral doses of GRT extract administered daily at 74 or 740 mg/kg body weight (BW) for 10 weeks. Controls receiving only water, and pioglitazone administrated orally at a dose of 10 mg/kg BW was included as a positive control. Data expressed as mean ± SD of eight mice per group. mRNA is expressed relative to that of β-actin. *p< 0.05, **p< 0.01 compared to control.

4.2.6 The effects of GRT extract on cholesterol synthesis genes of obese *db/db* and lean *db*/+ mice liver samples

GRT extract did not significantly affect HMGCR mRNA expression in both the lean *db/+* and obese *db/db* mice (Figure 4.23A and B). The expression of HMGCS was increased significantly in obese *db/db* mice ($p < 0.01$). GRT extract modulated this increase in mRNA expression of HMGCS with a dose of 74 mg/kg being the most effective ($p < 0.01$) (Figure 4.23D).

GRT extract did not significantly affect APOA1 mRNA expression of lean *db/+* mice. APOA1 mRNA expression was significantly increased in the obese *db/db* mice ($p < 0.01$). GRT treatment reduced APOA1 expression non-significantly, whilst pioglitazone significantly reduced APOA1 mRNA expression ($p < 0.01$).

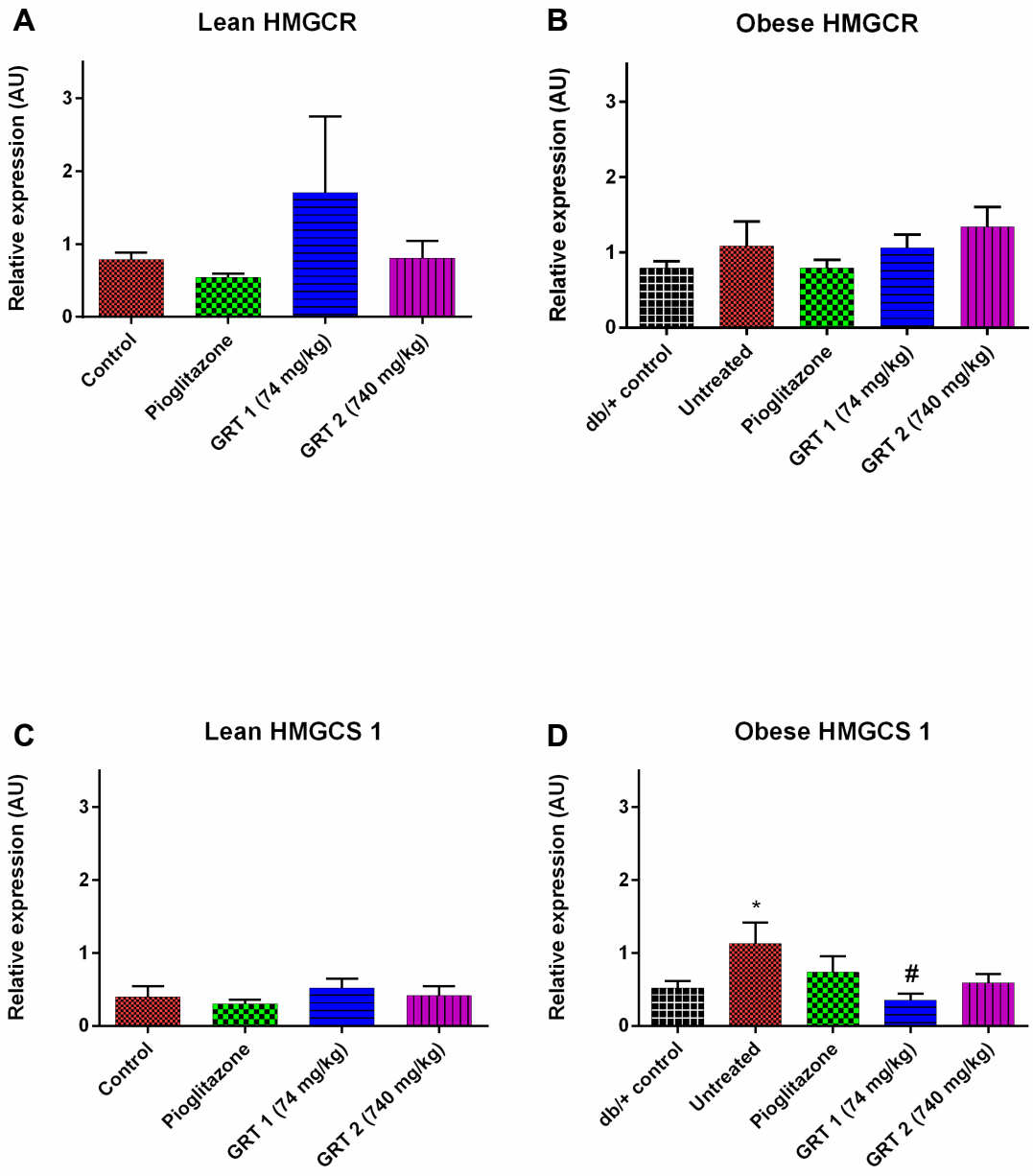

Figure 4.23: Relative mRNA expression of HMGCR and HMGCS in the livers of lean *db/+* and obese *db/db* mice treated with GRT extract.

Lean *db/+* (A) and obese *db/db* (B) mice received daily oral doses of GRT extract administered daily at 74 or 740 mg/kg body weight (BW) for 10 weeks. Controls receiving only water, and pioglitazone administrated orally at a dose of 10 mg/kg BW was included as a positive control. Data expressed as mean ± SD of eight mice per group. mRNA is expressed relative to that of β-actin. *p< 0.05 compared to control. #p< 0.05 compared to untreated.

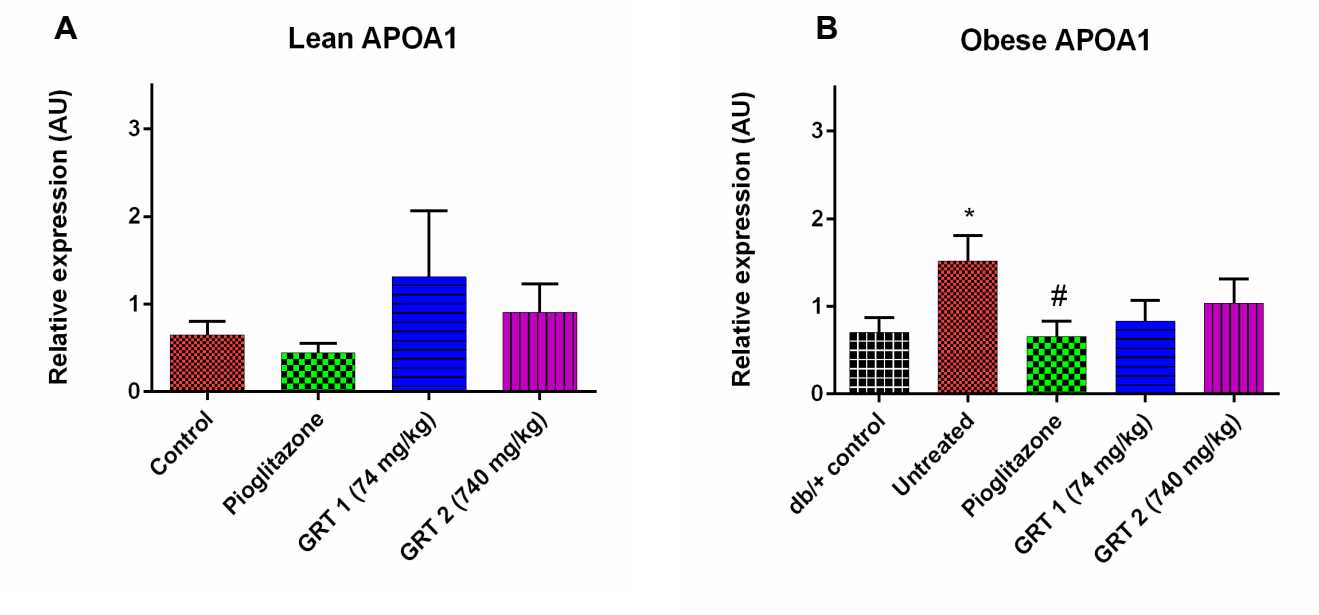

Figure 4.24: Relative mRNA expression of APOA 1 in the livers of lean *db*/+ and obese *db/db* mice treated with GRT extract.
Lean *db*/+ (A) and obese *db/db* (B) mice received daily oral doses of GRT extract administered daily at 74 or 740 mg/kg body weight (BW) for 10 weeks. Controls receiving only water, and pioglitazone administrated orally at a dose of 10 mg/kg BW was included as a positive control. Data expressed as mean ± SD of eight mice per group. mRNA is expressed relative to that of β-actin. *p< 0.05 compared to control and #p < 0.05 compared to *db/db* untreated.

4.3 The effects of GRT extract on Western blot protein expression of obese *db/db* and lean *db/+* mice liver samples

Western blot analysis of the proteins involved in the fat metabolism were performed on obese *db/db* and lean *db/+* mice liver samples. The proteins analyzed were PPAR-α, SREBP 1c, FASN, ACC and CPT 1.

Western blot analysis for the transcription factor SREBP 1c showed a varied response to GRT treatment with the 74 mg/kg dose increasing SREBP 1c expression ($p < 0.001$) while the higher dose of 740 mg/kg had no effect on SREBP 1c (Figure 4.25A). GRT treatment of obese *db/db* mice dose dependently increased PPAR-α protein expression ($p < 0.05$ and $p < 0.01$, respectively) (Figure 4.25B).

Further Western blot analysis showed that ACC protein expression was increased in obese *db/db* mice compared to their lean *db/+* litter mates. GRT extract did not significantly affect the protein expression in the obese *db/db* mice (Figure 4.26A). Similarly, ACC, FASN and CPT 1 protein expression were also increased in obese *db/db* mice, and GRT treatment failed to modulate this effect (Figure 4.26B). However, pioglitazone reduced the protein expression of CPT1 (Figure 4.26C).

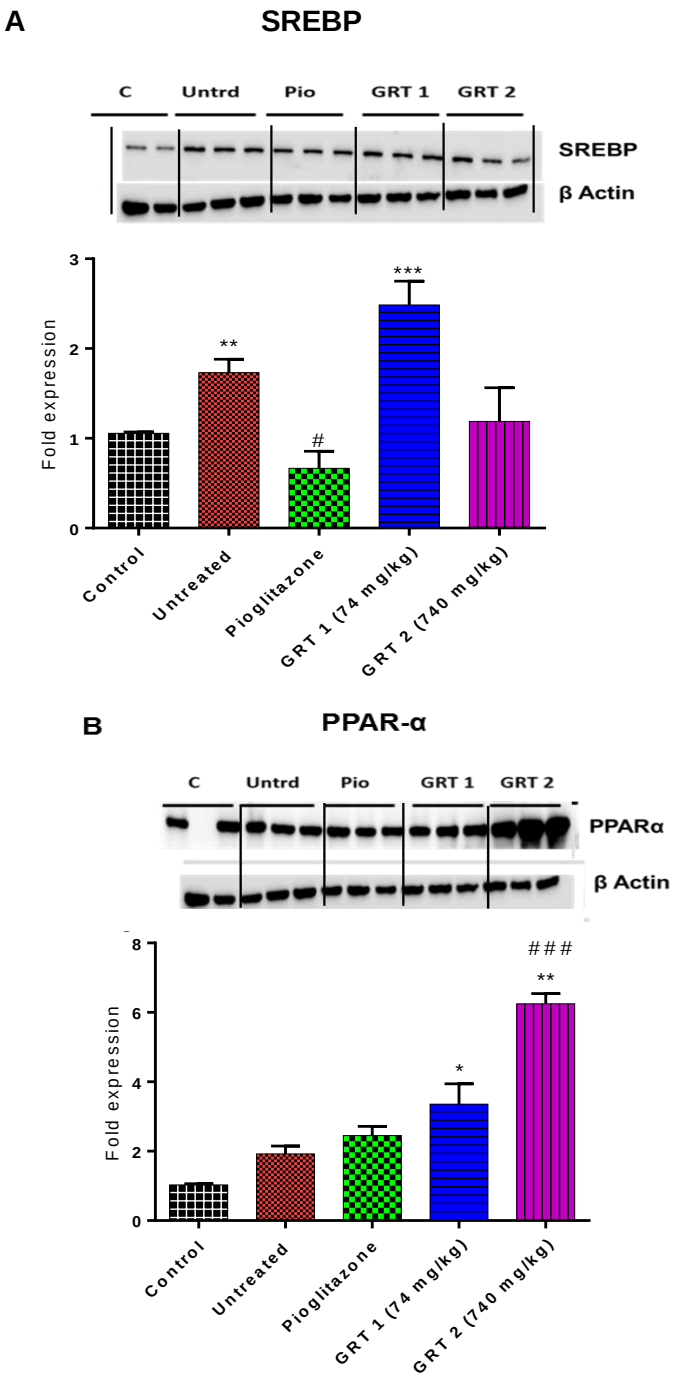

Figure 4.25: Western blot protein expression of SREBP 1C (A) and PPAR alpha (B) in the livers of obese *db/db* mice treated with GRT extract.

Obese db/db mice received daily oral doses of GRT extract at 74 or 740 mg/kg body weight (BW) for 10 weeks. Lean litter mate controls and obese controls, receiving only water were included as controls. Pioglitazone at an oral dose of 10 mg/kg BW was included as a positive control. Data expressed as mean ± SD of eight mice per group. P values *p<0.05 vs control; **p<0.01 vs control; ***p<0.001 vs control; #p<0.05 vs untreated and ###p<0.001 vs untreated.

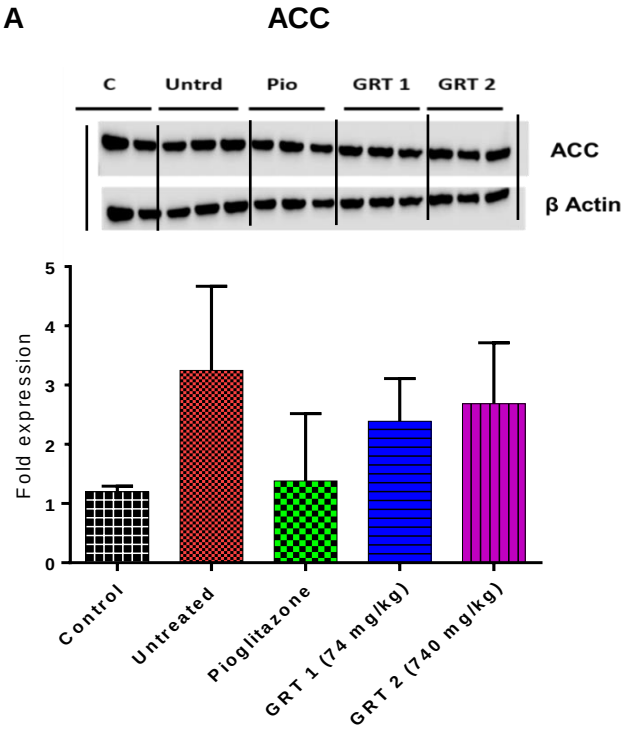
A
ACC
C
Untrd
Pio
GRT 1
GRT 2
ACC
β Actin
Fold expression
0
1
2
3
4
5
Control
Untreated
Pioglitazone
GRT 1 (74 mg/kg)
GRT 2 (740 mg/kg)

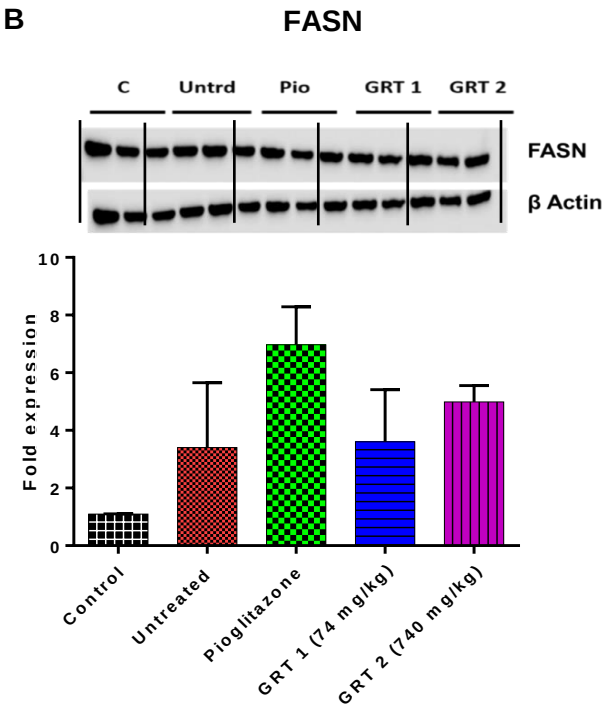
B
FASN
C
Untrd
Pio
GRT 1
GRT 2
FASN
β Actin
Fold expression
0
2
4
6
8
10
Control
Untreated
Pioglitazone
GRT 1 (74 mg/kg)
GRT 2 (740 mg/kg)

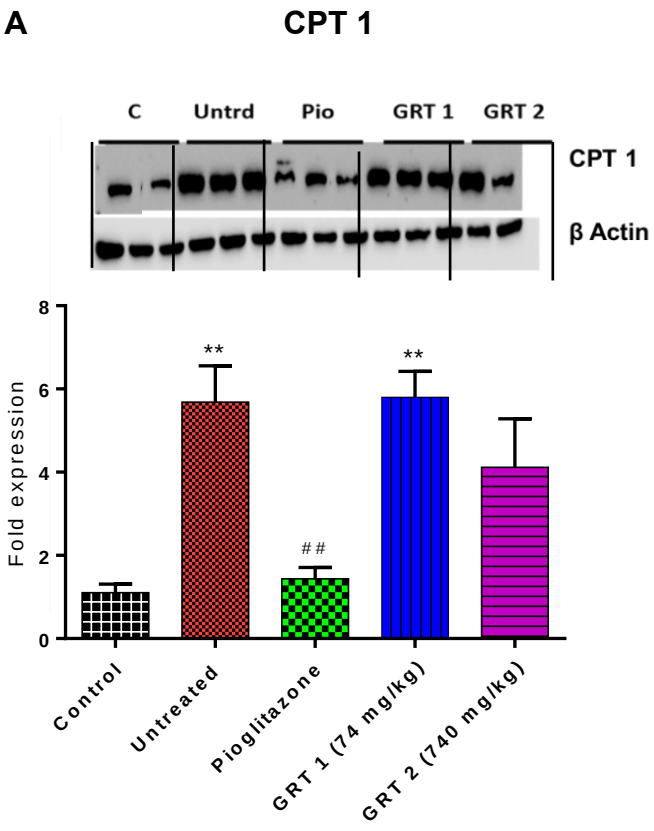

Figure 4.26: Western blot protein expression of ACC, FASN and CPT1 in the livers of obese *db/db* mice treated with GRT extract.

Obese *db/db* mice received daily oral doses of GRT extract with the diet at 74 or 740 mg/kg body weight (BW) for 10 weeks. Lean litter mate controls and obese controls, receiving only the diet, were included as controls. Pioglitazone at an oral dose of 10 mg/kg BW was included as a positive control. Data expressed as mean ± SD of eight mice per group. P values **p< 0.05 vs control; ##p< 0.01 vs untreated.

4.4 The effects of GRT extract on NAFLD model

The effect of GRT extract on the animal model was confirmed by histology. Mice liver sections stained with H&E showed more lipid accumulation for the untreated group and a partial reduction in the GRT treated group when compared to the control group.

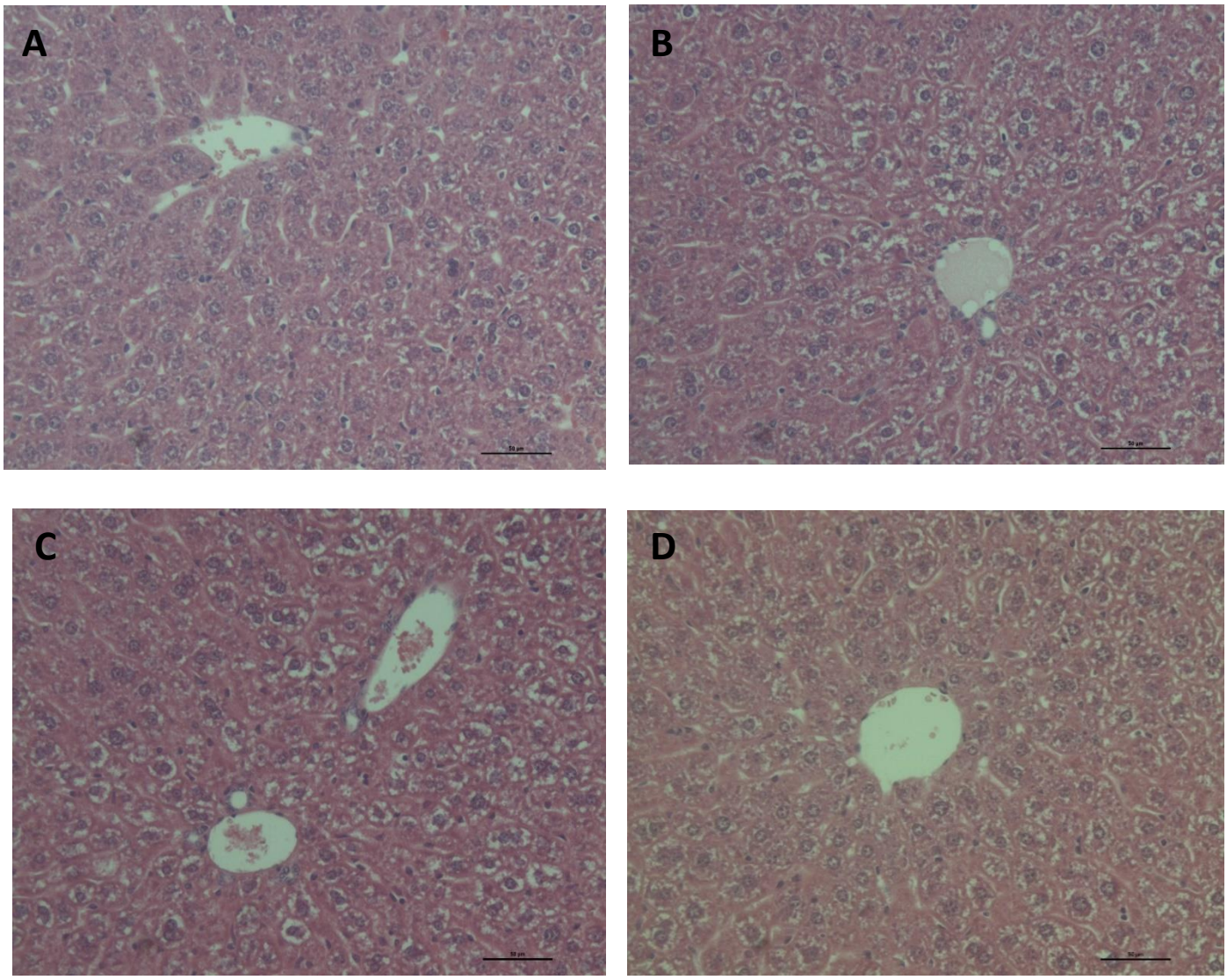

Figure 4.27: Histopathology of the livers of lean *db*/+ mice treated with GRT extract.
Lean *db*/+ mice were treated with daily oral doses of GRT extract of 74 or 740 mg/kg body weight (BW) for 10 weeks. Mice receiving only water were included as controls and pioglitazone at a dose of 10 mg/kg BW was included as a positive control. Liver sections, stained with haematoxylin and eosin (H&E) include untreated control (A), GRT extract dose 74 mg/kg (B), GRT extract dose 740 mg/kg (C) and pioglitazone (D), respectively. Bars are 50 µm.

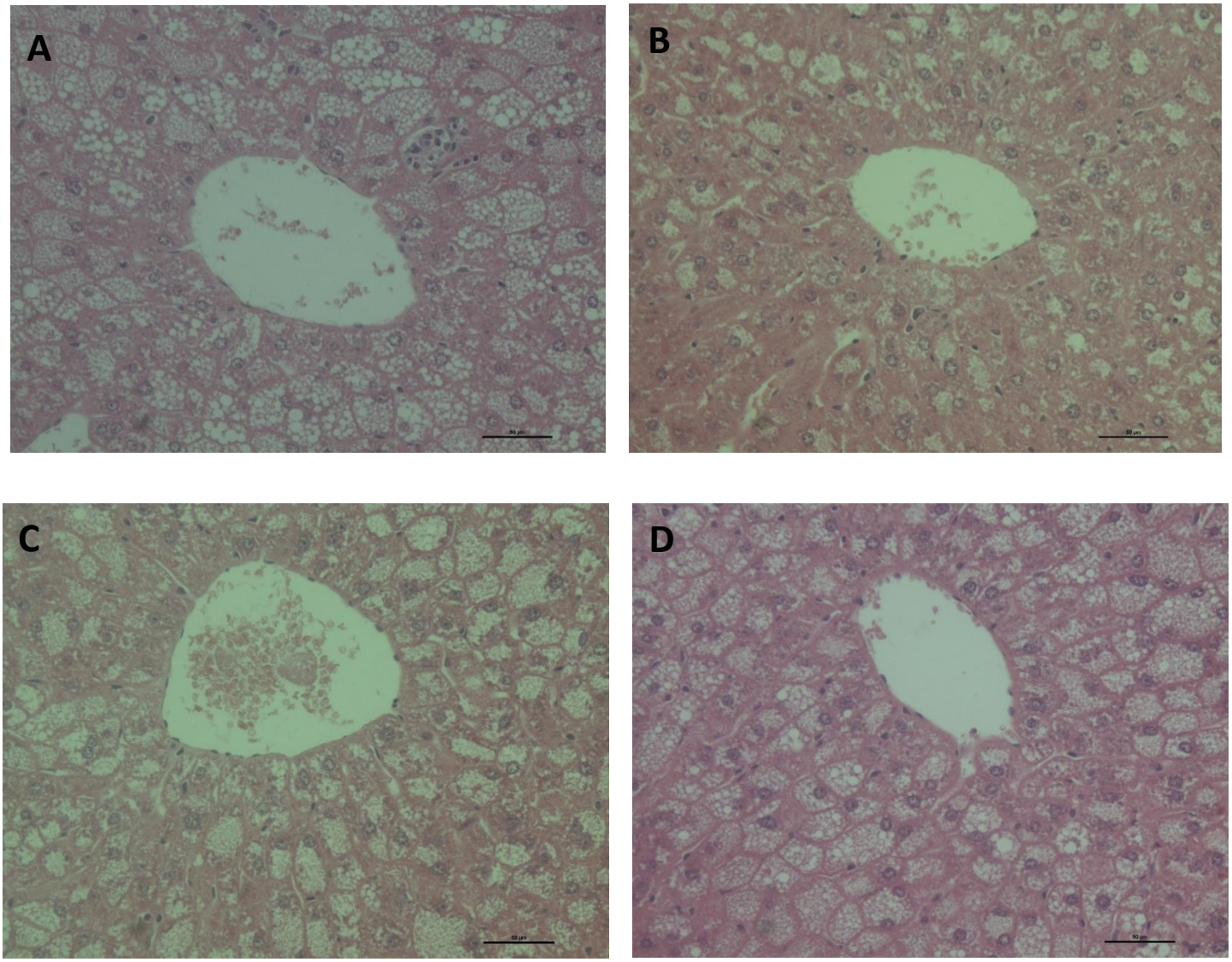

Figure 4.28: Histopathology of the livers of obese *db/db* mice treated with GRT extract.
Obese *db/db* mice were treated with daily oral doses of GRT extract of 74 or 740 mg/kg body weight (BW) for 10 weeks. Mice receiving only water were included as controls and pioglitazone at a dose of 10 mg/kg BW was included as a positive control. Liver sections, stained with haematoxylin and eosin (H&E) include untreated control (A), GRT extract dose 74 mg/kg (B), GRT extract dose 740 mg/kg (C) and pioglitazone (D), respectively. Bars are 50 µm.

4.4.1 Histopathological analysis

Steatosis severity was assessed histologically using the histological scoring system adapted from Trak-Smayra et al. (2011). Scoring was classified according to the abundance of intracellular microvesicular, mediovesicular and macrovacuolar lipid accumulation as shown in Table 4.1 below.

Table 4.1: Histopathological scoring of liver steatotic severity in both lean and obese mice after 10 weeks of treatment with GRT extract.

	Lean				Obese			
Steatosis severity	**Control**	**Pio**	**GRT 1**	**GRT 2**	**Control**	**Pio**	**GRT 1**	**GRT 2**
Micro	++	++	++	++	+++	+++	+++	+++
Medio	+	+	+	+	++	+++	++	+++
Macro	+	+	-	-	+	+	+	+

Steatosis severity after 10 weeks treatment with GRT.

CHAPTER FIVE

DISCUSSION

5.1 DISCUSSION

5.1.1 Establishment of the NAFLD models

The present study aimed to investigate the effect of GRT extract using *in vitro* (C3A liver cells) and *in vivo* (*db/db* mouse) models of experimentally induced NAFLD. Oleic acid was used to induce steatosis in C3A liver cells and obese *db/db* mice, that spontaneously develop hyperglycemia, hyperinsulinemia, insulin resistance and fatty livers (Santhekadur, Kumar, and Sanyal, 2018) were included as the animal model.

5.1.2 *In vitro* liver model of induced steatosis

Hepatic steatosis results from an increased flux of fatty acids into the hepatocytes (Geisler and Renquist, 2017). The first approach of this study was to create an *in vitro* model for NAFLD to study the efficacy of GRT extract in modulating oleic acid induced steatosis. Previous studies charaterise NAFLD as a chronic condition ranging from modest steatosis to more chronic liver injury (McPherson *et al*., 2015; Stål P, 2015). Despite this, the optimal treatment for NAFLD has not been established. Several conventional drugs have been tested to treat NAFLD. However, most of these drugs have presented with severe side effects. For example, vitamin E 800 IU/day used to treat NAFLD increases risk of prostate cancer, while pioglitazone 30 mg/day has been associated with osteoporosis and weight gain (Torres *et al*., 2012; Lisboa, Costa and Couto, 2016).

In this study intracellular lipid content was quantified using oil red O (ORO) staining, normalized for cell number by crystal violet staining. Results demonstrated a significant increasing fat content in C3A cells in response to oleic acid treatment for both 24 and 48 hrs, in a concentration dependent manner. This confirmed our *in vitro* models' usefulness as an inducer of hepatic steatosis that is associated with the development of NAFLD. Our findings are in agreement with numerous other studies (Alkhatatbeh *et al*., 2016; Cao *et al*., 2016; Cui, Chen and Hu, 2010; Liu *et al*., 2011; Moravcová *et al*., 2015). In our study lipid accumulation continued with oleic acid treatment for 48 hours, however the cells started detaching from the surface of the plate at the highest concentration. This suggests

that after 24 hrs the increasing accumulation of intracellular lipid content increases cellular buoyancy and that overcomes the cells ability to adhere to the growth surface. As cells containing most lipid were detaching first and floating into the media, this could be erroneously interpreted as a reduction in lipid accumulation. Therefore, as oleic acid had induced significant lipid accumulation after 24 hrs, all further experiments were performed over 24 hrs at a concentration of 1 mM oleic acid. Cytotoxicity experiments using MTT confirmed that 1 mM was non-toxic to C3A cells during steatogenesis.

A study by Ricchi et al. (2009) demonstrated that oleic acid induces steatosis but not apoptosis, as is the case of palmitic acid in HepG2, HuH7, and WRL68 cells. In a study performed on isolated rat hepatocytes, palmitic acid concentrations as low as 0.025 mM induced significant LDH leakage which was not observed for the oleic acid up to 1 mM concentration (Moravcová *et al*., 2015). A study by Garcia, Amankwa-Sakyi and Flynn, 2011 also confirmed the enhanced lipid accumulation in HepG2/C3A cells treated with 1 mM oleic acid compared to the combination of oleic acid with palmitate. Based on these studies, and our own concentration studies using HepG2/C3A liver cells, 1 mM oleic acid was confirmed to be be a suitable inducer of steatosis over a 24-hour period.

5.1.3 Obese *db/db* mouse model for NAFLD

The use of the *db/db* mouse model for NAFLD has been well reported with various studies reporting the spontaneity in the development of obesity and diabetes in mice fed a normal chow diet *ad libitum* which dates back to as far as the study by Mayer et al. (1951). where they described the development of NAFLD in obese *db/db* mice. However, to induced more advanced stages of liver disease e.g. NASH further dietary insults like the use of methionine and choline-deficient diet (MCD), high-fat, high glucose, high sucrose, high fructose, choline-deficient L-amino-defined (CDAA) diet, high cholesterol diet (HCD), cholesterol and cholate arerequired (Santhekadur, Kumar, and Sanyal, 2018).

In our study the *db/db* and *db/+* mice were fed a standard rodent chow *ad libitum* for ten weeks. As expected the *db/db* mice gained weight more quickly than their lean *db/+* littermates. By six weeks of age the db/db mice were approximately 40% heavier than the lean *db/+* littermates and by the end of the study at 10 weeks they had almost doubled their body weight. The *db/db* mice also developed mild hyperglycaemia (10.5 ±1.4 mmol/L versus 6.4 ±1.4 mmol/L) and glucose intolerance.

5.1.4 Anti-steatotic effect of GRT extract in experimentally induced hepatic steatosis.

Most pharmacological therapies available for NAFLD are directed towards insulin sensitivity (Soccio, Chen, and Lazar, 2015) and body weight reduction (Takahashi *et al.,* 2015). Herbal medicine has gained growing attention as potential therapeutic agents, demonstrating low-risk side effects in most studies (Yao *et al*., 2016). Rooibos recently showed beneficial effects in improving dyslipidemia, insulin sensitivity and reducing cardiovascular risk factors (Kawano *et al*., 2009; Sasaki, Nishida and Shimada, 2018, reviewed by Johnson *et al*., 2018). Hence, this study aimed at investigating the beneficial effects of GRT extract containing ca. 12% aspalathin in modulating hepatic steatosis.

The therapeutic probability that rooibos can modulate or prevent NAFLD was based on previous studies confirming the hypoglycemic activity of an aspalathin-enriched green rooibos extract *in vitro* and *in vivo* (Mazibuko *et al*., 2015; Kamakura *et al*., 2014; Muller *et al*., 2012; Son *et al*., 2012). Rooibos has also been shown to protect the liver against liver toxins such as CCl_4 (Ulicná *et al*., 2003) and *tert*-butyl hydroperoxide (Olawale *et al*., 2013) which further supports the likely potential hepatoprotective effects of rooibos. To the best of our knowledge, it is unknown whether rooibos affecting NAFLD has been previously assessed. Therefore, this present study was to establish if an aspalathin rich green rooibos extract GRT is able to modulate or prevent the excessive fat accumulation in experimental models of NAFLD.

Treatment of non-steatotic C3A cells, not exposed to oleic acid (control group), with GRT extract reduced lipid content by ~30%. A study by Mazibuko et al. (2019) investigated the effect of an aspalathin enriched green rooibos extract (GRE) on insulin resistance, induced by palmitate (0.75 mM) in C3A liver cells, and demonstrated that GRE attenuated the palmitate-induced impairment of glucose and lipid metabolism by activating the AMPK-mediated pathway. Although the effect of GRT on AMPK protein expression was not assessed in this study, the reduction of lipid content by GRT extract in the present study likely involves AMPK which regulates beta oxidation by controlling ACC (Mazibuko *et al*., 2019).

In the presence of oleic acid, GRT extract at a concentration of 100 µg/ml markedly increased lipid accumulation in C3A cells. The effect was similar to that of pioglitazone which increased lipid content. Pioglitazone, a thiazolidinedione class oral T2D drug, is a nuclear receptor peroxisome proliferator-activated receptor gamma (PPARγ) agonist and insulin sensitizer (Berger *et al*., 2002). Pioglitazone's primary effect is on white adipose tissue and macrophages, where it decreases the release of free fatty acids through storage of triglycerides and inhibits the production of proinflammatory cytokines. The secondary effect is on the liver and skeletal muscle where it reduces lipid accumulation and improves insulin sensitivity. However, rooibos has been shown to be PPAR-γ antagonistic, and able to modulate PPAR-γ activity (Mueller and Jungbauer, 2009), suggesting that the observed increase in lipid accumulation induced by GRT was not mediated via PPAR-γ. Alternatively, ppioglitazone has been shown to increase the livers proliferation capacity (Czaja *et al*., 2009).

The MTT results show that GRT concentration dependently increased cellular mitochondrial activity in the simultaneous and post treatment groups. The increase in MTT activity could be interpreted in three ways. Firstly, it has been reported that polyphenolic compounds could interfere with the MTT assay (Wang *et al*., 2015). In this study, because MTT activity in the control cells was not affected by GRT, it validates that the observed increase in MTT activity in the oleic acid treated cells was not due to GRT

interference with MTT. The other possibility is that GRT and pioglitazone enhanced proliferation and that the increase in lipid accumulation observed in the presence of oleic acid was due to increased cell numbers. However, as oil red O staining was normalised for cell number by crystal violet staining, it is unlikely that GRT increased proliferation. The most likely scenario is that GRT and pioglitazone increases mitochondrial bioactivity in oleic acid treated cells. This could be facilitated by activation of energy producing pathways such as AMPK. Activation of AMPK increases peroxisome proliferator-activated receptor gamma coactivator-1α (PGC-1α), a transcriptional regulator for genes involved in fatty acid oxidation andgluconeogenesis, and is considered the master regulator for mitochondrial biogenesis (Uguccioni *et al*., 2010). In a study Valenti et al. (2013) showed that an anthocyanin-rich extract derived from Mulberry increased pAMPK and pACC, PPARα, CPT1 and FFAs oxidation in HepG2 cells.

5.1.5 Effect of GRT extract on obese *db/db* mice.

Leptin-resistant (*db/db*) mice in all treatment group showed a weekly increase in body weight gain, increasing the risk factor for NAFLD. Our findings were in line with a study conducted by Milagro, Campión and Martínez., (2006) which shows that obese *db/db* mice had gained more body weight compared to the lean *db/*+ mice. Treatment with GRT extract did not affect body weight. In terms of the liver to body ratio, an increase in liver weight was observed in the obese group compared to lean (control). GRT at the highest dose induced a small but significant decrease in the liver to body weight ratio of lean *db/*+ mice but did not affect the obese *db/db* mice liver to body weight ratios. A similar effect was seen in a study conducted by Beltrán-Debón et al. (2011) which showed that rooibos extract used in that study decreased liver weights in mice fed high fat diet. Increased fat content in the liver is highly associated with insulin resistance (Fabbrini *et al*., 2010).

Food intake (supplemented with GRT extract) for the obese group did not significantly differ from the lean group, suggesting that the improvement in glucose tolerance was not due to the reduced food intake, but due to the action of GRT extract. These results are comparable to the study conducted by Kamakura et al. (2014) that demonstrated

hypoglycemic effects of GRE extract and aspalathin in type 2 diabetic KK-Ay mice treated for 5 weeks. GRT extract has been proven to regulate glucose homeostasis, one of the steps required for reversing the progression of NAFLD. Reduced glucose metabolism increased fasting blood glucose and compromised glucose tolerance correlates with obesity, a major causative factor for NAFLD.

5.1.6 The effects of GRT extract on mRNA expression and protein expression

Enhanced hepatic lipid accumulation provokes activation of major pathways like glycolysis and lipogenesis. Glycolysis favours an increased rate of fatty acid synthesis as its produces acetyl CoA as an end product, which is a precursor for fatty acid synthesis. Hence, the liver's ability to synthesis fats, through *de novo* lipogenesis relies on the activation of several transcriptional factors such as sterol regulatory element-binding protein (SREBP), peroxisome proliferator-activated receptors alpha (PPAR-α) and carbohydrate-response element-binding protein (ChREBP), which are activated by hyperinsulinemia and increased glucose concentrations respectively (Ferré and Foufelle, 2010; Wang *et al*., 2015). Activation of these transcription factors stimulate the activation of lipogenic genes which drive fat accumulation in hepatocytes (Jump *et al*., 2013).

SREBP is expressed abundantly in the liver and promotes the expression of several genes controlling the synthesis of fatty acids, cholesterol and phospholipids (Hampton, 2002; Horton *et al*., 2002). In the present study, GRT extract downregulated the mRNA levels of SREBP. The downregulation of SREBP *in vitro* is in accordance with previously conducted studies (Ziamajidi *et al*., 2013) where they evaluated the effect of chicory seed extract on oleic acid induced steatosis in HepG2 cells. The results obtained showed that the extract downregulated the mRNA expression of SREBP and PPARα. The possible mechanism by which GRT ameliorated lipid content is by supressing the transcription gene expression of SREBP and ChREBP thereby downregulating downstream lipogenic genes including fatty acid synthase (FASN) (Sanderson *et al*., 2014) and glucogenic gene glucokinase (GCK) (Valentová *et al*., 2007). The mRNA expression of lipogenic genes were highly expressed in untreated group and improved by treating with GRT extract.

In contrast, the third transcription factor PPAR-α which controls lipid beta-oxidation was upregulated by GRT extract. The regulation of PPAR-α transcription in combination with carnitine palmitoyltransferase I (Carnitine palmitoyltransferase-CPT1) controls mitochondrial lipid beta-oxidation (Souza-Mello, 2015). GRT treatment increase both PPAR-α and CPT 1 protein expression suggesting that GRT increases beta-oxidation. This corresponds with a study conducted by Leea and Jia. (2015) where the bioactive compounds found in tea exerted a hypolipidemic effect by regulating PPARs. The suppression of PPARs by green tea was also seen in a study conducted by Chen et al. (2009).

To confirm *in vitro* results, we further investigated the effects of aspalathin enriched green rooibos extract using a leptin-resistant (*db/db*) mouse model. By feeding *db/db* mice *ad libitum*, the mice develop obesity with changes in liver architecture towards steatosis over the duration of feeding. Six-week-old obese *db/db* and lean control *db/+* mice were treated with either GRT extract or pioglitazone, both treatments known to improve insulin resistance, one of the risk factors to NAFLD development. The possible mechanism by which GRT extract exerted its effects on glucose metabolism is through down regulation of transcription factors to regulate lipid synthesis. ChREBP and SREBP were highly upregulated in the obese untreated group implying that hepatic fat occurs as a result of up-regulation of transcriptional factors. This was reversed by GRT extract reversed this to almost the same level as the pioglitazone treated mice. Our results were in accordance with a study conducted by Mazibuko et al. (2015) which demonstrate that aspalathin improve glucose uptake and lipid metabolism *in vivo*.

Lipid synthesis is stimulated by transcription factors SREBP and ChREBP which are induced by hyperinsulinemia through the rate limiting enzyme glucokinase and elevated rates of glucose metabolism (Han *et al*., 2016). In the obese *db/db* mice, the transcription factors that regulate downstream lipid synthesizing acetyl-CoA carboxylase (ACACA) and fatty acid synthase (FASN) were significantly increased compared to the lean *db/+* mice. The study showed that both ACACA and FASN were significantly reduced by GRT extract

suggesting that GRT could modulate hepatic lipid synthesis. These results were in accordance with a study conducted by Chen et al. (2009).

The increased expression of 3-hydroxy-3-methylglutaryl coenzyme A (HMG-CoA) synthase (HMGCS 1) mRNA observed in the obese diabetic *db/db* mice is consistent with previous findings that relate the increased expression of HMGCS 1 with hypercholesterolaemia in mice fed a high fat diet (Suzuki *et al*., 2013; Yamashita *et al*., 2016). The modulation of HMGCS 1 support supports the cholesterol lowering effect of GRT seen in diabetic vervet monkeys fed a high fat diet (Orlando *et al*., 2017). In addition, high density lipoprotein (HDL) promotes the removal of cholesterol from tissues to the liver for excretion and is encoded by apoliproteins (A). Hence, upregulation of these genes promotes cholesterol removal through bile secretion. Data obtained in this study displayed that apolipoprotein 1 (APO A1) was elevated in obese *db/db* mice compared to the lean group. GRT extract modulated this increase (P = NS to lean control) suggesting that GRT suppresses hepatic cholesterol synthesis and promotes cholesterol removal, thereby could reduce cholesterol levels.

5.1.7 Histology

The extent of fatty liver disease in South Africa is unknown. In Western countries, such as the USA and Europe, it is estimated that up to 30% of adults have liver steatosis (Yeh and Blunt, 2007). In *db/db* mice lipoprotein lipase (LPL) activity is reduced by ca. 72% compared to the *db/+* littermates (Kobayashi *et al*., 2000). The reduced LPL activity and hyperfagia contributes to their dyslipidaemia. In addition, the *db/db* mice develop insulin resistance from 4 weeks of age with resultant hyperinsulinaemia. The resultant hyperinsulinaemia drives lipid synthesis in the liver (Petta *et al*., 2016). The effect of GRT extract on obese diabetic *db/db* mice was assessed histologically by an experienced histologist using a steatotic severity scoring system adapted from Trak-Smayra et al. (2011).

To avoid observational bias, the histologist was blinded to the different groups and the slides from the different groups were randomly assessed. Histological diagnostic criteria for NAFLD defines that greater than ≥ 5% of the hepatocytes per liver acinus are steatotic (Yeh and Blunt, 2007). In this study, the *db/db* obese diabetic mice demonstrated a clear increase in microvesicular, mediovesicular and microvacular steatosis that was limited to zone 3, the central vein area, of the liver acinus. Zone 1, the peri portal tract area was clear of steatotic hepatocytes. This is the most common zonal pattern for steatosis in adults and is associated with the metabolic syndrome (Chalasani *et al*., 2008).

Apart from hepatic steatosis in the mice, no histopathological evidence or features of NASH, i.e. signs of inflammation or fibrosis, was observed. This is consistent with other findings that *db/db* mice do not progress from NAFLD to steatohepatitis or liver fibrosis unless dietary or other insults are employed (Takahashi *et al*., 2012). In comparison to the lean *db/+* littermates, the *db/db* mice had an increased presence of micro- and mediovesicular steatosis. These results were supported by the increase in SREBP 1c mRNA expression that has been directly implicated in the development of liver steatosis (Takahashi *et al*., 2012; Brown *et al*., 2015). GRT treatment did not significantly improve the steatosis severity score in the *db/db* mice. However, GRT did increase protein expression of PPAR-α and CPT 1 suggesting that GRT enhances beta-oxidation of lipids but the effect was not substantial enough to reverse NAFLD in this obese and diabetic *db/db* mouse model.

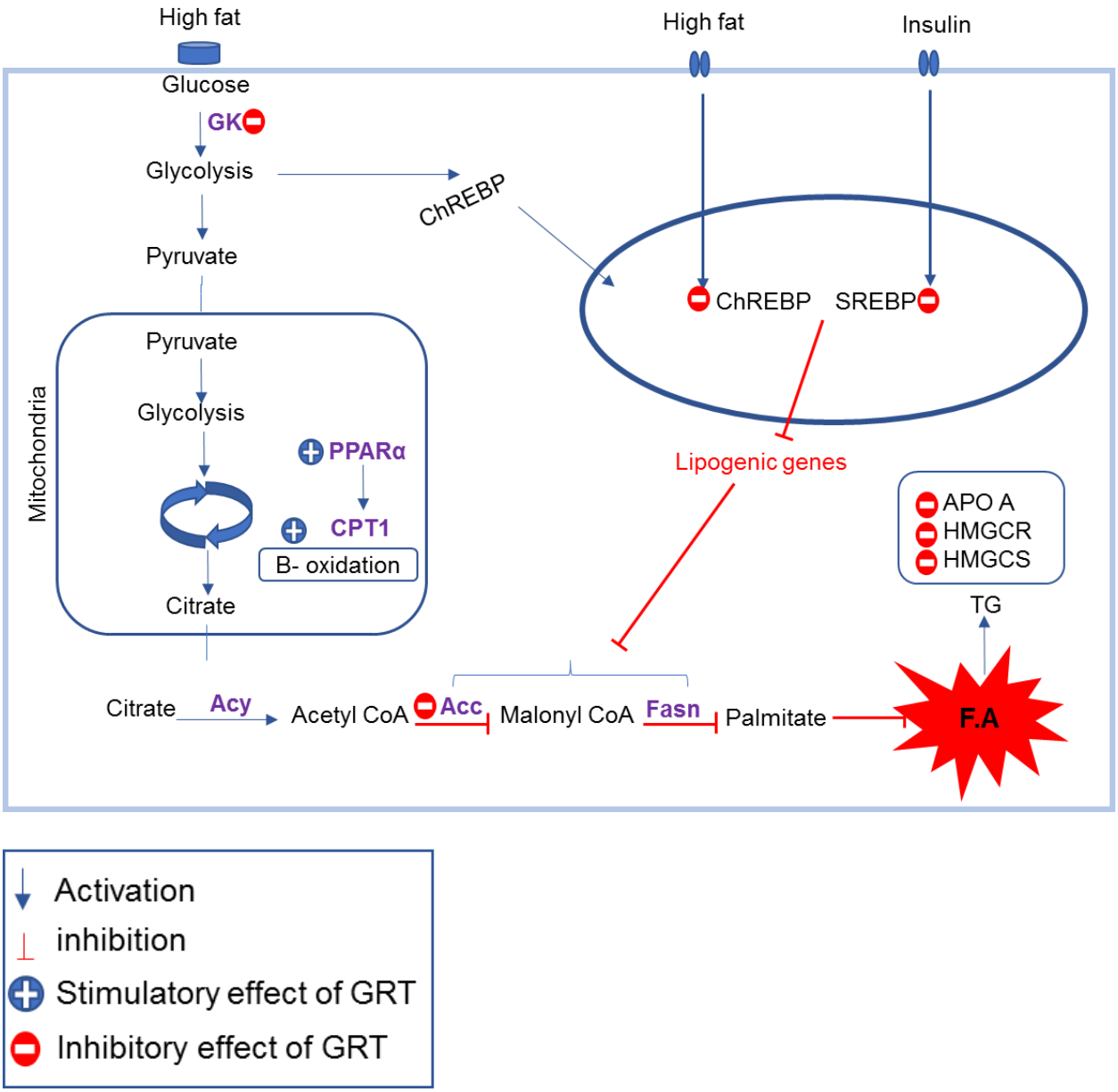

Figure 5.1: Brief Summary of anti-steatotic effect of an aspalathin rich green rooibos (GRT) extract.

An obesogenic environment results in enhanced lipid accumulation, insulin resistance as well as disturbances in metabolic syndrome. Hepatic *de novo* lipogenesis is regulated by hyperglycemia and hyperinsulinaemia. Which further activates lipogenic genes resulting in enhanced free fatty acids that are not oxidized. GRT effectively ameliorated these metabolic complications by reducing lipid accumulation and inflammation. In the liver, GRT suppressed lipid synthesis by decreasing SREBP 1c, a transcriptional factor involved in fat synthesis, and by increasing peroxisome proliferator-activated receptors alpha (PPAR-α) and CPT 1 promote beta-oxidation of lipids.

CHAPTER SIX

CONCLUSION AND LIMITATIONS

6.0 CONCLUSION

In conclusion, our findings showed that GRT effectively modulated oleic acid induced steatosis in C3A liver cells. At a mechanistic level, GRT extract modulated several genes relevant to hepatic steatosis including genes involved in cellular glucose metabolism (ChREBP and GCK), lipids synthesis (SEBP 1c and FASN) and inflammation (TNF-α). Of interest was that GRT extract also reduced PPAR-α a transcription factor involved in beta-oxidation. This together with the lack of effect on CPT-1 expression suggests that the activity observed *in vitro* was due to a reduction in the synthesis of lipids rather than increased lipolysis. In the obese diabetic *db/db* mouse, the GRT extract improved glucose tolerance but did not significantly affect liver weight or ameliorate liver steatosis. At a gene level, GRT extract reduced gene expression of SREBP, FASN and HMGCS 1; genes that control lipid and cholesterol synthesis. At a protein expression level, GRT treatment enhanced PPAR-α levels. PPAR-α plays several hepatoprotective effects such as increasing beta-oxidation, reducing inflammation and limiting fibrosis.

Taken together, this study confirmed the potential modulatory benefits of GRT extract treatment on the development of steatosis. However, more studies are required to fully elucidate the mechanism using other models.

6.1 Shortcoming of this study

- In terms of the *in vitro* study, the effects of GRT extract on protein expression and activation of relevant effector proteins, such as AMPK, PI3K and AKT, would have provided further information on the mechanisms of action of GRT. Additionally, a glycerol release assay would have provided further information of lipolysis but this was not performed due to time and financial constraints.
- As only ca. 10% of the litter homozygously express the obese *db/db* phenotype, the *in vivo* part of the project was completed in two studies with n=4/group. This contributed to the higher variation of the response to treatment and resultant lack of significance in terms of glycaemia as well as variation in the histopathology which could be ascribed to the fact that the results of two studies differed slightly.
- The *db/db* study was a shared study, and due to small volumes of serum, and other agreed uses of the serum, we were unable to do lipograms.

6.2 Future studies will include

- It would have also been useful if the treatment had commenced before the mice were overtly obese and diabetic. It would have been of interest if the study could have started at 4 weeks when the *db/db* mice are becoming obese, rather than at 6 weeks when the mice were already overtly obese and diabetic. It could have provided an insight into the ability of GRT to protect against steatosis rather than treat established NAFLD.
- To maximize the chances of identifying the benefits of treatment on NAFLD, proteomics and gene arrays will be used to further elucidate relevant pathways and effector genes.

CHAPTER SEVEN

REFERENCES

7.0 Bibliography

Abd El-Kader, S.M., and El-Den Ashmawy, E.M. (2015). Non-alcoholic fatty liver disease: The diagnosis and management. *World Journal of Hepatology*, *7*(6): 846-58. doi: 10.4254/wjh.v7.i6.846.

Abdel-Misih, S.R.Z. and Bloomston, M. (2010). Liver Anatomy. *Surgical Clinics of North America*, 90(4): 643–53. doi: 10.1016/J.SUC.2010.04.017.

Ables, G.P. (2012). Update on PPARγ and nonalcoholic Fatty liver disease. *PPAR Research*, 2012: 5. doi: 10.1155/2012/912351.

Adams, L.A., Angulo, P., and Lindor, K.D. (2005). Nonalcoholic fatty liver disease. *Canadian Medical Association Journal,* 172(7): 899-905. doi: 10.1503/cmaj.045232

Ajuwon, O.R., Katengua-Thamahane, E., Van Rooyen, J., Oguntibeju, O.O., and Marnewick, J.L. (2013). Protective effects of Rooibos (Aspalathus linearis) and/or red palm oil (*Elaeis guineensis*) supplementation on tert-butyl hydroperoxide-Induced oxidative hepatotoxicity in wistar rats. *Evidence-Based Complementary & Alternative Medicine*, 2013: 9847273. doi: 10.1155/2013/984273.

Ajuwon, O.R., Oguntibeju, O.O., and Marnewick, J.L. (2014). Amelioration of lipopolysaccharide-induced liver injury by aqueous rooibos (*Aspalathus linearis*) extract via inhibition of pro-inflammatory cytokines and oxidative stress. *BMC Complementary and Alternative Medicine*, 14: 392. doi:10.1186/1472-6882-14-392.

Alabraba, E.B., Curbishley, S.M., Lai, W.K., Wigmore, S.J., Adams, D.H., and Afford, S.C. (2007). A new approach to isolation and culture of human Kupffer cells. *Journal of Immunological Methods*, 326(1–2): 139–44. doi: 10.1016/j.jim.2007.06.014.

Alam, S., Fahim, S.M., Chowdhury, M., Hassan, M.Z., Azam, G., Mustafa, G., Ahsan, M., Ahmad, N. (2018). Prevalence and risk factors of non-alcoholic fatty liver disease in Bangladesh. *JGH open, 2*(2): 39-46. doi: 10.1002/jgh3.12044.

Albhaisi, S. and Sanyal, A. (2018). Recent advances in understanding and managing non-alcoholic fatty liver disease. *F1000 Research*, 7: 720. doi: 10.12688/f1000research.14421.1

Albhaisi, S., Issa, D. and Alkhouri, N. (2018). Non-alcoholic fatty liver disease: a pandemic disease with multisystem burden. *Hepatobiliary Surgery and Nutrition*, 7(5): 389-391. doi: 10.21037/hbsn.2018.07.01

Alkhatatbeh, M.J., Lincz, L.F., and Thorne, R.F. (2016). Low simvastatin concentrations reduce oleic acid-induced steatosis in HepG2 cells: An *in vitro* model of non-alcoholic fatty liver disease. *Experimental and Therapeutic Medicine*, 11(4): 1487-92. doi: 10.3892/etm.2016.3069

Ameer, F., Scandiuzzi, L., Hasnain, S., Kalbacher, H., and Zaidi, N., (2014). *De novo* lipogenesis in health and disease. *Metabolism*. 63(7): 895–902. doi: 10.1016/j.metabol.2014.04.003.

Anderson, B., Rafferty, A. P., Lyon-Callo, S., Fussman, C., and Imes, G. (2011). Fast-food consumption and obesity among Michigan adults. *Preventing Chronic Disease*, *8*(4): A71.

Anstee, Q.M, and Goldin, R. D. (2006). Mouse models in non-alcoholic fatty liver disease and steatohepatitis research. *International Journal of Experimental Pathology*, 87(1): 1–16. doi: 10.1111/j.0959-9673.2006.00465.x.

Antonucci, L., Porcu, C., Iannucci, G., Balsano, C., and Barbaro, B. (2017). Non-Alcoholic Fatty Liver Disease and Nutritional Implications: Special Focus on Copper. *Nutrients*, *9*(10): 1137. doi: 10.3390/nu9101137.

Araújo, A.R., Rosso, N., Bedogni, G., Tiribelli, G., and Bellentani, S. (2018). Global epidemiology of non-alcoholic fatty liver disease/non-alcoholic steatohepatitis: What we need in the future. *Liver International*, 38(1): 47–51. doi: 10.1111/liv.13643.

Arguello, G., Balboa, E., Arrese, M., and Zanlungo, S. (2015) Recent insights on the role of cholesterol in non-alcoholic fatty liver disease. *BBA-Molecular Basis of Disease*, 1852(9): 1765-78. doi: 10.1016/j.bbadis.2015.05.015.

Arshad, S., Butt, J., Ahmed, R., and Ijaz, M.(2018). Pharmacogenetics; mini review. *Journal of Analytical & Pharmaceutical Research*, 7(2): 147–50. doi: 10.15406/japlr.2018.07.00215.

Ayisi, C.L., Yamei, C., and Zhao, J. (2017). Genes , transcription factors and enzymes involved in lipid metabolism in fin fish. *Agri Gene*, 7: 7–14. doi: 10.1016/j.aggene.2017.09.006.

Azam, G., Alam, S., Hasan, S.N., Noor-E-Alam, S., Kabir, J., and Alamu, A.K. (2016). Insulin Resistance in Nonalcoholic Fatty Liver Disease: Experience from Bangladesh. *Bangladesh Critical Care Journal*, 4 (2): 86-91. doi: 10.3329/bccj.v4i2.30022.

Bainor, A., Chang, L., McQuade, T., Webb, B. and Gestwicki, J. (2011). Bicinchoninic acid (BCA) assay in low volume. *Analytical Biochemistry*, 410(2): 310-12. doi: 10.1016/j.ab.2010.11.015

Bale, S.S., Golberg, I., Jindal, R., McCarty, W.J., Luitje, M., Hegde, M., Bhushan, A., Usta, O.B. and Yarmush, M.L. (2014). Long-term coculture strategies for primary hepatocytes and liver sinusoidal endothelial cells. *Tissue Engineering. Part C,* Methods, 21(4): 413-22. doi: 10.1089/ten

Bellentani, S., Scaglioni, F., Marino, M. and Bedogni, G. (2010). Epidemiology of Non-Alcoholic Fatty Liver Disease. *Digestive Diseases*, 28(1): 155-61. doi: 10.1159/000282080

Beltrán-Debón, R., Rull, A., Rodríguez-Sanabria, F., Iswaldi, I., Herranz-López, M., Aragonès, G., Camps, J., Alonso-Villaverde, C., Menéndez, J.A., Micol V., Segura-Carretero, A., and Joven, J. (2011). Continuous administration of polyphenols from aqueous Rooibos (*Aspalathus linearis*) extract ameliorates dietary-induced metabolic

disturbances in hyperlipidemic mice. *Phytomedicine,* 18(5): 414–24. doi: 10.1016/j.phymed.2010.11.008

Benedict, M., and Zhang, X. (2017). Non-alcoholic fatty liver disease: An expanded review. *World Journal of Hepatology*, *9*(16): 715-32. doi: 10.4254/wjh.v9.i16.715

Benhamed, F., Dentin, R., Pégorier, J., Foufelle, F., Ferré, P., Fauveau, V., Magnuson, M.A., Girard, J., and Postic*, C.* (2004). Hepatic Glucokinase is required for the Synergistic Action of ChREBP and SREBP-1c on Glycolytic and Lipogenic gene expression. *Journal of Biological Chemistry,* 279(19): 20314–26. doi: 10.1074/jbc.M312475200.

Berger, J. and Moller, D. (2002). The Mechanisms of Action of PPARs. *Annual Review of Medicine*, 53(1): 409-35. doi: 10.1146/annurev.med.53.082901.104018

Berlanga, A., Guiu-Jurado, E., Porras, J.A., and Auguet, T. (2014). Molecular pathways in non-alcoholic fatty liver disease. *Clinical and Experimental Gastroenterology*, *7*: 221-39. doi: 10.2147/CEG.S62831.

Bhatt, S., Nigam, P., Misra, A., Guleria, R., Luthra, K., Vaidya, M., Jain, S. and Pasha, M. (2011). SREBP-2 1784G/CGenotype is Associated with Non-Alcoholic Fatty Liver Disease in North Indians. *Disease Markers*, 31(6): 371-77. doi: 10.3233/DMA-2011-0852

Boden, G. and Shulman, G.I. (2002), Free fatty acids in obesity and type 2 diabetes: defining their role in the development of insulin resistance and β-cell dysfunction. *European Journal of Clinical Investigation*, 32: 14-23. doi: 10.1046/j.1365-2362.32.s3.3.

Boursier, J., Mueller, O., Barret, M., Machado, M., Fizanne, L., Araujo-Perez, F., Guy, C. D., Seed, P.C., Rawls, J.F., David, L.A., Hunault, G., Oberti, F., Calès, P., and Diehl, A.M. (2016). The severity of nonalcoholic fatty liver disease is associated with gut dysbiosis and shift in the metabolic function of the gut microbiota. *Hepatology (Baltimore, Md.)*, 63(3): 764-75. doi: 10.1002/hep.28356

Brandon, E.F.A., Christiaan, D., Raap, C.D., Meijerman, I., Beijnen, J.A., and

Schellensa, J.S.M. (2003). An update on *in vitro* test methods in human hepatic drug biotransformation research: Pros and cons'. *Toxicology and Applied Pharmacology*, 189(3): 233–46. doi: 10.1016/S0041-008X(03)00128-5.

Bril, F., and Cusi, K. (2017). Management of Nonalcoholic Fatty Liver Disease in Patients With Type 2 Diabetes: A Call to Action. *Diabetes Care,* 40(3): 419-30; doi: 10.2337/dc16-1787.

Brown, G.T., and Kleiner, D.E. (2015). Histopathology of nonalcoholic fatty liver disease and nonalcoholic steatohepatitis. *Metabolism: Clinical and Experimental*, 65(8): 1080-86. doi: 10.1016/j.metabol.2015.11.008

Browning, J.D., and Horton, J.D. (2004). Molecular mediators of hepatic steatosis and liver injury. *The Journal of Clinical Investigation*, 114(2): 147-52. doi: 10.1172/JCI22422

Brunt, E.M., Kleiner, D.E., and Welson, L.A. (2011). Nonalcoholic fatty liver disease (NAFLD) activity score and the histopathologic diagnosis in NAFLD: Distinct clinic pathologic meanings. *Hepatology,* 53: 810-20. doi: 10.1002/hep.24127

Buettner, R., Parhofer, K., Woenkhaus, M., Wrede, C., Kunz-Schughart, L., Scholmerich, J., Bollheimer, L.C. (2006). Defining high-fat rat models:metabolic and molecular effects of different fat types. *Journal of Molecular Endocrinology*, 36(3): 485-501. doi: 10.1677/jme.1.01909

Byrne, C.D., and Targher, G. (2015) 'NAFLD: A multisystem disease', European Association for the Study of the Liver. *Journal of Hepatology*, 62(1): S47–S64. doi: 10.1016/j.jhep.2014.12.012.

Caballero, B. (2007). The Global Epidemic of Obesity: An Overview. *Epidemiologic Reviews*, 29(1): 1–5. doi: 10.1093/epirev/mxm012.

Canda, B.D., Oguntibeju, O.O. and Marnewick, J.L. (2014). Effects of consumption of rooibos (*Aspalathus linearis*) and a rooibos-derived commercial supplement on hepatic

tissue injury by tert -butyl hydroperoxide in Wistar rats. *Oxidative Medicine and Cellular Longevity*, 2014(2014): 716832. doi: 10.1155/2014/716832

Cao, P., Huang, G., Yang, Q., Guo, J., and Su, Z. (2016). The effect of chitooligosaccharides on oleic acid-induced lipid accumulation in HepG2 cells. *Saudi Pharmaceutical Journal*, 24(3): 292-98. doi: 10.1016/j.jsps.2016.04.023

Carr, D., Friedman, M.A. and Jaffe, K. (2007). Understanding the relationship between obesity and positive and negative affect : The role of psychosocial mechanisms. *Body Image*, 4(2): 165–77. doi: 10.1016/j.bodyim.2007.02.004.

Castro, R.E. and Diehl, A.M. (2018). Towards a definite mouse model of NAFLD. *Journal of Hepatology*, 69(2): 272–74. doi: 10.1016/j.jhep.2018.05.002.

Cave, M.C., Clair, H.B., Hardesty, J.E., Falkner, K.C., Feng, W., Clark, B.J., Sidey, J., Shi, H., Aqel, B.A., McClain, C.J., and Prough, R.A. (2016). Nuclear receptors and nonalcoholic fatty liver disease. *Biochimica et Biophysica acta*, 1859(9): 1083-99. doi: 10.1016/j.bbagrm.2016.03.002

Chalasani, N., Wilson, L., Kleiner, D.E., Cummings, O.W., Brunt, E.M., Unalp, A., NASH Clinical Research Network (2008). Relationship of steatosis grade and zonal location to histological features of steatohepatitis in adult patients with non-alcoholic fatty liver disease. *Journal of Hepatology*, 48(5): 829-34. doi: 10.1016/j.jhep.2008.01.016

Chalasani, N., Younossi, Z., Lavine, J.E., Charlton, M., Cusi, K., Rinella, M., Harrison, S.A., Brunt, E.M. and Sanyal, A.J. (2018), The diagnosis and management of nonalcoholic fatty liver disease: Practice guidance from the American Association for the Study of Liver Diseases. *Hepatology*, 67: 328-57. doi: 10.1002/hep.29367.

Chang, E., Park, C.Y., and Park, S.W. (2013). Role of thiazolidinediones, insulin sensitizers, in non-alcoholic fatty liver disease. *Journal of Diabetes Investigation*, 4(6), 517-24. doi: 10.1111/jdi.12107

Chen, N., Bezzina, R., Hinch, E., Lewandowski, P., Cameron-Smith, D., Mathai, M., Jois, M., Sinclair, A., Begg, D., Wark, J., Weisinger, H. and Weisinger, R. (2009). Green tea,

black tea, and epigallocatechin modify body composition, improve glucose tolerance, and differentially alter metabolic gene expression in rats fed a high-fat diet. *Nutrition Research*, 29(11): 784-93. doi: 10.1016/j.nutres.2009.10.003.

Chiu, C.C., Ching, Y.H., Li, Y.P., Liu, J.Y., Huang, Y.T., Huang, Y.W., Yang, S.S., Huang, W.C., andChuang, H.L. (2017). Nonalcoholic Fatty Liver Disease Is Exacerbated in High-Fat Diet-Fed Gnotobiotic Mice by Colonization with the Gut Microbiota from Patients with Nonalcoholic Steatohepatitis. *Nutrients*, 9(11): 1220. doi: 10.3390/nu9111220.

Cioboată, R., Găman, A., Traşcă, D., Ungureanu, A., Docea, A.O., Tomescu, P., Gherghina, F., Arsene, A.L., Badiu, C., Tsatsakis, A.M., Spandidos, D.A., Drakoulis, N., and Călina, D. (2017). Pharmacological management of non-alcoholic fatty liver disease: Atorvastatin versus pentoxifylline. *Experimental and Therapeutic Medicine*, 13(5): 2375-81. doi: 10.3892/etm.2017.4256.

Cui, W., Chen, S.L., and Hu, K.Q. (2010). Quantification and mechanisms of oleic acid-induced steatosis in HepG2 cells. *American Journal of Translational Research*, 2(1): 95-104.

Czaja M.J. (2009). Pioglitazone: more than just an insulin sensitizer. *Hepatology (Baltimore, Md.)*, 49(5): 1427-30. doi: 10.1002/hep.22983

Day, C.P. (2002). Pathogenesis of steatohepatitis. *Best Practice & Research Clinical Gastroenterology,* 16(5): 663-78. doi: 10.1053/bega.2002.0333.

Dowman, J.K., Tomlinson, J.W., and Newsome, P.N. (2009). Pathogenesis of non-alcoholic fatty liver disease. *QJM: Monthly Journal of the Association of Physicians*, 103(2): 71-83. doi: 10.1093/qjmed/hcp158.

Du, J., Ma, Y.Y., Yu, C.H., and Li, Y.M. (2014). Effects of pentoxifylline on nonalcoholic fatty liver disease: a meta-analysis. *World Journal of Gastroenterology*, 20(2): 569-77. doi: 10.3748/wjg.v20.i2.569.

Dyson, J.K., Anstee, Q.M. and Mcpherson, S. (2014). 'Non-alcoholic fatty liver disease:

a practical approach to diagnosis and staging'. *Frontline Gastroenterology*, 5: 211–18. doi:10.1136/flgastro-2013-100403.

Eleazu, C.O., Eleazu, K.C., Chukwuma, S., and Essien, U.N. (2013). Review of the mechanism of cell death resulting from streptozotocin challenge in experimental animals, its practical use and potential risk to humans. *Journal of Diabetes and Metabolic Disorders*, 12(1): 60. doi:10.1186/2251-6581-12-60.

Fabbrini, E., Sullivan, S., and Klein, S. (2010). Obesity and nonalcoholic fatty liver disease: biochemical, metabolic, and clinical implications. *Hepatology (Baltimore, Md.)*, 51(2): 679-89. doi: 10.1002/hep.23280

Facey, A., Dilworth, L., Irving, R. (2017). A Review of the Leptin Hormone and the Association with Obesity and Diabetes Mellitus. *Journal of Diabetes & Metabolism,* 8:727. doi: 10.4172/2155-6156.1000727.

Fatima, W., Shahid, A., Imran, M., Manzoor, J., Hasnain, S., Rana, S., and Mahmood, S. (2011). Leptin deficiency and leptin gene mutations in obese children from Pakistan. *International Journal of Pediatric Obesity.* 6(5-6): 419-27. doi: 10.3109/17477166.2011.608431.

Fengler, V.H.I., Macheiner, T. and Sargsyan, K. (2016). Manifestation of non-alcoholic fatty liver disease / non-alcoholic steatohepatitis in different dietary mouse models. *EMJ Hepatology*, 4(1): 94–102.

Ferramosca, A., Di Giacomo, M., and Zara, V. (2017). Antioxidant dietary approach in treatment of fatty liver: New insights and updates. *World Journal of Gastroenterology*, 23(23): 4146-4157. doi: 10.3748/wjg.v23.i23.4146.

Ferré, P. and Foufelle, F. (2010). Hepatic steatosis: a role for *de novo* lipogenesis and the transcription factor SREBP-1c. *Diabetes, Obesity and Metabolism*, 12: 83-92. doi: 10.1111/j.1463-1326.2010.01275.x.

Francisco, V., Pino, J., Campos-Cabaleiro, V., Ruiz-Fernández, C., Mera, A., Gonzalez-Gay, M.A., Gómez, R., and Gualillo, O. (2018). Obesity, Fat Mass and Immune System:

Role for Leptin. *Frontiers in Physiology*, 9: 640. doi:10.3389/fphys.2018.00640.

Garcia, M., Amankwa-Sakyi, M. and Flynn, T. (2011). Cellular glutathione in fatty liver *in vitro* models. *Toxicology in vitro*, 25(7): 1501-1506. doi: 10.1016/j.tiv.2011.05.011

GBD 2015 Mortality and Causes of Death Collaborators (2016). Global, regional, and national life expectancy, all-cause mortality, and cause-specific mortality for 249 causes of death, 1980-2015: a systematic analysis for the Global Burden of Disease Study 2015. *The Lancet*, *388*(10053): 1459-1544. doi.10.1016/S0140-6736(16)31012-1

Geisler, C. and Renquist, B. (2017). Hepatic lipid accumulation: cause and consequence of dysregulated glucoregulatory hormones. *Journal of Endocrinology*, 234(1): R1-R21. doi: 10.1530/JOE-16-0513

Genel, S., Aurelia, C., Donca, V. and Emanuela, F. (2015). Is the non-alcoholic fatty liver disease part of metabolic syndrome. *Journal of Diabetes and Metabolism*, 6: 4. doi: 10.4172/2155-6156.1000526

Green, C.J., Charlton, C.A., Wang, L.M., Silva, M., Morten, K. J., and Hodson, L. (2017). The isolation of primary hepatocytes from human tissue: optimising the use of small non-encapsulated liver resection surplus. *Cell and Tissue Banking*, *18*(4): 597-604. doi: 10.1007/s10561-017-9641-6.

Guillouzo, A. (1998). Liver cell models in *in vitro* toxicology. *Environmental Health Perspectives*, *106 Suppl 2 (Suppl 2)*, 511: 32. doi: 10.1289/ehp.98106511

Gunn, N.T., and Shiffman, M.L. (2018). The use of liver biopsy in nonalcoholic fatty liver disease: when to biopsy and in whom. *Clinics in Liver Disease,* 22(1): 109-19. doi: 10.1016/j.cld.2017.08.006.

Hadi, H.E., Vettor, R., and Rossato, M. (2018). Vitamin E as a Treatment for nonalcoholic fatty liver disease: reality or myth?. *Antioxidants*, *7*(1): 12. doi:10.3390/antiox7010012.

Hall, J.E., da Silva, A.A., do Carmo, J.M., Dubinion, J., Hamza, S., Munusamy, S., Smith, G., andStec, D.E. (2010). Obesity-induced hypertension: role of sympathetic nervous system, leptin, and melanocortins. *The Journal of Biological Chemistry*, *285*(23): 17271-76. doi: 10.1074/jbc.R110.113175

Hampton, R. (2008). A cholesterol toggle switch. *Cell Metabolism*, 8(6): 451-53. doi: 10.1016/j.cmet.2008.11.006

Han, H.S., Kang, G., Kim, J.S., Choi, B.H., and Koo, S.H. (2016). Regulation of glucose metabolism from a liver-centric perspective. *Experimental & Molecular Medicine*, 48(3): e218. doi:10.1038/emm.2015.122.

Han, L., Shen, W.J., Bittner, S., Kraemer, F.B., and Azhar, S. (2017). PPARs: regulators of metabolism and as therapeutic targets in cardiovascular disease. Part I: PPAR-α. *Future Cardiology*, 13(3): 259-78. doi: 10.2217/fca-2016-0059

Han, S.J., and Boyko, E.J. (2018). The Evidence for an Obesity Paradox in Type 2 Diabetes Mellitus. *Diabetes and Metabolism Journal*, 42(3): 179-87. doi: 10.4093/dmj.2018.0055.

Hansen, H.H., Feigh, M., Veidal, S.S. , Rigbolt, K.T., Vrang, N., and Fosgerau, K. (2017). Mouse models of nonalcoholic steatohepatitis in preclinical drug development. *Drug Discovery Today*, 22(11): 1707–18. doi: 10.1016/J.DRUDIS.2017.06.007.

Harada, N., Oda, Z., Hara, Y., Fujinami, K., Okawa, M., Ohbuchi, K., Yonemoto, M., Ikeda, Y., Ohwaki, K., Aragane, K., Tamai, Y., and Kusunoki, J. (2007). Hepatic *de novo* lipogenesis is present in liver-specific ACC1-deficient mice. *Molecular and Cellular Biology,* 27(5): 1881-88; doi: 10.1128/MCB.01122-06.

Hatting, M., Tavares, C., Sharabi, K., Rines, A.K., and Puigserver, P. (2017). Insulin regulation of gluconeogenesis. *Annals of the New York Academy of Sciences*, 1411(1): 21-35. doi: 10.1111/nyas.13435

Hijona, E., Hijona, L., Arenas, J.I., and Bujanda, L.(2010). Inflammatory mediators of hepatic steatosis. *Mediators of Inflammation,* 2010: 7. doi: 10.1155/2010/837419.

Horton, J.D., Goldstein, J.L., and Brown, M.S. (2002). SREBPs: activators of the complete program of cholesterol and fatty acid synthesis in the liver. *The Journal of Clinical Investigation*, 109(9): 1125-31. doi:10.1172/JCI15593

Howard, R.B., Christensen, A.K., Gibbs, F.A., and Pesch, L.A. (1967). The enzymatic preparation of isolated intact paranchymal cells from rat liver. *The Journal of Cell Biology*, 35(3): 675-84. doi: 10.83/jcb.35.3.675.

Hruby, A., and Hu, F.B. (2015). The epidemiology of obesity: A big picture. *PharmacoEconomics*, 33(7): 673-89. doi: 10.1007/s40273-014-0243-x.

Huang, J., Zhou, Y., Wan, B., Wang, Q., and Wan, X. (2017). Green tea polyphenols alter lipid metabolism in the livers of broiler chickens through increased phosphorylation of AMP-activated protein kinase. *PloS One*, 2(10): e0187061. doi: 10.1371/journal.pone.0187061.

Huh, J.H., Kim, K.J., Kim, S.U., Han, S.H., Kwang-Hyub Han, K., Cha, B., Choon Hee Chung, C.H., Lee, B. (2017). Obesity is more closely related with hepatic steatosis and fibrosis measured by transient elastography than metabolic health status. *Metabolism*, 66: 23-31. https://doi.org/10.1016/j.metabol.2016.10.003.

Inzucchi, S.E., Bergenstal, R.M., Buse, J.B., Diamant, M., Ferrannini, E., Nauck, M., and Peters, A.L., Tsapas, A., Wender, R., and Matthews, D.R. (2015). Management of hyperglycemia in type 2 diabetes, 2015: A patient-centered approach: update to a position statement of the American Diabetes Association and the European Association for the Study of Diabetes. *Diabetes Care*, 38:140–49. doi: 10.2337/dc14-2441.

Ipsen, D.H., Lykkesfeldt, J., and Tveden-Nyborg, P. (2018). Molecular mechanisms of hepatic lipid accumulation in non-alcoholic fatty liver disease. *Cellular and molecular life sciences : CMLS*, *75*(18): 3313-27. doi: 10.1007/s00018-018-2860-6.

Ishida, H., Takizawa, M., Ozawa, S., Nakamichi, Y., Yamaguchi, S., Katsuta, H., Tanaka, T., Maruyama, M., Katahira, H., Yoshimoto, K., Itagaki, E. and Nagamatsu, S. (2004). Pioglitazone improves insulin secretory capacity and prevents the loss of β-cell mass in

obese diabetic *db/db* mice: possible protection of β cells from oxidative stress. *Metabolism*, 53(4): 488-94. doi: 10.1016/j.metabol.2003.11.021

Jiang, Z.G., Robson, S.C., and Yao, Z. (2012). Lipoprotein metabolism in nonalcoholic fatty liver disease. *Journal of Biomedical Research*, 27(1): 1-13. doi: 10.7555/JBR.27.20120077.

Johnson, R., Beer, D., Dludla, P., Ferreira, D., Muller, C. and Joubert, E. (2018). *Aspalathin* from Rooibos (*Aspalathus linearis*): A bioactive C-glucosyl dihydrochalcone with potential to target the metabolic syndrome. *Planta Medica*, 84(09/10): 568-83. doi: 10.1055/s-0044-100622

Joubert, E. and de Beer, D. (2011). Rooibos (*Aspalathus linearis*) beyond the farm gate: From herbal tea to potential phytopharmaceutical. *South African Journal of Botany*, 77(4): 869-86. doi: 10.1016/j.sajb.2011.07.004.

Joubert, E., Jolley, B., Koch, I., Muller, M., Van der Rijst, M. and de Beer, D. (2016). Major production areas of rooibos (*Aspalathus linearis*) deliver herbal tea of similar phenolic and phenylpropenoic acid glucoside content. *South African Journal of Botany*, 103: 162-69. doi: 10.1016/j.sajb.2015.08.015.

Jump, D.B., Tripathy, S., and Depner, C. M. (2013). Fatty acid-regulated transcription factors in the liver. *Annual Review of Nutrition*, *33*: 249-69. doi: 10.1146/annurev-nutr-071812-161139.

Jung, U.J., and Choi, M.S. (2014). Obesity and its metabolic complications: the role of adipokines and the relationship between obesity, inflammation, insulin resistance, dyslipidemia and nonalcoholic fatty liver disease. *International Journal of Molecular Sciences*, 15(4): 6184-223. doi: 10.3390/ijms15046184.

Kaleta, C., de Figueiredo, L.F., Werner, S., Guthke, R., Ristow, M., and Schuster, S. (2011). In silico evidence for gluconeogenesis from fatty acids in humans. *PLoS Computational Biology*, 7(7): 1-10. doi: 10.1371/journal.pcbi.1002116.

Kamakura, R., Son, M., de Beer, D., Joubert, E., Miura, Y. and Yagasaki, K. (2014). Antidiabetic effect of green rooibos (*Aspalathus linearis*) extract in cultured cells and type 2 diabetic model KK-Ay mice. *Cytotechnology*, 67(4): 699-710. doi: 10.1007/s10616-014-9816-y

Kanda. Y., Shimoda, M., Hamamoto, S., Tawaramoto, K., Kawasaki, F., Hashiramoto, M., Nakashima, K., Matsuki, M., and Kaku, K. (2010). Molecular mechanism by which pioglitazone preserves pancreatic b-cells in obese diabeteic mice: evidence for acute and chronic actions as a PPARy agaonist. *American Journal of Physiology- Endocrinology and Metabolism*, 298(2). E278-66 doi: 10.1152/ajpendo.00388.2009

Kang, Y., Kim, J., Joung, K., Lee, J., You, B., Choi, M., Ryu, M., Ko, Y., Lee, M., Lee, J., Ku, B., Shong, M., Lee, K. and Kim, H. (2016). The roles of adipokines, proinflammatory cytokines, and adipose tissue macrophages in obesity-associated insulin resistance in modest obesity and early metabolic dysfunction. *PLOS ONE*, 11(4): e0154003. doi: 10.1371/journal.pone.0154003.

Kanuri, G. and Bergheim, I. (2013). *In vitro* and *in vivo* models of non-alcoholic fatty liver disease (NAFLD). *International Journal of Molecular Sciences*, 14(6): 11963-80. doi: 10.3390/ijms140611963.

Kaur, P., Robin, Mehta, R., Arora, S. and Singh, B. (2018). Progression of conventional hepatic cell culture models to bioengineered HepG2 cells for evaluation of herbal bioactivities. *Biotechnology Letters*, 40(6): 881-93. doi: 10.1007/s10529-018-2547-y.

Kawano, A., Nakamura, H., Hata, S., Minakawa, M., Miura, Y. and Yagasaki, K. (2009). Hypoglycemic effect of aspalathin, a rooibos tea component from *Aspalathus linearis*, in type 2 diabetic model *db/db* mice. *Phytomedicine*, 16(5): 437-43. doi: 10.1016/j.phymed.2008.11.009.

Kawano, Y., and Cohen, D.E. (2013). Mechanisms of hepatic triglyceride accumulation in non-alcoholic fatty liver disease. *Journal of Gastroenterology*, 48(4): 434-41. doi: 10.1007/s00535-013-0758-5.

Kershaw, E. and Flier, J. (2004). Adipose tissue as an endocrine organ. *The Journal of Clinical Endocrinology & Metabolism*, 89(6): 2548-56. doi: 10.1210/jc.2004-0395.

Khoonsari, M., Mohammad Hosseini Azar, M., Ghavam, R., Hatami, K., Asobar, M., Gholami, A., Rajabi, A., Safarnezhad Tameshkel, F., Amirkalali, B., and Sohrabi, M. (2017). Clinical manifestations and diagnosis of nonalcoholic fatty liver disease. *Iranian Journal of Pathology*, *12*(2): 99-105.

Kim, S.H., Lim, Y., Park, J.B., Kwak, J.H., Kim, K.J., Kim, J.H., Song, H., Cho, J.Y., Hwang, D.Y., Kim, K.S., and Jung, Y.S. (2017). Comparative study of fatty liver induced by methionine and choline-deficiency in C57BL/6N mice originating from three different sources. *Laboratory Animal Research*, *33*(2): 157-64. doi: 10.5625/lar.2017.33.2.157

Kim, Y.J., Kim, S.I., Hong, K. and Kang, M.W. (2012), Reply. *Internal Medicine Journal*, 42: 1368-69. doi: 10.1111/imj.12004.

Kitade, H., Chen, G., Ni, Y., and Ota, T. (2017). Nonalcoholic fatty liver disease and insulin resistance: New insights and potential new treatments. *Nutrients*, 9(4): 387. doi:10.3390/nu9040387.

Kobayashi, K., Forte, T.M., Taniguchi, S., Ishida, B.Y., Oka K. and Chan, L. (2000). The *db/db* mouse, a model for diabetic dyslipidemia: molecular characterization and effects of Western diet feeding. *Metabolism*. 49(1): 22-31. doi: 10.1016/S0026-0495(00)90588-2

Koeppen, B.H. and Roux, D.G. (1965). C-Glycosylflavonoids. The chemistry of orientin and iso-orientin. *The Biochemical Journal*, *97*(2): 444-48.

Kohli, R., Kirby, M., Xanthakos, S., Softic, S., Feldstein, A., Saxena, V., Tang, P., Miles, L., Miles, M., Balistreri, W., Woods, S. and Seeley, R. (2010). High-fructose, medium chain trans fat diet induces liver fibrosis and elevates plasma coenzyme Q9 in a novel murine model of obesity and nonalcoholic steatohepatitis. *Hepatology*, 52(3): 934-44. doi: 10.1002/hep.23797.

Kolnes, A., Birk, J., Eilertsen, E., Stuenæs, J., Wojtaszewski, J. and Jensen, J. (2015). Epinephrine-stimulated glycogen breakdown activates glycogen synthase and increases insulin-stimulated glucose uptake in epitrochlearis muscles. *American Journal of*

Physiology-Endocrinology and Metabolism, 308(3): E231-40. doi: 10.1152/ajpendo.00282.2014.

Koo, S.H. (2013). Nonalcoholic fatty liver disease: molecular mechanisms for the hepatic steatosis. *Clinical and Molecular Hepatology*, 19(3): 210-15. doi: 10.3350/cmh.2013.19.3.210.

Koppe, S. and Green, R. (2003). Pentoxifylline attenuates methionine choline deficient (MCD) diet induced steatohepatitis. *Gastroenterology*, 124(4): A707. doi: 10.1016/j.jhep.2004.06.030.

Kotsis, V., Stabouli, S., Papakatsika, S., Rizos, Z. and Parati, G. (2010). Mechanisms of obesity-induced hypertension. *Hypertension Research*, 33(5): 386-93. doi: 10.1038/hr.2010.9.

Kraft, G., Coate, K., Winnick, J., Dardevet, D., Donahue, E., Cherrington, A., Williams, P. and Moore, M. (2017). Glucagon's effect on liver protein metabolism *in vivo*. *American Journal of Physiology-Endocrinology and Metabolism*, 313(3):E263-E272. doi: 10.1152/ajpendo.00045.2017

Krishna, M. (2013). Microscopic anatomy of the liver. *Clinical Liver Disease*, 2: S4-7. doi:10.1002/cld.147.

Kristina, M. Utzschneider, and Steven E. Kahn (2006). The Role of Insulin Resistance in Nonalcoholic Fatty Liver Disease. T*he Journal of Clinical Endocrinology & Metabolism* 91(12): 4753– 61. doi: 10.1210/jc.2006-0587

Lau, J.K., Zhang, X., and Yu, J. (2016). Animal models of non-alcoholic fatty liver disease: current perspectives and recent advances. *The Journal of Pathology*, 241(1): 36-44. doi: 10.1002/path.4829

Lavoie, J. and Gauthier, M. (2006). Regulation of fat metabolism in the liver: link to non-alcoholic hepatic steatosis and impact of physical exercise. *Cellular and Molecular Life Sciences*, 63(12): 1393-1409. doi: 10.1007/s00018-006-6600-y.

Lee, C.A., Sinha, S., Fitzpatrick, E., and Dhawan, A. (2018). Hepatocyte transplantation and advancements in alternative cell sources for liver-based regenerative medicine. *Journal of Molecular Medicine*, 96(6): 469-81. doi: 10.1007/s00109-018-1638-5.

Lee, S. and Jia, Y. (2015). The effect of bioactive compounds in tea on lipid metabolism and obesity through regulation of peroxisome proliferator-activated receptors. *Current Opinion in Lipidology*, 26(1): 3-9. doi: 10.1097/MOL.0000000000000145.

Lee, W. and Bae, J. (2015). Anti-inflammatory effects of Aspalathin and Nothofagin from Rooibos (*Aspalathus linearis*) *in vitro* and *in vivo*. *Inflammation*, 38(4): 1502-16. doi: 10.1007/s10753-015-0125-1.

Lillie, R.D., and Ashburn L.L. (1943). Supersaturated solutions of fat stains in dilute isopropanol for demonstration of acute fatty degeneration not shown by Herxheimer's technique. *Archives of Pathology and Laboratory Medicine*, 36: 432-40.

Limdi, J. and Hyde, G. (2003). Evaluation of abnormal liver function tests. *Postgraduate Medical Journal*, 79(932): 07-312. doi: 10.1136/pmj.79.932.307.

Linardi, D. "Pathophysiology of Insulin Resistance and Type II Diabetes Mellitus" (2018). Master of Science in Nursing (MSN) Student Scholarship. 282. https://digitalcommons.otterbein.edu/stu_msn/282.

Linden, A., Li, S., Choi, H., Fang, F., Fukasawa, M., Uyeda, K., Hammer, R., Horton, J., Engelking, L. and Liang, G. (2018). Interplay between ChREBP and SREBP-1c coordinates postprandial glycolysis and lipogenesis in livers of mice. *Journal of Lipid Research*, 59(3): 475-87. doi: 10.1194/jlr.M081836.

Lisboa, Q., Costa, S. and Couto, C. (2016). Current management of non-alcoholic fatty liver disease. *Revista da Associação Médica Brasileira*, 62(9): 872-78. doi: 10.1590/1806-9282.62.09.872

Liu, Y., Wang, D., Zhang, D., Lv, Y., Wei, Y., Wu, W., Zhou, F., Tang, M., Mao, T., Li, M. and Ji, B. (2011). Inhibitory effect of blueberry polyphenolic compounds on oleic acid-induced hepatic steatosis *in vitro*. *Journal of Agricultural and Food Chemistry*, 59(22): 12254-63.

Lomonaco, R., Sunny, N., Bril, F. and Cusi, K. (2013). Nonalcoholic Fatty Liver Disease: Current Issues and Novel Treatment Approaches. *Drugs*, 73(1): 1-14. doi: 10.1007/s40265-012-0004-0.

Lu, X., Shi, P., Luo, C., Zhou, Y., Yu, H., Guo, C. and Wu, F. (2013). Prevalence of hypertension in overweight and obese children from a large school-based population in Shanghai, China. *BMC Public Health*, 13(1). doi: 10.1186/1471-2458-13-24.

Ma, Y., Wang, W., Zhang, J., Lu, Y., Wu, W., Yan, H., and Wang, Y. (2012). Hyperlipidemia and atherosclerotic lesion development in Ldlr-deficient mice on a long-term high-fat diet. *PloS One*, *7*(4): e35835. doi: 10.1371/journal.pone.0035835.

Mahomoodally, M. (2013). Traditional Medicines in Africa: An Appraisal of Ten Potent African Medicinal Plants. *Evidence-Based Complementary and Alternative Medicine*, 2013: 1-14. doi: 10.1155/2013/617459

Mailleux, J., Timmermans, S., Nelissen, K., Vanmol, J., Vanmierlo, T., van Horssen, J., Bogie, J. and Hendriks, J. (2017). Low-density lipoprotein receptor deficiency attenuates neuroinflammation through the induction of apolipoprotein E. *Frontiers in Immunology*, 8: 1–12. doi: 10.3389/fimmu.2017.01701.

Majno, P., Mentha, G., Toso, C., Morel, P., Peitgen, H. and Fasel, J. (2014). Anatomy of the liver: An outline with three levels of complexity – A further step towards tailored territorial liver resections. *Journal of Hepatology*, 60(3): 654-62. doi: 10.1016/j.jhep.2013.10.026.

Malviya, N., Jain, S. and Malviya, S. (2010). Antidiabetic potential of medicinal plants. Acta Poloniae Pharmaceutica - *Drug Research*, 67 (2): 113-18.

Martin-Rodriguez, J.L., Gonzalez-Cantero, J., Gonzalez-Cantero, A., Arrebola, J.P., and Gonzalez-Calvin, J.L. (2017). Diagnostic accuracy of serum alanine aminotransferase as biomarker for nonalcoholic fatty liver disease and insulin resistance in healthy subjects, using 3T MR spectroscopy. *Medicine*, *96*(17): e6770. doi: 10.1097/MD.0000000000006770.

Masuoka, H.C., and Chalasani, N. (2013). Nonalcoholic fatty liver disease: an emerging threat to obese and diabetic individuals. *Annals of the New York Academy of Sciences*, 1281(1): 106-22. doi: 10.1111/nyas.12016.

Mathijs, K., Kienhuis, A., Brauers, K., Jennen, D., Lahoz, A., Kleinjans, J. and van Delft, J. (2009). Assessing the Metabolic Competence of Sandwich-Cultured Mouse Primary Hepatocytes. *Drug Metabolism and Disposition*, 37(6): 1305-11. doi: 10.1124/dmd.108.025775.

Mavrogiannaki, A.N., and Migdalis, I.N. (2013). Nonalcoholic Fatty liver disease, diabetes mellitus and cardiovascular disease: newer data. *International Journal of Endocrinology*, *2013*: 450639. doi: 10.1155/2013/450639.

May, T., Hauser, H. and Wirth, D. (2004). Transcriptional control of SV40 T-antigen expression allows a complete reversion of immortalization. *Nucleic Acids Research*, 32(18): 5529-38. doi: 10.1093/nar/gkh887. doi: 10.1093/nar/gkh887

Mayer, J., Bates, M. and Dickie, M. (1951). Hereditary Diabetes in Genetically Obese Mice. *Science*, 113(2948): 746-47. doi: 10.1126/science.113.2948.746

Mazibuko, S., Joubert, E., Johnson, R., Louw, J., Opoku, A. and Muller, C. (2015). Aspalathin improves glucose and lipid metabolism in 3T3-L1 adipocytes exposed to palmitate. *Molecular Nutrition & Food Research*, 59(11): 2199-208. doi: 10.1002/mnfr.201500258.

Mazibuko-Mbeje, S., Dludla, P., Roux, C., Johnson, R., Ghoor, S., Joubert, E., Louw, J., Opoku, A. and Muller, C. (2019). Aspalathin-Enriched Green Rooibos Extract Reduces

Hepatic Insulin Resistance by Modulating PI3K/AKT and AMPK Pathways. *International Journal of Molecular Sciences*, 20(3): 633. doi: 10.3390/ijms20030633

Mazza, A., Fruci, B., Garinis, G., Giuliano, S., Malaguarnera, R. and Belfiore, A. (2012). The Role of Metformin in the Management of NAFLD. *Experimental Diabetes Research*, 2012, pp.1-13. doi: 10.1155/2012/716404.

McCracken, E., Monaghan, M. and Sreenivasan, S. (2018). Pathophysiology of the metabolic syndrome. *Clinics in Dermatology*. Elsevier Inc., 36(1): 14–20. doi: 10.1016/j.clindermatol.2017.09.004.

Mckay, D.L. and Blumberg, J.B. (2006). A Review of the Bioactivity of South African Herbal Teas : Rooibos (*Aspalathus linearis*) and Honeybush (*Cyclopia intermedia*). *Phytotherapy Research* 21(1): 1–16. doi: 10.1002/ptr.1992

McPherson, S., Hardy, T., Henderson, E., Burt, A., Day, C. and Anstee, Q. (2015). Evidence of NAFLD progression from steatosis to fibrosing-steatohepatitis using paired biopsies: Implications for prognosis and clinical management. *Journal of Hepatology*, 62(5): 1148-55. doi: 10.1016/j.jhep.2014.11.034.

Meagher, C., Arreaza, G., Peters, A., Strathdee, C., Gilbert, P., Mi, Q., Santamaria, P., Dekaban, G. and Delovitch, T. (2007). CCL4 Protects From Type 1 Diabetes by Altering Islet -Cell-Targeted Inflammatory Responses. *Diabetes*, 56(3): 809-17. doi: 10.2337/db06-0619.

Milagro, F., Campión, J. and Martínez, J. (2006). Weight Gain Induced by High-Fat Feeding Involves Increased Liver Oxidative Stress*. *Obesity*, 14(7): 1118-23. doi: 10.1038/oby.2006.128

Milić, S., Lulić, D. and Štimac, D. (2014) Non-alcoholic fatty liver disease and obesity : Biochemical , *Metabolic and clinical presentations*,20(28): 9330–37. doi: 10.3748/wjg.v20.i28.9330.

Mirza M. S. (2011). Obesity, Visceral Fat, and NAFLD: Querying the Role of Adipokines in the Progression of Nonalcoholic Fatty Liver Disease. *ISRN Gastroenterology*, *2011*: 592404. doi: 10.5402/2011/592404

Moravcová, A., Červinková, Z., Kučera, O., Mezera, V., Rychtrmoc, D. and Lotková H. (2015). The Effect of Oleic and Palmitic Acid on Induction of Steatosis and Cytotoxicity on Rat Hepatocytes in Primary Culture. *Physiological Research*, 64(5): S627-S636.

Mosmann, T. 1983. Rapid colorimetric assay for cellular growth and survival: Application to proliferation and cytotoxicity assays. *J Immunol Methods*, 65(1-2): 55-63. doi.org/10.1016/0022-1759(83)90303-4

Mueller, M and Jungbauer A. (2009) Culinary plants, herbs and spices- A rich source of PPARγ ligands. *Food Chemistry*, 117: 660-67. doi: 10.1016/j.foodchem.2990.04.063

Muller, C.F.J., Joubert, E., Pheiffer, C., Ghoor, S., Sanderson, M., Chellan, N., Fey,. S. J., Louw, J.(2013). Z-2-(β-d-glucopyranosyloxy)-3-phenylpropenoic acid, an α-hydroxy acid from rooibos (*Aspalathus linearis*) with hypoglycemic activity. *Molecular Nutrition and Food Research*, 57(12): 2216–22. doi: 10.1002/mnfr.201300294.

Muller, C., Joubert, E., de Beer, D., Sanderson, M., Malherbe, C., Fey, S. and Louw, J. (2012). Acute assessment of an aspalathin-enriched green rooibos (*Aspalathus linearis*) extract with hypoglycemic potential. *Phytomedicine*, 20(1): 32-39. doi: 10.1016/j.phymed.2012.09.010.

Muller, C., Malherbe, C., Chellan, N., Yagasaki, K., Miura, Y. and Joubert, E. (2017). Potential of rooibos, its major C-glucosyl flavonoids, and Z-2-(β-D-glucopyranosyloxy)-3-phenylpropenoic acid in prevention of metabolic syndrome. *Critical Reviews in Food Science and Nutrition*, 58(2): 227-46. doi:10.1080/10408398.2016.1157568

Musso, G., Gambino, R. and Cassader, M. (2009). Non-alcoholic fatty liver disease from pathogenesis to management: an update. *Obesity Reviews*, 11(6): 430-45. doi: 10.1111/j.1467-789X.2009.00657.x.

Nadulska, A., Szwajgier, D. and Opielak, G. (2017). Obesity and metabolic syndrome.

MEDtube Science, 1.

Najafian, M., Najafian, B. and Najafian, Z. (2016). The effect of aspalathin on levels of sugar and lipids in streptozotocin-induced diabetic and normal rats., *Zahedan Journal of Research in Medical Sciences*, 18(11): e4963. doi: 10.17795/zjrms-4963.

Nalbantoglu, I. L., and Brunt, E.M. (2014). Role of liver biopsy in nonalcoholic fatty liver disease. *World Journal of Gastroenterology*, 20(27): 9026-37. doi: 10.3748/wjg.v20.i27.9026.

Nguyen, P. , Leray, V. , Diez, M. , Serisier, S. , Bloc'h, J.L., Siliart, B. and Dumon, H. (2008), Liver lipid metabolism. *Journal of Animal Physiology and Animal Nutrition*, 92: 272-83. doi:10.1111/j.1439-0396.2007.00752.

Nishikawa, M., Kojima, N., Komori, K., Yamamoto, T., Fujii, T. and Sakai, Y. (2008). Enhanced maintenance and functions of rat hepatocytes induced by combination of on-site oxygenation and coculture with fibroblasts. *Journal of Biotechnology*, 133(2): 253-60. doi: 10.1016/j.jbiotec.2007.08.041

Ober, E.A. and Lemaigre, F.P. (2018). Development of the liver: Insights into organ and tissue morphogenesis. *Journal of Hepatology*. European Association for the Study of the Liver, 68(5): 1049–62. doi: 10.1016/j.jhep.2018.01.005.

Oh, Y.S., Bae, G.D., Baek, D.J., Park, E.Y., and Jun, H.S. (2018). Fatty Acid-Induced Lipotoxicity in Pancreatic Beta-Cells During Development of Type 2 Diabetes. *Frontiers in Endocrinology*, *9*(384): 1-10. doi:10.3389/fendo.2018.00384.

Olawale R. Ajuwon, Emma Katengua-Thamahane, Jacques Van Rooyen, Oluwafemi O. Oguntibeju, and Jeanine L. Marnewick, "Protective Effects of Rooibos (*Aspalathus linearis*) and/or Red Palm Oil (*Elaeis guineensis*) Supplementation on tert-Butyl Hydroperoxide-Induced Oxidative Hepatotoxicity in Wistar Rats," *Evidence-Based Complementary and Alternative Medicine*, 2013: 984273. doi: 10.1155/2013/984273

Oligschlaeger, Y. (2017). DNA Mouse Models for NASH : Are we there yet ?. *Journal of Genetics and DNA Research*, 1(1): 102.

Orlando, P., Chellan, N., Muller, C.J., Louw, J., Chapman, C.C., Joubert, E., and Tiano, L. (2017). Green Rooibos Extract improves plasma lipid profile and oxidative status in diabetic non-human primates. *Free Radical Biology and Medicine*, *108:* S97. doi.org/10.1016/j.freeradbiomed.2017.04.313

Ozougwu, J.C. (2017). Physiology of the liver. *International Journal of Research in Pharmacy and Biosciences,* 4(8): 13–24.

Ortiga-Carvalho, T.M., Oliveira, K.J., and Pazos-Moura*,* C.C*.* (2002) The role of leptin in the regulation of TSH secretion in the fed state: *In vivo* and *in vitro* studies. *Journal of Endocrinology*, 174(1): 121–25. doi: 10.1677/joe.0.1740121.

Pappachan, J.M., Babu, S., Krishnan, B., and Ravindran, N.C. (2017). Non-alcoholic Fatty Liver Disease: A Clinical Update. *Journal of Clinical and Translational Hepatology*, *5*(4): 384-93. doi: 10.14218/JCTH.2017.00013.

Parafati, M., Kirby, R.J., Khorasanizadeh, S., Rastinejad, F., and Malany, S. (2018). A nonalcoholic fatty liver disease model in human induced pluripotent stem cell-derived hepatocytes, created by endoplasmic reticulum stress-induced steatosis. *Disease Models & Mechanisms*, *11*(9): dmm033530. doi:10.1242/dmm.033530.

Parkash, J. and Patel, K. (2015). Hepatoprotective activity of chenopodium album leaves extract in CCl_4 induced hepatotoxicity in rats. *Journal of Drug Delivery and Therapeutics*, 5(2): 88–93. doi: 10.22270/jddt.v5i2.1063

Pauli, E., Staveley-O'Carroll, K.F., Brock, M.V., Efron, D.T., and Efron, G. (2012). A handy tool to teach segmental liver anatomy to surgical trainees. *Archives of Surgery*, *147*(8): 692-93. doi: 10.1001/archsurg.2012.689.

Petta, S., Gastaldelli, A., Rebelos, E., Bugianesi, E., Messa, P., Miele, L., Svegliati-Baroni, G., Valenti, L. and Bonino, F. (2016). Pathophysiology of Non-Alcoholic Fatty Liver Disease. *International Journal of Molecular Sciences*, 17(12): E2082. doi: 10.3390/ijms17122082

Petta, S., Muratore, C. and Craxì, A. (2009). Non-alcoholic fatty liver disease

pathogenesis: The present and the future. *Digestive and Liver Disease*, 41(9): 615-25. doi: 10.1016/j.dld.2009.01.004.

Pinto, K.A., Griep, R.H., Rotenberg, L., da Conceição Chagas Almeida, M., Barreto, R. S., and Aquino, E.M.L., (2018). Gender, time use and overweight and obesity in adults: Results of the Brazilian Longitudinal Study of Adult Health (ELSA-Brasil). *PLoS ONE*, 13(3). doi: 10.1371/journal.pone.0194190

Pocai, A., Obici, S., Schwartz, G. and Rossetti, L. (2005). A brain-liver circuit regulates glucose homeostasis. *Cell Metabolism*, 1(1): 53-61. doi: 10.1016/j.cmet.2004.11.001.

Ponmari, G., Annamalai, A., Gopalakrishnan, V., Lakshmi, P. and Guruvayoorappan, C. (2014). NF-κB activation and proinflammatory cytokines mediated protective effect of Indigofera caerulea Roxb. on CCl_4 induced liver damage in rats. *International Immunopharmacology*, 23(2): 672-680. doi: 10.1016/j.intimp.2014.10.021.

Poteser, M. (2017). Cell-based *in vitro* models in environmental toxicology: a review. *Biomonitoring*, 4(1): 11–26. doi: 10.1515/bimo-2017-0002.

Puchalska, P., and Crawford, P. A. (2017). Multi-dimensional Roles of Ketone Bodies in Fuel Metabolism, Signaling, and Therapeutics. *Cell metabolism*, *25*(2): 262-84. doi: 10.1016/j.cmet.2016.12.022.

Puigserver, P., Rhee, J., Donovan, J., Walkey, C., Yoon, J., Oriente, F., Kitamura, Y., Altomonte, J., Dong, H., Accili, D. and Spiegelman, B. (2003). Insulin-regulated hepatic gluconeogenesis through FOXO1–PGC-1α interaction. *Nature*, 423(6939): 550-55. https://doi.org/10.1038/nature01667.

Puri, P. and Sanyal, A. (2012). Nonalcoholic fatty liver disease: Definitions, risk factors, and workup. *Clinical Liver Disease*, 1(4): 99-103. doi: 10.1002/cld.81

Ramadori, P., Weiskirchen, R., Trebicka, J. and Streetz, K. (2015). Mouse models of metabolic liver injury. *Laboratory Animals*, 49(1): 47-58. doi: 10.1177/0023677215570078.

Reagan-shaw, S., Nihal, M., and Ahmad, N. (2008). Dose translation from animal to human studies revisited. *The FASEB Jornal*. 22(3): 659-61. doi:10.1096/fj.07-9574LSF

Reddy, J. and Sambasiva Rao, M. (2006). Lipid Metabolism and Liver Inflammation. II. Fatty liver disease and fatty acid oxidation. *American Journal of Physiology-Gastrointestinal and Liver Physiology*, 290(5): G852-58. doi:10.1152/ajpgi.00521.2005

Ricchi, M., Odoardi, M., Carulli, L., Anzivino, C., Ballestri, S., Pinetti, A., Fantoni, L., Marra, F., Bertolotti, M., Banni, S., Lonardo, A., Carulli, N. and Loria, P. (2009). Differential effect of oleic and palmitic acid on lipid accumulation and apoptosis in cultured hepatocytes. *Journal of Gastroenterology and Hepatology*, 24(5): 830-40. doi:10.1111/j.1440-1746.2008.05733.x

Rinella, M.E., Loomba, R., Caldwell, S.H., Kowdley, K., Charlton, M., Tetri, B., and Harrison, S.A. (2014). Controversies in the Diagnosis and Management of NAFLD and NASH. *Gastroenterology & Hepatology*, 10(4): 219-27.

Romero-Gómez, M., Zelber-Sagi, S. and Trenell, M. (2017). Treatment of NAFLD with diet, physical activity and exercise. *Journal of Hepatology*, 67(4): 829-46. doi: 10.1016/j.jhep.2017.05.016.

Rouabhia, S., Milic, N. and Abenavoli, L. (2014). Metformin in the treatment of non-alcoholic fatty liver disease: safety, efficacy and mechanism. *Expert Review of Gastroenterology & Hepatology*, 8(4): 343-49. doi: 10.1586/17474124.2014.894880.

Rui, L. (2014). Energy metabolism in the liver. *Comprehensive Physiology*, *4*(1): 177-97. doi: 10.1002/cphy.c130024.

Sanders, F.W., and Griffin, J.L. (2015). *De novo* lipogenesis in the liver in health and disease: more than just a shunting yard for glucose. *Biological reviews of the Cambridge Philosophical Society*, 91(2): 452-68. doi: 10.1111/brv.12178.

Sanders, F., Acharjee, A., Walker, C., Marney, L., Roberts, L.D., Imamura, F., Jenkins, B., Case, J., Ray, S., Virtue, S., Vidal-Puig, A., Kuh, D., Hardy, R., Allison, M., Forouhi, N., Murray, A.J., Wareham, N., Vacca, M., Koulman, A. and Griffin, J.L. (2018). Hepatic

steatosis risk is partly driven by increased *de novo* lipogenesis following carbohydrate consumption. *Genome Biology*, 19(1): 79. doi:10.1186/s13059-018-1439-8.

Sanderson, M., Mazibuko, S., Joubert, E., de Beer, D., Johnson, R., Pheiffer, C., Louw, J. and Muller, C. (2014). Effects of fermented rooibos (*Aspalathus linearis*) on adipocyte differentiation. *Phytomedicine*, 21(2): 109-17. doi: 10.1016/j.phymed.2013.08.011.

Santhekadur, P.K., Kumar, D.P., and Sanyal, A.J. (2017). Preclinical models of non-alcoholic fatty liver disease. *Journal of Hepatology*, 68(2): 230-37.

Sanyal, A.J., Chalasani, N., Kowdley, K.V., McCullough, A., Diehl, A.M., Bass, N.M., Neuschwander-Tetri, B.A., Lavine, J.E., Tonascia, J., Unalp, A., Van Natta, M., Clark, J., Brunt, E. M., Kleiner, D.E., Hoofnagle, J.H., Robuck, P.R., NASH CRN (2010). Pioglitazone, vitamin E, or placebo for nonalcoholic steatohepatitis. *The New England Journal of Medicine*, 362(18): 1675-85. doi: 10.1056/NEJMoa0907929.

Sartorio, A., Del Col, A., Agosti, F., Mazzilli, G., Bellentani, S., Tiribelli, C., and Bedogni, G. (2007). Predictors of non-alcoholic fatty liver disease in obese children. *European Journal of Clinical Nutrition,* 61:877–83 doi: 10.1038/sj.ejcn.1602588.

Sasaki, M., Nishida, N., and Shimada, M. (2018). A Beneficial Role of Rooibos in Diabetes Mellitus: A Systematic Review and Meta-Analysis. *Molecules (Basel, Switzerland)*, *23*(4): 839. doi: 10.3390/molecules23040839.

Sass, D., Chang, P. and Chopra, K. (2005). Nonalcoholic Fatty Liver Disease: A Clinical Review. *Digestive Diseases and Sciences*, 50(1): 171-80. doi: 10.1007/s10620-005-1267-z

Schonborn, J.L. (2010). The role of the liver in drug metabolism anaesthesia tutorial of the week 179.*Drug metabolism.*

Serván, P. R. (2013). Obesity and Diabetes. *Nutricion Hospitalaria*, 28 (5): 138-43. doi: 10.3305/nh.2013.28.sup5.6929.

Singh, V., Sharma, P. and Alam, M. (2018). Metabolism of drugs with inhibition of

enzymes. *Journal of Drug Metabolism & Toxicology*, 09(01). doi: 10.4172/2157-7609.1000233.

Sinisalo, M., Enkovaara, A.L. and Kivistö, K.T. (2010). Possible hepatotoxic effect of rooibos tea: A case report. *European Journal of Clinical Pharmacology*, 66(4): 427–28. doi: 10.1007/s00228-009-0776-7.

Smith, P., Krohn, R., Hermanson, G., Mallia, A., Gartner, F., Provenzano, M., Fujimoto, E., Goeke, N., Olson, B. and Klenk, D. (1985). Measurement of protein using bicinchoninic acid. *Analytical Biochemistry*, 150(1): 76-85. doi: 10.1016/0003-2697(85)90442-7

Soccio, R.E., Chen, E.R., and Lazar, M.A. (2014). Thiazolidinediones and the promise of insulin sensitization in type 2 diabetes. *Cell Metabolism*, *20*(4): 573-91. doi: 10.1016/j.cmet.2014.08.005.

Solinas, G., Borén, J. and Dulloo, A.G. (2015). *De novo* lipogenesis in metabolic homeostasis : More friend than foe ? *Molecular Metabolism*, 4(5): 367–377. doi: 10.1016/j.molmet.2015.03.004.

Son, M., Minakawa, M., Miura, Y. and Yagasaki, K. (2013). Aspalathin improves hyperglycemia and glucose intolerance in obese diabetic *ob/ob* mice. *European Journal of Nutrition*, 52(6): 1607-1619. doi: 10.1007/s00394-012-0466-6

Song, Z., Xiaoli, A. and Yang, F. (2018). Regulation and metabolic significance of *de novo* lipogenesis in adipose tissues. *Nutrients*, 10(10): 1383. doi: 10.3390/nu10101383.

Souza, M., Diniz, M., Medeiros-Filho, J. and Araújo, M. (2012). Metabolic syndrome and risk factors for non-alcoholic fatty liver disease. *Arquivos de Gastroenterologia*, 49(1): 89-96. doi.org/10.1590/S0004-28032012000100015

Souza-Mello, V. (2015). Peroxisome proliferator-activated receptors as targets to treat non-alcoholic fatty liver disease. *World Journal of Hepatology*, 7(8): 1012-19. doi: 10.4254/wjh.v7.i8.1012.

Stål P. (2015). Liver fibrosis in non-alcoholic fatty liver disease - diagnostic challenge with prognostic significance. *World Journal of Gastroenterology*, 21(39): 11077-87. doi: 10.3748/wjg.v21.i39.11077.

Sumida, Y., and Yoneda, M. (2017). Current and future pharmacological therapies for NAFLD/NASH. *Journal of Gastroenterology*, 53(3): 362-376. doi: 10.1007/s00535-017-1415-1.

Takahashi, Y. and Fukusato, T. (2010). Pediatric nonalcoholic fatty liver disease: Overview with emphasis on histology. *World Journal of Gastroenterology*, 16(42): 5280. doi: 10.3748/wjg.v16.i42.5280.

Takahashi, Y. and Fukusato, T. (2014). Histopathology of nonalcoholic fatty liver disease/nonalcoholic steatohepatitis. *World Journal of Gastroenterology*, 20(42): 15539. doi: 10.3748/wjg.v20.i42.15539.

Takahashi, Y., Soejima, Y., and Fukusato, T. (2012). Animal models of nonalcoholic fatty liver disease/nonalcoholic steatohepatitis. *World Journal of Gastroenterology*, 18(19): 2300-08. doi: 10.3748/wjg.v18.i19.2300.

Takahashi, Y., Sugimoto, K., Inui, H., and Fukusato, T. (2015). Current pharmacological therapies for nonalcoholic fatty liver disease/nonalcoholic steatohepatitis. *World Journal of Gastroenterology*, 21(13): 3777-85. doi: 10.3748/wjg.v21.i13.3777

Tall, A. (2008). Cholesterol efflux pathways and other potential mechanisms involved in the athero-protective effect of high density lipoproteins. *Journal of Internal Medicine*, 263(3): 256-73. doi: 10.1111/j.1365-2796.2007.01898.x.

Ter Horst, K.W., and Serlie, M.J. (2017). Fructose consumption, lipogenesis, and non-alcoholic fatty liver disease. *Nutrients*, 9(9): 981. doi: 10.3390/nu9090981.

Tian, J., Zhong, R., Liu, C., Tang, Y., Gong, J., Chang, J., Lou, J., Ke, J., Li, J., Zhang, Y., Yang, Y., Zhu, Y., Gong, Y., Xu, Y., Liu, P., Yu, X., Xiao, L., Du, M., Yang, L., Yuan, J., Wang, Y., Chen, W., Wei, S., Liang, Y., Zhang, X., He, M., Wu, T., Yao, P. and Miao, X. (2016). Association between bilirubin and risk of non-alcoholic fatty liver disease based

on a prospective cohort study. *Scientific reports*, 6: 31006. doi:10.1038/srep31006

Torres, D.M., William,s C.D., Harrison, S.A. (2012). Features, diagnosis, and treatment of nonalcoholic fatty liver disease. *Clinical Gastroenterol and Hepatology*, 10(8): 837-58. doi: 10.1016/j.cgh.2012.03.011.

Trak-Smayra, V., Paradis, V., Massart, J., Nasser, S., Jebara, V., and Fromenty, B. (2011). Pathology of the liver in obese and diabetic *ob/ob* and *db/db* mice fed a standard or high-calorie diet. *International Journal of Experimental Pathology*, 92(6): 413-21. doi: 10.1111/j.1365-2613.2011.00793.x

Trauner, M., Arrese, M. and Wagner, M. (2009). Fatty liver and lipotoxicity. *(BBA) - Molecular and Cell Biology of Lipids*, 1801(3): 299-310. doi: 10.1016/j.bbalip.2009.10.007.

Tsai, M., Chen, C., Pan, Y., Wang, S., Mersmann, H. and Ding, S. (2015). Alleviation of Carbon-Tetrachloride-Induced Liver Injury and Fibrosis by Betaine Supplementation in Chickens. *Evidence-Based Complementary and Alternative Medicine*, 2015: 1-12. doi: 10.1155/2015/725379

Uguccioni, G., D'souza, D. and Hood, D. (2010). Regulation of PPARγ Coactivator-1α Function and Expression in Muscle: Effect of Exercise. *PPAR Research*, 2010, pp.1-7. doi: 10.1155/2010/937123.

Ulicná O., Greksák M., Vancová O., Zlatos L., Galbavý S., Bozek P., and Nakano M. (2003). Hepatoprotective effect of Rooibos tea (*Aspalathus linearis*) on CCl4-induced liver damage in rats. *Physiological Research / Academia Scientiarum Bohemoslovaca*, 52(4): 461–66.

University of Zululand. Faculty of Biochemistry and Microbiology, Buthelezi N.N. (2017). An *in vitro* and *in vivo* hepatotoxicity study of an aspalathin-rich green rooibos extract.

Uyeda, K. and Repa, J. (2006). Carbohydrate response element binding protein, ChREBP, a transcription factor coupling hepatic glucose utilization and lipid synthesis. *Cell Metabolism*, 4(2): 107-10. doi: 10.1016/j.cmet.2006.06.008.

Valenti, L., Riso, P., Mazzocchi, A., Porrini, M., Fargion, S. and Agostoni, C. (2013). Dietary Anthocyanins as Nutritional Therapy for Nonalcoholic Fatty Liver Disease. *Oxidative Medicine and Cellular Longevity*, 2013: 1-8. doi: 10.1155/2013/145421

Valentová, K., Truong, N., Moncion, A., de Waziers, I. and Ulrichová, J. (2007). Induction of glucokinase mRNA by dietary phenolic compounds in rat liver cells *in vitro*. *Journal of Agricultural and Food Chemistry*, 55(19): 7726-31. doi: 10.1021/jf0712447

Van de Bovenkamp, M. , Groothuis, G. M., Meijer, D. K., and Olinga, P. (2007). Liver fibrosis *in vitro*: Cell culture models and precision-cut liver slices. *Toxicology in Vitro*, 21(4): 545–57. doi: 10.1016/j.tiv.2006.12.009.

Van De Wier, B., Koek, G., Bast, A. and Haenen, G. (2015). The potential of flavonoids in the treatment of non-alcoholic fatty liver disease. *Critical Reviews in Food Science and Nutrition*, 57(4): 834-55. doi: 10.1080/10408398.2014.952399

van der Merwe, J., de Beer, D., Joubert, E. and Gelderblom, W. (2015). Short-term and sub-chronic dietary exposure to Aspalathin-enriched green Rooibos (*Aspalathus linearis*) extract affects rat liver function and antioxidant status. *Molecules*, 20(12): 22674-90. doi: 10.3390/molecules201219868.

Van Herck, M., Vonghia, L. and Francque, S. (2017). Animal models of nonalcoholic fatty liver disease—A starter's guide. *Nutrients*, 9(10): 1072. doi: 10.3390/nu9101072.

Vendel Nielsen, L., Krogager, T., Young, C., Ferreri, C., Chatgilialoglu, C., Nørregaard Jensen, O. and Enghild, J. (2013). Effects of elaidic acid on lipid metabolism in HepG2 cells, investigated by an integrated approach of lipidomics, transcriptomics and proteomics. *PLoS ONE*, 8(9): e74283. doi: 10.1371/journal.pone.0074283.

von Wettstein-Knowles, P., Olsen, J., McGuire, K. and Henriksen, A. (2006). Fatty acid

synthesis. Role of active site histidines and lysine in Cys-His-His-type beta-ketoacyl-acyl carrier protein synthases. *FEBS Journal*, 273(4): 695-710. doi: 10.1111/j.1742-4658.2005.05101.x.

Wang, B., Chandrasekera, P.C., and Pippin, J.J. (2014). Leptin- and leptin receptor-deficient rodent models: relevance for human type 2 diabetes. *Current Diabetes Reviews*, *10*(2):131-45. doi: 10.2174/1573399810666140508121012.

Wang, S., Sun, T., Whitaker, B. and Faust, M. (1988). Effect of paclobutrazol on membrane lipids in apple seedlings. *Physiologia Plantarum*, 73(4): 560-64. doi: 10.1111/j.1399-3054.1988.tb05441.x.

Wang, Y., Viscarra, J., Kim, S.J., and Sul, H.S. (2015). Transcriptional regulation of hepatic lipogenesis. *Nature Reviews. Molecular Cell Biology*, 16(11): 678-89. doi: 10.1038/nrm4074.

Wang, Y., Viscarra, J., Kim, S.J., and Sul, H.S. (2015). Transcriptional regulation of hepatic lipogenesis. *Nature Reviews. Molecular Cell Biology*, 16(11): 678-89. doi: 10.1038/nrm4074

Weyermann, J., Lochmann, D.,and Zimmer, A. 2005. A practical note on the use of cytotoxicity assays. *International Journal of Pharmaceutics*, 288(2): 369-76. doi: 10.1016/j.ijpharm.2004.09.018

Woods, A., Williams, J. R., Muckett, P.J., Mayer, F.V., Liljevald, M., Bohlooly-Y, M., and Carling, D. (2017). Liver-Specific Activation of AMPK Prevents Steatosis on a High-Fructose Diet. *Cell reports*, *18*(13): 3043-51. doi: 10.1016/j.celrep.2017.03.011.

Wu, H., Deng, X., Shi, Y., Su, Y., Wei, J. and Duan, H. (2016). PGC-1α, glucose metabolism and type 2 diabetes mellitus. *Journal of Endocrinology*, 229(3): R99-R115. doi:10.1530/JOE-16-0021

Yang, J., Gadi, R., Paulino, R. and Thomson, T. (2010). Total phenolics, ascorbic acid,

and antioxidant capacity of noni (Morinda citrifolia L.) juice and powder as affected by illumination during storage. *Food Chemistry*, 122(3): 627-32. doi: 10.1016/j.foodchem.2010.03.022

Yang, X., Fu, Y., Hu, F., Luo, X., Hu, J., and Wang, G. (2018). PIK3R3 regulates PPAR α expression to stimulate fatty acid β-oxidation and decrease hepatosteatosis. *Experimental & Molecular Medicine,* 50(1): e431. doi:10.1038/emm.2017.243.

Yao, H., Qiao, Y.J., Zhao, Y. L., Tao, X.F., Xu, L.N., Yin, L.H., Qi, Y. and Peng, J.Y. (2016). Herbal medicines and nonalcoholic fatty liver disease. *World Journal of Gastroenterology*, *22*(30): 6890-905.

Ye, J., Chao, J., Chang, M., Peng, W., Cheng, H., Liao, J. and Pao, L. (2016). Pentoxifylline ameliorates non-alcoholic fatty liver disease in hyperglycaemic and dyslipidaemic mice by upregulating fatty acid β-oxidation. *Scientific Reports*, 6(1). DOI:10.1038/srep33102.

Yeh, M.M. and Brunt, E.M. (2007). Pathology of nonalcoholic fatty liver disease. *American Journal of Clinical Pathology*, 128: 837–47. doi: 10.1309/RTPM1PY6YGBL2G2R

Yoneda, M., Yoneda, M., Mawatari, H., Fujita, K., Endo, H., Iida, H., Nozaki, Y., Yonemitsu, K., Higurashi, T., Takahashi, H., Kobayashi, N., Kirikoshi, H., Abe, Y., Inamori, M., Kubota, K., Saito, S., Tamano, M., Hiraishi, H., Maeyama, S., Yamaguchi, N., Togo, S. and Nakajima, A. (2008). Noninvasive assessment of liver fibrosis by measurement of stiffness in patients with nonalcoholic fatty liver disease (NAFLD). *Digestive and Liver Disease*, 40(5): 371-78. doi: 10.1016/j.dld.2007.10.019

Zang, M. (2016).The Molecular basis of hepatic *de novo* lipogenesis in insulin resistance. *Hepatic De Novo Lipogenesis and Regulation of Metabolism*, 33–58. doi: 10.1007/978-3-319-25065-6_2.

Zhang, Y., Guan, Q., Liu, Y., Zhang, Y., Chen, Y., Chen, J., Liu, Y. and Su, Z. (2018). Regulation of hepatic gluconeogenesis by nuclear factor Y transcription factor in

mice. *Journal of Biological Chemistry*, 293(20): 7894-7904. doi: 10.1074/jbc.RA117.000508

Zhang, Y., Yin, L. and Hillgartner, F. (2003). SREBP-1 integrates the actions of thyroid hormone, insulin, cAMP, and medium-chain fatty acids on ACCα transcription in hepatocytes. *Journal of Lipid Research*, 44(2): 356-68. doi: 10.1194/jlr.M200283-JLR200.

Zhou, Z., Xu, M.J., and Gao, B. (2015). Hepatocytes: a key cell type for innate immunity. *Cellular & Molecular Immunology*, *13*(3): 301-15. doi: 10.1038/cmi.2015.97.

Ziamajidi, N., Khaghani, S., Hassanzadeh, G., Vardasbi, S., Ahmadian, S., Nowrouzi, A., Ghaffari, S. and Abdirad, A. (2013). Amelioration by chicory seed extract of diabetes- and oleic acid-induced non-alcoholic fatty liver disease (NAFLD)/non-alcoholic steatohepatitis (NASH) via modulation of PPARα and SREBP-1. *Food and Chemical Toxicology*, 58: 198-209. doi: 10.1016/j.fct.2013.04.018.

CHAPTER EIGHT

APPENDIX

8.0 APPENDIX

8.1.1 Ethical approval (SAMRC-ECRA REF.05/17)

saMRC advancinglife

ETHICS COMMITTEE FOR RESEARCH ON ANIMALS (ECRA)

29 March 2017

Miss Y Ntamo
BRIP
MEDICAL RESEARCH COUNCIL

Dear Miss Ntamo,

CERTIFICATE OF FINAL APPROVAL – REF. 05/17 "Amelioration of the longer term effects of diabetes on pancreatic beta cells and hepatotoxicity by *Aspalathus linearis* (Rooibos) in db/db mice"

The ECRA Committee reviewed your corrected Application and it was final approved.

Attached herewith please find your Certificate of Approval for the period 30 March 2017 – 31 July 2-18. Should this study period not be long enough, please write a letter to the ECRA Committee requested an extension on the study.

Should you encounter any difficulties duties your study or sudden death of the animals, please do not hesitate to inform the ECRA thereof as well as the reason for the death. You will need to submit every 6 months an interim report on the study to the ECRA Committee. The secretariat will inform you thereof in time.

Kind regards.

PROF D DU TOIT

Animal Ethics Approval Certificate

Decision of the Animal Ethics Committee for the use of living vertebrates for research, diagnostic procedures and product development

APPROVAL PERIOD: 30 March 2017 – 31 July 2018

PROJECT NUMBER:	05/17			
PROJECT TITLE:	**"Amelioration of the longer term effects of diabetes on pancreatic beta cells and hepatotoxicity by *Asapalthus linearis* (Rooibos) in db/db mice"**			
PROJECT LEADER:	Miss Yonela Ntamo			
DIVISION:	Biomedical Research and Innovation Platform (BRIP)			
CATEGORY:	Diabetes			
SPECIES OF ANIMAL:	Mouse BKS.Cg-Dock7 (m)	+/+ Lepr (db)/J	6 week old males 30gr	
NUMBER OF ANIMALS:	200			
NOT APPROVED:	n/a			
APPROVED:	29 March 2017			

PLEASE NOTE: Should the number or species of animal(s) required, or the experimental procedure(s) change, please submit a revised animal ethics clearance form to the animal ethics committee for approval before commencing with the experiment

PROF D DU TOIT **DATE** **29 March 2017**

CHAIRPERSON ANIMAL ETHICS COMMITTEE

8.1.2 Ethical clearance (UZREC 171110-030)

UNIVERSITY OF ZULULAND
RESEARCH ETHICS COMMITTEE
(Reg No: UZREC 171110-030)

RESEARCH & INNOVATION
Website: http://www.unizulu.ac.za
Private Bag X1001
KwaDlangezwa 3886
Tel: 035 902 6731
Fax: 035 902 6222
Email: DlaminJA@unizulu.ac.za

ETHICAL CLEARANCE CERTIFICATE

Certificate Number	**UZREC 171110-030 PGM 2017/479**						
Project Title	**A STUDY OF THE PROTECTIVE EFFECTS OF AN ASPALATHIN ENRICHED GREEN EXTRACT ON EXPERIMENTALLY-INDUCED HEPATIC STEATOSIS**						
Principal Researcher/ Investigator	NT Khuboni						
Supervisor and Co-supervisor	Prof AP Kappo Dr K Gabuza		Prof C Muller Dr R Mosa				
Department	Biochemistry and Microbiology						
Faculty	SCIENCE AND AGRICULTURE						
Type of Risk	Low Risk– Data collection from animals						
Nature of Project	Honours/4th Year		Master's	x	Doctoral		Departmental

The University of Zululand's Research Ethics Committee (UZREC) hereby gives ethical approval in respect of the undertakings contained in the above-mentioned project. The Researcher may therefore commence with data collection as from the date of this Certificate, using the certificate number indicated above.

Special conditions:

(1) This certificate is valid for 3 years from the date of issue.
(2) Principal researcher must provide an annual report to the UZREC in the prescribed format [due date-30 April 2018]
(3) Principal researcher must submit a report at the end of project in respect of ethical compliance.
(4) The UZREC must be informed immediately of any material change in the conditions or undertakings mentioned in the documents that were presented to the meeting.

The UZREC wishes the researcher well in conducting research.

Professor Gideon De Wet
Chairperson: University Research Ethics Committee
Deputy Vice-Chancellor: Research & Innovation
08 March 2018

CHAIRPERSON
UNIVERSITY OF ZULULAND RESEARCH ETHICS COMMITTEE (UZREC)
REG NO: UZREC 171110-30
09 -03- 2018
RESEARCH & INNOVATION OFFICE

8.1.3 Proofreading and report

GRANTS INNOVATION & PRODUCT DEVELOPMENT
BIOMEDICAL RESEARCH & INNOVATION PLATFORM

05 March 2019

The Post-graduate Examination Committee
University of Zululand

MSc thesis Proof reading report Ms Noxolo Khuboni

I have proof read the above thesis for English language correctness and readability and hereby certify that the thesis titled "**A study of the protective effects of an aspalathin enriched green rooibos extract on experimentally induced hepatic steatosis**" is acceptable in its current form for examination and publication.

I hope you find this in order.

Yours sincerely,

CSChapman

Mrs. C.S. Chapman

Laboratory Manager
Biomedical Research and Innovation Platform

8.2 Reagents and buffers solutions

Product name	Supplier	Product number
Oleic acid	Sigma-Aldrich, St Louis, MO, USA	SLBQ9717V
Pioglitazone	Sigma-Aldrich, St Louis, MO, USA	LRAA5299
MTT Reagent	Sigma-Aldrich, St Louis, MO, USA	MKBW0847V
Crystal Violet		
Oil Red O	Sigma, St Louise, MO, USA	1320-06-5
Isopropanol	Sigma-Aldrich, St Louis, MO, USA	I9516
Neutral Buffered formalin	Sigma-Aldrich, St Louis, MO, USA	HT501128
Ethanol	Sigma-Aldrich, St Louis, MO, USA	0030123.328
Water (TC grade)	Sigma-Aldrich, St Louis, MO, USA	BE 17-724Q
PBS	Lonza, Walkersville, MD, USA	BE17-513F
Dulbecco`s phosphate buffered saline (DPBS)	Lonza, Walkersville, MD, USA	17-513F
Eagle's minimum essential medium (EMEM)	Lonza, Walkersville, MD, USA	BE12-662F
Trypsin	Millipore, Bellerica, MA, USA	2500-056
Trypan blue	Invitrogen, Carlsbad, CA, USA	15050-065
Albumin, Bovine Fraction V (fatty acid-free)	Melford Laboratories, Ipswich Suffolk, U.K.	A1302

Fetal Bovine Serum (FBS)	Sigma-Aldrich, St Louis, MO, USA	F2442
L-Glutamine	Lonza, Walkersville, MD, USA	BE17-605E
Dimethyl sulfoxide (DMSO)	Sigma-Aldrich, St Louis, MO, USA	276855
Phenylmethanesulfonyl fluoride (PMSF)	Roche, Basel, Switzerland	11206893001
Cell extraction lysis Buffer	Life Technologies Corporation, Carlsbad, CA, USA	FNN0011
PMSF	Fluka	78830
Ammonium persulfate (APS)	Bio-Rad, Hercules, CA, USA	1610700
Acrylamide	Bio-Rad, Hercules, CA, USA	1610156
Non-fat milk powder (Elite Clover SA)	Pick n Pay	N/A
Whatman paper	Merck	3031-915
Hybond-P PVDF membrane	Amersham	RPN1416F
Methanol	Fluka	65543
Tris	Fluka	93352
Stainless steel beads	Qiagen	69989
High capacity cDNA reverse transcription kit	Applied Biosystems, Foster City, CA, USA	4368814
TaqMan® Gene Expression Cells-to-CT™ Kit	Ambion by life technologies	1205047
RNase inhibitor	Applied Biosystems, Foster City, CA, USA	N8080119
High capacity reverse transcription kit	Applied Biosystems, Foster City, CA, USA	00325750
Precision plus protein ™ western c ™standards	Bio-Rad, Hercules, CA, USA	161-0376
Precision protein™ strep tactin-HPRTN conjugate	Bio-Rad, Hercules, CA, USA	1610381

Entellan	Merck	1.07961.0500
Nuclease-free water	Ambion	1701323
Restore™ Plus western blot stripping buffer	Thermo Scientific	SL258473
Clarity™ western ECL substrate	Bio-Rad	170-5061
Pierce™ BCA protein assay kit	Thermo Scientific	MA152117
Tween 20	Sigma-Aldrich, St Louis, MO, USA	MKCD6838
Trans-blot Turbo™ 5x transfer buffer	Bio-Rad, Hercules, CA, USA	100266958
Chloroform	Sigma-Aldrich, St Louis, MO, USA	136112-00-0
Isopropanol	Sigma-Aldrich, St Louis, MO, USA	I9516
Lysis buffer	Cell Signalling Technology, Danvers, MA, USA	9803
β-mercaptoethanol	Sigma-Aldrich, St Louis, MO, USA	60-24-2
Coomasie blue stain	Bio-Rad, Hercules, CA, USA	161-0437

8.3: List of consumables

Product name	Supplier	Product number
PCR plates	Applied Biosystems, Foster City, CA, USA	N8010560
0. 2 PCR tubes, flat cap	Axgyen, Corning, NY	AX/PCR-02-C/S
0.5 mL Eppendorf safe-lock tubes	Eppendorf, Hamburg, German	0030 123.301
1.5 mL Eppendorf safe- lock tubes	Eppendorf, Hamburg, Germany	0030 123.328
2 mL Eppendorf safe- lock tubes	Eppendorf, Hamburg, Germany	0030 123. 344
15 mL centrifuge tubes	NEST Biotechnology, Jiangsu China Wuxi	602072
50 mL centrifuge tubes	NEST Biotechnology, Jiangsu China Wuxi	601001
CELLBIND- 6 well plates	Corning, MA, USA	3335
CELLBIND -96well clear plates	Corning, MA, USA	3300
Filter Pads	Sigma-Aldrich, St Louis, MO, USA	23385
T75 Flasks	Greiner bio-one, Frickenhausen, Germany	658975
Cell counting chamber slides	C10228	Life Technologies Corporation, Carlsbad, CA, USA
Stainless steel beads 5mm	Qiagen, Hilden, Germany	69989
Whatman3MMChr sheets	Sigma-Aldrich, St Louis, MO, USA	3030-931
Cryotubes	Corning, MA, USA	430659

Polyvinylidene Fluoridine Membrane (PVDF)	88585	Pierce, Rockford, IL, USA

8.4: Equipment's

Product name	Supplier	Product number
FLX800 Fluorescence microplate reader	Bio-Tek, Winooski, VT, USA	Gen5v.1.05
Quantity One Software	Bio-Rad, Hercules, CA, USA	170-9600
Tissue lyser	Qiagen, Hilden, Germany	85600
Countess® automated cell counter	Invitrogen, Carlsbad, CA, USA	C10311
Bio-Rad chemiDoc	Bio-Rad, Hercules, CA, USA170	-8265
Microscope NIS elements software with a Nikon Eclipse Ti inverted microscope	(Nikon, Kanagawa, Japan)	
Graphpad Prism ®	Graphpad Software Inc, CA, USA	Version 5.02

8.5 Buffers and media used in this study

Eagle's Minimum Essential Medium (EMEM)

90% complete growth media (containing 100 mM Sodium Pyruvate, 1% non-essential amino acids (NEAAs) was supplemented with 10% foetal bovine serum (FBS), 2 ml glutamine and 2 ml penicillin-streptomycin.

Oil red O solution

1% (w/v) ORO stock solution was prepared by dissolving 1 g of ORO powder in 100 ml isopropanol and left to mix on a magnetic stirrer overnight. An ORO working solution 70% (v/v) was made from the stock by diluting 70 ml stock solution with 30 ml distilled water. The solution was filtered to remove any precipitate.

Crystal violet solution

2% (w/v) CV stock solution was prepared by dissolving 2 g of crystal violet powder in 100 ml of TC grade water, stirred using a magnetic stirrer. A working solution was prepared by diluting 250 µl of stock solution (2%) with 50ml of distilled water. The working solution was prepared fresh every time before use.

MTT reagent

1 mg/ml solution was prepared by dissolving 43 mg of MTT reagent in 43 ml of DPBS. This reagent was filter sterilized then covered with foil as it is light sensitive.

Sorenson's Glycine buffer

0.751 g glycine (0.1 M) and 0.584 g sodium chloride (NaCl) (0.1 M) were weighed and dissolved in 100 ml TC water. The pH was adjusted to 10.5 using sodium hydroxide (NaOH).

5x transfer buffer

5 x transfer buffer was prepared by dissolving 3.03 g 25 mM Tris (MW=121.1) and 14.41 g 192 mM glycine (MW= 75.07) in 800 ml double distilled water.

1x transfer buffer

1 x transfer buffer was prepared by mixing 200 ml 5 x transfer buffer with 600 ml double distilled water and 200 ml ethanol (molecular grade 95~99% purity).

10x Tris-buffered saline (10x TBS pH= 7.6)

10 x TBS was prepared by dissolving 24.22 g 200 mM Tris and 80.06 g 1.37 mM NaCl (MW=58.44) made up to 1 L with double distilled water.

1x Tris-buffered saline and Tween 20 (1x TBST)

1 x TBST was prepared by diluting 100 ml 10x TBS with 900 ml double distilled water and adding 1 ml Tween-20.

10% Ammonium persulphate solution

10% APS was prepared by dissolving in 10 g APS in 10 ml of double distilled water.

8.6 Preparations of stock treatments

B1: showing how stock solutions per treatment were prepared

Description	EMEM	GRT	BSA	Oleic acid	PIOGLITAZONE
GRT stock solution	2 ml	2 mg	-	-	-
BSA stock solution	45 ml	-	0.9 g	-	-
Oleic acid 10mM Stock solution	3488,3 µl with BSA	-	-	11.7 µl	-
1mM Pioglitazone	0.5 ml	-	-	-	0.196 g
10M Pioglitazone	990 µl				10 µl of 1M stock solution

8.7 *In vivo* data

OGTT 10 WEEKS RAW DATA (Obese)

Obese Control	Mice no							
Time	**1**	**2**	**3**	**4**	**5**	**6**	**7**	**8**
0.	18.8	22.8	10.5	15.0	19.2	25.1	27.7	22.6
15.	29.6	33.3	31.4	32.6	26.1	31.1	33.3	33.3
30.	26.9	33.3	27.2	33.3	27.1	30.2	27.8	33.3
60.	18.1	27.3	16.2	25.3	26.6	28.9	31.1	30.6
120.	9.8	14.6	10.9	18.8	11.7	12.5	10.4	11.2

Obese Pioglitazone	Mice no							
Time	**1**	**2**	**3**	**4**	**5**	**6**	**7**	**8**
0	8.8	7.2	8.1	9.0	20.1	21.5	20.6	25.3
15	28.2	24.4	32.7	32.6	32.4	28.9	27.2	29.7
30	18.2	19.3	32.8	22.5	33.3	27.1	31.2	33.1
60	7.6	8.4	14.2	16.7	31.2	33.3	26.7	25.1
120	6.2	5.6	9.8	12.5	11.8	10.6	7.0	12.0

Obese GRT 1 (74 mg/kg)	Mice no							
Time	**1**	**2**	**3**	**4**	**5**	**6**	**7**	**8**
0	6.3	7.4	31.9	10.2	24.2	14.6	21.3	15.0
15	28.6	19.6	33.3	31.8	31.0	28.3	33.3	33.3
30	17.6	16.2	33.3	24.8	30.2	29.6	27.6	25.2
60	16.0	6.1	29.4	12.1	19.8	24.6	22.3	18.1
120	5.1	4.9	25.4	6.5	14.6	12.6	10.7	7.9

Obese GRT 1 (740 mg/kg)	Mice no							
Time	**1**	**2**	**3**	**4**	**5**	**6**	**7**	**8**
0	16.1	20.2	6.7	30.1	22.2		15.7	21.8
15	28.3	22.2	19.2	33.3	23.9		29.2	33.3
30	29.0	23.8	25.2	33.3	23.3		24.3	33.3
60	7.2	17.8	9.8	29.3	14.9		16.4	28.4
120	8.1	8.8	4.4	18.8	7.8		6.6	6.5

OGTT 10 WEEKS RAW DATA (Lean)

Lean Control	Mice no							
Time	**1**	**2**	**3**	**4**	**5**	**6**	**7**	**8**
0	9.6	8.4	7.4	9.9	7.9	9.1	9.4	9.4
15	12.7	13.5	15.1	14.3	10.2	12.0	14.4	14.6
30	9.1	9.2	9.6	12.2	13.1	9.5	14.6	10.5
60		9.2	7.1	8.6	8.4	12.3	11.0	10.3
120	6.9	7.1	7.1	9.0	6.1	5.8	7.3	8.8

Lean Pioglitazone	Mice no							
Time	**1**	**2**	**3**	**4**	**5**	**6**	**7**	**8**
0	9.7	7.8	7.1	6.2	5.2	6.4	9.1	
15	7.9	12.2	15.0	12.2	9.8	10.3	10.5	
30	8.2	9.4	12.2	10.3	7.8	11.1	9.7	
60	8.6	7.2	7.9	7.3	6.2	9.3	9.4	
120	5.8	6.0	6.4	5.6	5.7	5.7	8.4	

Lean GRT 1 (74 mg/kg)	Mice no							
Time	**1**	**2**	**3**	**4**	**5**	**6**	**7**	**8**
0	7.8	6.0	4.9	4.8	10.8	9.8	3.3	11.8
15	12.3	8.8	12.4	11.1	13.6	11.5	10.3	15.9
30	9.4	6.9	8.5	8.8	12.6	12.1	5.7	14.4
60	10.5	9.2	5.8	5.4	11.4	8.8	4.2	12.2
120	7.9	6.6	5.5	4.0	8.9	5.9	3.7	10.2

Lean GRT 1 (740 mg/kg)	Mice no							
Time	**1**	**2**	**3**	**4**	**5**	**6**	**7**	**8**
0	9.0	9.8	7.3	7.3	9.9	11.6	9.3	8.3
15	11.6	11.1	11.3	11.6	17.6	13.2	10.3	11.3
30	9.4	10.7	10.4	10.9	12.9	12.6	10.1	7.7
60	6.7	9.1	7.6	7.6	9.7	10.6	13.0	7.2
120	5.8	5.4	7.3	7.4	7.8	8.4	7.6	6.3

FASTING BLOOD GLUCOSE 10 WEEKS RAW DATA (Obese)

Obese Control	Mice no						
1	**2**	**3**	**4**	**5**	**6**	**7**	**8**
9.1	9.7	9.9	8.3	3.8	4.0	5.0	4.2
8.2	8.4	33.3	17.6	16.8	15.9	18.4	25.8
4.9	5.2	9.9	9.3	10.7	6.7	6.5	6.9
5.3	6.6	10.7	10.9	9.7	9.3	11.8	12.4
7.3	10.4	9.7	11.9	10.8	11.2	8.8	12.6
6.9	13.9	7.0	11.6	14.2	13.1	7.1	7.1
5.9	13.2	5.8	13.3	9.1	10.6	7.7	14.0
8.4	13.0	7.4	8.6	11.8	11.4	8.4	9.2
8.5	14.4	6.1	14.1	15.1	19.2	10.5	11.7

Obese Pioglitazone	Mice no						
1	2	3	4	5	6	7	8
6.3	14.0	9.0	7.6	5.6	4.2	5.7	3.2
9.6	7.9	7.4	8.6	17.0	17.1	25.2	20.1
6.3	6.3	4.8	4.4	9.2	6.2	8.9	11.6
9.4	6.7	2.6	5.1	9.2	6.2	8.9	12.6
6.2	7.0	5.7	6.1	13.7	8.1	8.6	12.0
5.4	7.9	5.6	7.4	9.0	6.8	9.7	8.9
5.8	5.8	5.4	7.8	6.9	7.3	11.7	13.4
4.6	4.7	4.0	4.8	11.3	11.4	6.7	9.2
8.1	9.0	8.8	6.3	12.2	9.1	8.3	12.2

Obese GRT 1 (74 mg/kg)	Mice no						
1	2	3	4	5	6	7	8
7.9	6.9	8.8	8.4	3.9	3.8	5.2	5.1
14.8	10.3	14.8	13.3	15.1	13.7	16.9	21.9
13.8	8.1	8.9	4.9	6.1	10.1	9.8	9.9
4.6	4.9	14.2	6.1	9.1	12.1	10.8	8.9
7.7	5.8	16.8	4.8	8.1	7.1	11.4	9.6
6.4	7.9	32.9	6.0	8.9	10.2	12.6	8.3
10.1	7.4	22.9	17.8	8.4	9.6	11.3	8.7
5.6	6.2	33.3	8.8	12.5	8.6	10.4	8.1
7.3	6.9	32.7	9.8	16.4	7.4	15.9	9.8

Obese GRT 1 (740 mg/kg)				Mice no			
1	2	3	4	5	6	7	8
8.2	5.3	9.7	16.1	7.2	7.7	5.2	3.4
10.2	8.4	11.4	16.9	23.6	25.7	17.1	12.9
13.9	4.1	4.1	8.2	11.1	13.2	7.2	8.5
6.8	5.3	6.9	11.7	10.6	11.2	9.2	10.5
4.9	4.9	5.8	15.6	11.1	8.9	9.3	12.4
7.3	7.7	5.6	13.3	9.8	8.3	7.6	7.3
6.4	7.9	7.3	14.6	7.1	8.3	8.4	13.7
6.6	6.3	5.5	19.5	8.3	10.2	9.7	8.0
13.6	10.2	7.9	14.9	12.4	13.6	9.9	11.3

FASTING BLOOD GLUCOSE 10 WEEKS RAW DATA (LEAN)

Lean Control				Mice no			
1	2	3	4	5	6	7	8
5.3	4.9	7.1	9.7	2.3	2.3	1.6	1.8
8.8	10.3	6.2	6.2	7.3	8.4	8.6	6.6
5.8	7.6	5.8	5.8	5.6	6.9	5.7	6.8
3.0	3.3	3.5	4.0	7.3	8.4	8.6	6.6
6.8	6.7	7.8	9.5	5.6	7.6	6.2	6.7
5.9	6.3	7.4	10.6	6.2	6.8	6.9	7.5
4.0	3.9	5.2	4.8	6.2	6.6	9.1	6.5
5.9	6.8	6.7	8.2	7.5	8.8	9.4	8.1
6.1	6.5	8.9	11.1	6.3	9.1	8.3	7.5

Lean Pioglitazone			Mice no				
1	2	3	4	5	6	7	8
6.6	6.7	7.5	7.6	2.4	2.3	5.2	3.8
8.6	8.3	7.0	7.3	7.2	5.4	6.6	6.1
6.6	7.6	7.2	6.9	6.2	6.1	5.4	
3.5	2.9	4.1	4.6	7.2	5.4	6.6	
7.4	8.2	7.8	5.9	5.9	6.4	6.3	
7.7	8.2	6.3	7.2	4.8	5.8	5.3	
4.7	2.9	4.0	3.1	4.9	5.8	7.0	
9.8	7.2	7.8	6.3	5.1	6.4	6.1	
7.4	7.2	8.2	5.3	6.2	4.7	8.6	

Lean GRT 1 (74 mg/kg)			Mice no				
1	2	3	4	5	6	7	8
4.3	2.8	2.2	3.7	2.1	1.9	2.8	1.8
7.8	9.0	7.3	7.0	9.3	5.9	6.3	7.3
5.3	5.4	6.2	5.8	7.6	5.4	5.6	5.3
3.5	3.9	6.8	4.1	9.3	5.9	6.3	7.3
8.1	7.2	5.7	11.9	6.7	5.7	5.4	5.9
7.2	6.6	8.2	9.4	6.5	5.3	5.9	6.6
3.8	2.7	3.4	3.4	8.8	4.7	5.5	5.7
7.2	5.8	7.2	6.2	8.8	5.8	8.8	8.7
6.4	4.9	7.9	9.5	7.8	7.4	7.1	7.5

Lean GRT 1 (740 mg/kg)	Mice no							
	1	2	3	4	5	6	7	8
	3.0	2.3	3.6	3.0	3.2	3.2	3.4	3.0
	7.1	9.1	6.8	8.2	13.6	13.2	13.0	7.9
	6.6	8.4	6.6	5.4	6.1	7.0	6.2	5.7
	4.4	5.8	3.2	3.9	9.6	8.2	8.9	7.9
	7.4	7.1	9.2	8.1	5.2	6.1	6.4	6.3
	7.3	6.9	7.4	8.7	5.4	7.1	6.8	6.3
	3.4	3.7	3.3	3.5	7.7	5.3	7.4	6.3
	6.6	6.8	7.4	7.1	8.3	11.2	8.7	7.5
	7.5	7.2	5.8	8.8	8.9	8.6	8.8	7.6

BODY WEIGHT 10 WEEKS RAW DATA (LEAN)

Lean Control	Mice no							
Time	1	2	3	4	5	6	7	8
1	22	26	28	27	24	23	26	24
2	28	28	28	26	23	21	24	22
4	28	28	28	27	27	24	28	25
5	27	28	28	27	28	25	31	26
6	28	28	29	29	30	26	30	26
7	29	30	29	28	30	26	31	26
8	29	30	29	28	32	27	31	27
9	29	30	29	28	31	28	31	28
10	30	29	29	30	31	28	31	28

Lean Pioglitazone				Mice no				
Time	**1**	**2**	**3**	**4**	**5**	**6**	**7**	**8**
1	29	26	24	27	24	24	25	21
2	29	26	25	29	22	21	25	19
4	28	26	26	30	27	24	25	15
5	29	27	27	31	28	26	25	
6	27	27	32	30	28	26	24	
7	30	30	29	33	27	27	25	
8	30	30	29	33	30	28	25	
9	30	29	29	37	26	27	26	
10	30	29	29	34	30	29	26	

Lean GRT 1 (74 mg/kg)				Mice no				
Time	**1**	**2**	**3**	**4**	**5**	**6**	**7**	**8**
1	28	25	26	27	26	24	23	21
2	27	25	26	27	24	22	22	21
4	29	26	26	27	26	24	24	23
5	30	27	25	27	27	25	24	24
6	30	27	26	29	26	24	25	25
7	30	28	28	29	30	28	24	27
8	30	28	28	29	32	31	22	27
9	30	28	29	31	32	31	17	28
10	31	28	29	32	31	30	27	

Lean GRT 2 (740 mg/kg)					Mice no			
Time	**1**	**2**	**3**	**4**	**5**	**6**	**7**	**8**
1	29	26	26	25	24	22	23	23
2	29	26	26	25	22	21	20	23
4	31	28	27	26	24	25	23	24
5	31	28	26	27	26	26	24	25
6	31	28	27	27	26	27	26	27
7	31	28	27	28	27	28	26	26
8	31	28	27	28	27	27	26	25
9	31	27	28	28	27	27	26	24
10	32	28	28	29	27	26	26	26

BODY WEIGHT 10 WEEKS RAW DATA (Obese)

Obese Control					Mice no			
Time	**1**	**2**	**3**	**4**	**5**	**6**	**7**	**8**
1	43	42	43	40	30	32	30	29
2	46	45	37	45	29	31	30	28
4	52	52	47	50	35	37	37	34
5	54	53	50	53	36	38	38	36
6	55	55	55	54	38	40	39	36
7	57	56	55	56	40	42	41	39
8	57	56	56	58	43	45	46	43
9	59	60	59	59	45	47	48	52
10	60	60	60	59	47	48	47	46

Obese Control Pioglitazone					Mice no			
Time	**1**	**2**	**3**	**4**	**5**	**6**	**7**	**8**
1	45	48	39	46	29	30	30	30
2	47	49	42	49	28	30	29	30
4	56	56	47	53	34	38	36	37
5	58	57	47	53	35	40	38	39
6	58	60	49	56	38	41	39	41
7	59	59	49	58	40	45	42	43
8	61	59	49	58	44	48	47	48
9	64	63	50	60	49	48	50	48
10	66	65	51	62	50	53	48	49

Obese GRT 1 (74 mg/kg)					Mice no			
Time	**1**	**2**	**3**	**4**	**5**	**6**	**7**	**8**
1	46	45	43	42	33	32	36	35
2	39	49	45	48	31	27	34	34
4	41	54	48	53	38	35	39	38
5	45	55	49	55	40	37	40	39
6	49	56	50	56	42	39	41	40
7	53	58	50	57	44	42	43	42
8	54	59	50	58	46	45	49	47
9	59	64	51	59	47	48	48	50
10	61	64	52	61	52	46	51	49

Obese GRT 2 (740 mg/kg)					Mice no			
Time	**1**	**2**	**3**	**4**	**5**	**6**	**7**	**8**
1	46	38	39	38	35	33	33	33
2	44	52	41	44	34	35	33	32
4	48	57	42	48	38	39	38	36
5	50	59	48	49	38	40	41	37
6	51	61	51	51	40	42	43	39
7	53	62	53	53	42	44	47	42
8	53	63	55	53	46	48	51	45
9	54	65	56	54	50	48	52	46
10	64	52	61	64	49	50	53	47

FOOD INTAKE 10 WEEKS RAW DATA (Obese)

Obese Control					Mice no			
Time	**1**	**2**	**3**	**4**	**5**	**6**	**7**	**8**
1	17	17	19	19	19	19	19	19
2	18	18	19	19	17	17	19	19
4	20	20	16	16	18	18	19	19
5	20	20	20	20	20	20	20	20
6	21	21	21	21	22	22	20	20
7	26	26	25	25	24	24	25	25
8	26	26	25	25	26	26	27	27
9	30	30	30	30	31	31	31	31
10	30	30	30	30	31	31	31	31

Obese Pioglitazone					Mice no			
Time	**1**	**2**	**3**	**4**	**5**	**6**	**7**	**8**
1	18	18	19	19	18	18	18	18
2	19	19	19	19	19	19	19	19
4	18	18	19	19	22	22	19	19
5	21	21	20	20	21	21	20	20
6	22	22	22	22	20	20	22	22
7	24	24	24	24	24	24	23	23
8	27	27	27	27	27	27	26	26
9	31	31	30	30	31	31	31	31
10	31	31	30	30	31	31	31	31

Obese GRT 1 (74 mg/kg)					Mice no			
Time	**1**	**2**	**3**	**4**	**5**	**6**	**7**	**8**
1	19	19	17	17	19	19	18	18
2	16	16	19	19	19	19	18	18
4	21	20	20	16	16	18	18	19
5	20	18	18	18	18	20	20	18
6	21	18	18	16	16	18	18	18
7	25	25	25	25	25	23	23	25
8	26	20	20	20	20	20	20	20
9	32	32	32	32	31	31	31	31
10	32	32	32	32	31	31	31	31

Obese GRT 2 (740 mg/kg)					Mice no			
Time	**1**	**2**	**3**	**4**	**5**	**6**	**7**	**8**
1	18	18	19	19	20	20	18	18
2	21	21	20	20	19	19	18	18
4	19	18	18	19	19	22	22	19
5	18	18	18	18	18	18	18	18
6	18	20	20	18	18	20	20	18
7	25	25	25	25	25	25	25	25
8	20	21	21	20	20	21	21	20
9	30	30	32	32	30	30	30	30
10	30	30	32	32	30	30	30	30

FOOD INTAKE 10 WEEKS RAW DATA (Lean)

Lean Control					Mice no			
Time	**1**	**2**	**3**	**4**	**5**	**6**	**7**	**8**
1	17	17	19	19	19	19	19	19
2	18	18	19	19	17	17	19	19
4	20	20	19	19	19	19	16	16
5	22	22	24	24	24	24	23	23
6	24	24	24	24	24	24	26	26
7	27	27	27	27	26	26	26	26
8	30	30	30	30	30	30	29	29
9	24	24	23	23	23	23	24	24
10	25	25	24	24	24	24	24	24

Lean Pioglitazone					Mice no			
Time	**1**	**2**	**3**	**4**	**5**	**6**	**7**	**8**
1	18	18	19	19	18	18	18	18
2	19	19	19	19	19	19	19	19
4	20	20	19	19	21	21	18	18
5	21	21	24	24	22	22	22	22
6	23	23	26	26	26	26	25	25
7	25	25	26	26	24	24	27	27
8	29	29	30	30	27	27	30	30
9	24	24	24	24	23	23	25	25
10	24	24	25	25	23	23	24	24

Lean GRT 1 (74 mg/kg)					Mice no			
Time	**1**	**2**	**3**	**4**	**5**	**6**	**7**	**8**
1	19	19	17	17	19	19	18	18
2	16	16	19	19	19	19	18	18
4	19	19	20	20	20	20	19	19
5	24	24	21	21	21	21	24	24
6	26	26	26	26	25	25	26	26
7	28	28	28	28	27	27	25	25
8	28	28	28	28	27	27	25	25
9	26	26	26	26	27	27	25	25
10	24	24	26	26	26	26	25	25

Lean GRT 2 (740 mg/kg)					Mice no			
Time	**1**	**2**	**3**	**4**	**5**	**6**	**7**	**8**
1	18	18	19	19	20	20	18	18
2	21	21	20	20	19	19	18	18
4	19	19	20	20	20	20	20	20
5	20	20	21	21	23	23	23	23
6	25	25	23	23	26	26	26	26
7	28	28	26	26	24	24	27	27
8	28	28	26	26	24	24	27	27
9	26	26	26	26	22	22	25	25
10	26	26	26	26	23	23	26	26

Gene	Slope	R^2	no of points in std
Act B (lean)	-3.322	0.999	6
Act B (obese)	-3.207	0.988	6
HPRT (lean)	-3.08	0.997	5
HPRT (obese)	-3.27	0.998	6
FASN (lean)	-3.406	0.996	5
FASN (lean)	-3.226	0.984	6
ACACA (lean)	-3.08	0.982	5
ACACA (obese)	-3.31	0.998	6
APO A1 (lean)	-3.199	0.993	6
APO A1 (obese)	-3.133	0.995	5
APO A4 (lean)	-3.4	0.996	6
APO A4 (obese)		ND	
HSMGCR (lean)	-3.096	0.996	6
HSMGCR (obese)	-3.057	0.999	6
HSMGCS 1(lean)	-3.598	0.999	6
HSMGCS 1 (obese)	-3.068	0.987	5
ChREBP (lean)	-3.382	0.994	5
ChREBP (obese)	-3.111	0.988	5
PPAR a(lean)	-3.55	0.994	5
PPAR a(obese)	-3.362	0.998	6
SREBP 1c (lean)	-3.068	0.987	5
SREBP 1c (obese)	-3.403	0.98	6

Table 4: Gene expression results in lean and obese mice treated with GRT.